

# **Synthesis of an antiaromatic circulenophane**

**M.Sc. thesis**

**University of Jyväskylä**

**Department of Chemistry**

**Nanoscience Center**

**04.04.2020**

**Afra Pazhouhan Fekri**

## ABSTRACT

Otherwise unstable antiaromatic compounds can be studied when they are integrated into a bigger  $\pi$ -conjugated system. Cyclooctatetraene (COT) compounds are easy to synthesize and study, but they reside in a non-planar saddle-shaped conformation. Planarized COT, however, is an  $8\pi$  8-membered antiaromatic structure. A hetero[8]circulene is one option to overcome the non-planar conformation barrier. The surrounding aromatic  $\pi$ -system in a hetero[8]circulene core assists in creating a smaller bond angle, thus resulting in a planar diazadioxa[8]circulene.

This thesis addresses a synthetic pathway towards having a suitable compound for studying the concept of antiaromaticity in planarized cyclooctatetraenes (COTs). For further research, there are two means of evaluating aromaticity. According to the Nucleus-Independent Chemical Shift (NICS) values obtained by computational chemistry, magnetic current of the COT core can be investigated. Furthermore, the synthesized compound can be analysed using NMR spectroscopy. Antiaromaticity of the hetero[8]circulene can be proven by locating a proton near the COT core so that the chemical shift of the proton changes due to the proximity to the ring current.

To apply this theory, cyclophane-chemistry has been used to create a system in which a circulene substrate bearing a bridge-type linker containing protons is located in its centre. The linker is covalently bonded through the pyrrole nitrogen atoms of the circulene system. Creating this system enables us to study further the antiaromaticity of the circulenophane compound synthesized in this project.

## PREFACE

This work was done as a part of the Master's degree program in Nanoscience of The University of Jyväskylä under the supervision of Professor Maija Nissinen. The experimental part was done at The Department of Chemistry of The University of Copenhagen under the supervision of Associate Professor Michael Pittelkow.

There are many people involved in my studies, whom I would like to express my appreciation to them. I would like to thank Maija for giving me the opportunity to find my way and explore the working environment in other laboratories and broaden my experience as a chemist.

Then I would like to thank Michael for giving me the chance to be part of his group despite all the burdens and I would like to thank him for giving me the confidence to work independently in the lab.

I am thankful to all Pittelkow group who helped me throughout the work; especially Associate Professor Fadhil Kamounah, Postdoc researcher Stephan K. Pedersen and PhD students Kristina Eriksen, Nicolaj N. Andersen, Bodil Lousen and Line M. Langhorn who were always there to answer my questions.

I am thankful to all my friends in Denmark and Finland, who have been there for me, supported me and created valuable moments.

I would like to thank my family, who paved the way for me in the first place and encouraged me to realize my dreams.

At last, I would like to thank my dearest Jaakko I. Mastomäki for his support and professional advice on my work and most importantly for creating peace of mind for me.

## TABLE OF CONTENT

ABSTRACT .....	1
PREFACE .....	2
TABLE OF CONTENT .....	3
LIST OF ABBREVIATIONS .....	5
1 INTRODUCTION .....	1
2 AROMATICITY AND ANTIAROMATICITY .....	3
2.1 Introduction to aromaticity and antiaromaticity .....	3
2.2 Criteria and measurement of aromaticity and antiaromaticity .....	6
2.2.1 Chemical reactivity .....	6
2.2.2 Spectroscopic criteria.....	7
2.2.3 Energetic criteria.....	8
2.2.4 Magnetic criteria .....	9
3 CIRCULENES .....	12
3.1 Introduction to circulenes .....	12
3.1.1 Heterocirculenes .....	13
3.1.2 Modelling circulenes.....	15
3.1.3 Benzotetraoxa[8]circulene .....	17
3.2 Other works regarding hetero[n]circulenes .....	21
4 CYCLOPHANES AND RELATED SYSTEMS.....	24
4.1 Cyclophanes.....	24
4.2 Planar cyclooctatetraene systems .....	27
4.3 Circulenophanes .....	30
4.3.1 Forming a macrocycle.....	32
4.4 Bridge-type linkers .....	34
EXPERIMENTAL PART: TOWARDS THE SYNTHESIS OF A CIRCULENOPHANE....	37
5 MOTIVATION .....	38
6 SYNTHESIS APPROACH.....	39
6.1 Synthesis of diazadioxo[8]circulene 10 .....	39
6.2 Synthesis of bicyclo[2.2.2]octane containing linker 51 .....	41
6.3 Synthesis of linker 60 .....	43
6.4 Synthesis of a circulenophane .....	44
7 REACTION MECHANISMS.....	46
7.1 Diazadioxo[8]circulene .....	46
7.2 Synthesis of the bicyclo containing linker 51 .....	47

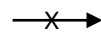

## IV

7.3 Mechanistic view towards the synthesis of DABCO containing linker 60 .....	51
8 MATERIAL AND INSTRUMENTATION .....	53
9 SYNTHESIS .....	54
9.1 Synthesis of dimethyl bicyclo[2.2.2]octane-1,4-dicarboxylate 53 .....	54
9.2 Synthesis of bicyclo[2.2.2]octane-1,4-dimethanol 54 .....	56
9.3 Synthesis of bicyclo[2.2.2]octane-1,4-dicarboxaldehyde 55 .....	58
9.4 Synthesis of 1,4-bis[2-(ethoxycarbonyl)ethen-1-yl]bicyclo[2.2.2]octane 56 .....	60
9.5 Synthesis of <i>N</i> -benzyl-2,7-di- <i>tert</i> -butyl-3,6-dimethoxy-9 <i>H</i> -carbazole 48 .....	62
9.6 Synthesis of 9-benzyl-2,7-di- <i>tert</i> -butyl-9 <i>H</i> -carbazole-3,6-diol 49 .....	64
9.7 Synthesis of 9,11-bis( <i>N</i> -benzyl)-2,3,6,7-tetra- <i>tert</i> -butyl diazadioxo[8]circulene 24 .....	66
9.8 Synthesis of 9,11 <i>H</i> -2,3,6,7-tetra- <i>tert</i> -butyl-diazadioxo[8]circulene 10 .....	68
9.9 Synthesis of 8-bromoquinoline 61 .....	70
9.10 Synthesis of 1-(3-bromopropoxy)-2-iodobenzene 62 .....	71
9.11 Synthesis of DABCO with 1-(3-bromopropoxy)-2-iodobenzene 60 .....	73
9.12 Synthesis of a circulenophane: Approach I 72 .....	75
9.13 Synthesis of a circulenophane: Approach II 72 .....	76
10 CONCLUSIONS AND OUTLOOK .....	77
LITERATURE REFERENCES .....	80

**LIST OF ABBREVIATIONS**

DCM	Dichloromethane
DMF	<i>N,N</i> -Dimethylformamide
DMSO	Dimethyl sulfoxide
DTT	Dithiothreitol
THF	Tetrahydrofuran
AcOH	Acetic acid
Ar	Aryl
Bn	Benzyl
Bu	Butyl
COT	Cyclooctatetraene
Et	Ethyl
Me	Methyl
<i>n</i> -BuLi	<i>n</i> -Butyllithium
<i>t</i> -Bu	<i>tert</i> -Butyl
TMS	Tetramethylsilane
$\delta$	Chemical shift
2D	Two dimensional
<i>C</i>	Number of Clar $\pi$ sextets
COSY	Correlation spectroscopy
DCVC	Dry column vacuum chromatography
EA	Elemental analysis
ESI	Electrospray ionization
FTMS	Fourier-transform mass spectroscopy
GC	Gas chromatography

## VI

HMBC	Heteronuclear single-quantum correlation spectroscopy
HPLC	High-performance liquid chromatography
HRMS	High-resolution mass spectroscopy
HSQC	Heteronuclear single-quantum correlation spectroscopy
<i>J</i>	Coupling constant
MALDI	Matrix-assisted laser desorption/ionization
MM	Molecular modelling
MP	Melting point
MS	Mass spectroscopy
NICS	Nucleus-independent chemical shift
NMR	Nuclear magnetic resonance
PG	Protecting group
R <sub>f</sub>	Retention factor
ROESY	Rotating frame nuclear Overhauser effect spectroscopy
r.t.	Room temperature
S <sub>N</sub> 2	Nucleophilic substitution
S <sub>N</sub> Ar	Nucleophilic aromatic substitution
TLC	Thin layer chromatography
UV	Ultra violet
	Failed reaction
	Synthesis was not carried out





## 1 INTRODUCTION

[ $n$ ]circulenes are fully conjugated systems consisting of annulated benzene rings.<sup>1</sup> This family of compounds has been analysed computationally from  $n = 3$  to  $n = 20$ .<sup>2</sup> Each compound appeared to have interesting structural properties and strain energy, based on the number of benzene rings in the [ $n$ ]circulene in comparison to the [6]circulene. [6]circulene, also known as coronene, is the only structure in a planar conformation and exists in nature in the form of mineral graphite; this also verifies the stability of this derivative.<sup>3,4</sup>

Up to this date, [8]circulenes are the largest synthesized [ $n$ ]circulenes in the form of highly substituted structures.<sup>5</sup> The crystal structures of these compounds demonstrate their saddle-shaped conformation making it rather difficult to investigate their properties.<sup>6</sup> However, [8]circulenes can be modified into planar conformations by substituting some of the atoms of the benzene rings with heteroatoms, such as oxygen, nitrogen, sulphur and selenium.<sup>1</sup> The synthesis of hetero[8]circulenes by a condensation reaction of 1,4-naphthoquinones in the presence of concentrated hydrochloric acid was rather serendipitous.<sup>7</sup> The result was an insoluble amorphous powder; yet it was not fully characterized until Erdtman studied the polymerization of 1,4-naphthoquinone, 1,4-benzoquinone and 2-methyl-1,4-benzoquinone.<sup>8</sup>

Hetero[8]circulenes have raised interest during the past decades due to their unique properties. The enforced planarity of this class of compounds resulted in specific electronic and magnetic properties due to their heteroatom substituents and made them easier to study in contrast to the saddle-shaped [8]circulenes.<sup>9</sup> The center of hetero[8]circulenes contains an 8-membered  $8\pi$  cyclooctatetraene (COT) core and a  $4n$   $\pi$ -system in their center which is considered to be antiaromatic when planar.<sup>10</sup>

Some hetero[8]circulenes have fluorescent properties making them potential candidates for the production of blue organic light-emitting diodes (OLEDs).<sup>11</sup> OLEDs consist of layers of organic electroluminescent substances, which are glowing when activated by an electric current. The organic layer could be, for example,  $\pi$ -conjugated systems that are electrically conductive as a result delocalization of  $\pi$  electrons. Due to their electroluminescent properties, OLEDs are independent of a backlight, which is needed in liquid crystal displays (LCDs). They also have enhanced picture quality and lower electricity consumption, making them a better choice than conventional LCDs. Pittelkow and Christensen<sup>12</sup> have found the potential application of tetraoxa[8]circulenes as the blue light emitter component of OLEDs.

In Pittelkow's group, a simple and efficient way to synthesize a series of hetero[8]circulenes has been established.<sup>13,14</sup> Their favourable properties, such as high thermal and chemical stability, substitutable nitrogen atoms in the pyrrole moieties, as well as cheap and commercially available 9*H*-carbazole **44** as the starting material, made them good candidates for studying the COT core.

To study these properties, the COTs can be included in a bigger system such as a functionalized COT. This allows placing a proton to the proximity of the COT core in order to investigate the NMR chemical shifts of the protons affected by the paratropic ring current of the antiaromatic ring.<sup>15</sup> The proton could be a part of a bridge-type linker spanned across the circulene plane (Figure 1).

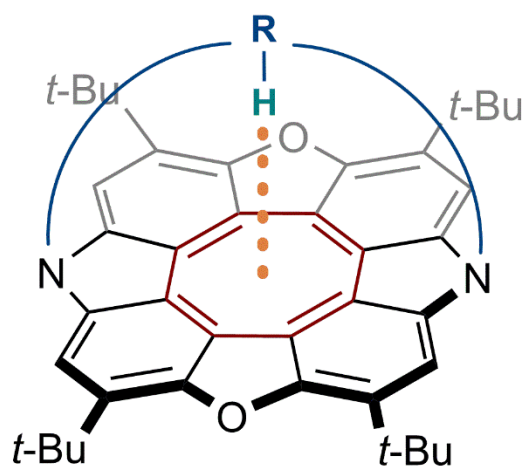


**Figure 1.** A bridge-functionalized hetero[8]circulene derivative having the bridge proton pointed towards the COT core.

This project aimed to synthesize a suitable bridge-type linker to span over the planar diazadioxo[8]circulene plane. This strategy was inspired by cyclophane chemistry, which is described in detail in Chapter 4. Diazadioxo[8]circulene has substitutable pyrrole moieties for the attachment of a ligand, covalently or non-covalently, to investigate its interactions with the COT core.

## 2 AROMATICITY AND ANTIAROMATICITY

### 2.1 Introduction to aromaticity and antiaromaticity

Aromaticity is an important concept in chemistry, and it has been a matter of interest to study for decades.<sup>16-17</sup> Benzene, discovered by Michael Faraday in 1825, is a classic example of an aromatic compound.<sup>18-19</sup> The structure of benzene, however, was not established before Kekulé proposed a structure and introduced aromaticity in 1865 and 1866. His idea about the presence of C<sub>6</sub> units in planar cyclic compounds has evolved dramatically ever since. These fundamental studies were inspired by the fact that the benzenoid hydrocarbons show different physical and chemical reactivity compared with their acyclic analogues. Other compounds showing similar properties<sup>20</sup> were suggested as well; few of the suggestions by Kekulé,<sup>19</sup> Prismane<sup>21</sup> and Dewar<sup>22</sup> are presented in Figure 2.

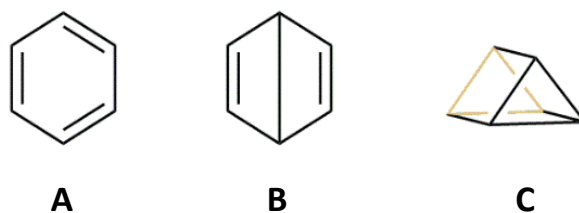


**Figure 2.** Proposed structures of benzene by Kekulé<sup>19</sup> (A), Dewar<sup>22</sup> (B) and Prismane<sup>21</sup> (C).

There is not a single formula that can describe aromaticity because of its multidimensional characteristics. Similarly to other fundamental chemical properties, such as charge, electronegativity or bond order, aromaticity is not a measurable property. Therefore it has to be defined and measured by a relative scale.<sup>23,24</sup> Aromatic compounds have been measured utilizing different indices, such as geometrical,<sup>25</sup> energetic,<sup>26</sup> electronic,<sup>27,28</sup> and magnetic<sup>29,30</sup> properties. As a result of these measurements, it is established that aromatic compounds show different energetic stability and chemical reactivity, as well as structural, magnetic and electronic properties.<sup>25</sup> Therefore, there are several ways to assess the aromatic or antiaromatic properties of molecules.<sup>31</sup> Furthermore, these measurements will give us an insight into the structure and chemical bonding of the molecules as well as help us to predict the reactivity and stability of both organic and inorganic compounds.

Delocalization of the  $\pi$ -electrons leads to equal bond length (1.39 Å) in the conjugated system, whereas localized single and double bonds (1.54 Å and 1.34 Å, respectively) show a significant difference in their bond lengths.<sup>32,33</sup> As a matter of fact, longer bond length (>1.39 Å) makes the molecule lean towards antiaromaticity due to the Jahn-Teller effect, which forces the molecule to bend geometrically to avoid antiaromaticity.<sup>34</sup> Since the bond length also affects the hybridization, planarity is another determining parameter for aromaticity of a compound. The molecular orbitals of the  $\pi$ -system can overlap only when they are planar to provide electron delocalization.

In 1931, Hückel<sup>35-36</sup> introduced a formula by which the aromaticity of compounds can be predicted. He claimed that not all conjugated systems are aromatic, but only those having  $4n + 2$  (where  $n = 1, 2, 3 \dots$ )  $\pi$ -electrons in addition to being planar, cyclic, and conjugated. This rule applies only to monocyclic conjugated systems. He explained the stability of benzene compared to cyclobutadiene and cyclooctatetraene through delocalization of the  $\pi$ -electrons in the ring. Many attempts were performed to expand this law to polycyclic systems. So far Erich Clar's<sup>37</sup>  $\pi$ -sextet rule introduced in 1972 is the most successful. His idea was inspired by work by Armit and Robinson<sup>38</sup> who used the term "aromatic sextet" for the first time in 1925. Clar's rule explains qualitatively the aromatic character of benzenoid species in polycyclic aromatic hydrocarbons (PAHs). He claims that the number of disjoint aromatic  $\pi$ -sextets describes the chemical properties of the molecule.

According to Clar's<sup>39</sup> theory, the ring that bears an aromatic sextet may be sharing an acenic portion with another ring. Therefore, several rings will have fractions of the  $\pi$ -electron sextets. As an example, in phenanthrene (Figure 3), there are two  $\pi$ -sextets, whereas in anthracene there is only one. The central ring of anthracene bears only two of the total 14  $\pi$ -electrons while the outermost rings have six  $\pi$ -electrons. The outermost rings are more inert since they have a high aromatic share in the molecule. Both anthracene and phenanthrene, however, undergo olefinic addition reactions. With anthracene, the reaction is faster and happens on the 9 and 10 positions in the central ring.<sup>40</sup> Phenanthrene is also thermochemically more stable than anthracene by 5 kcal·mol<sup>-1</sup>, which is obviously due to the more aromatic character of phenanthrene. Furthermore, it is established that increasing the portion of non-sextet rings in acenes will lower the stability of the molecule.<sup>41</sup>

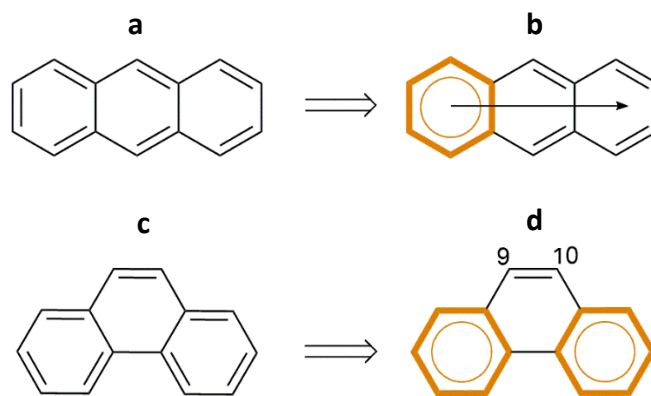


**Figure 3.** Top: The structure of anthracene proposed by Kekulé (**a**) and Clar (**b**) having a migrating  $\pi$ -sextet. Bottom: The structure of phenanthrene proposed by Kekulé (**c**) and Clar<sup>40</sup> (**d**) bearing two Clar's  $\pi$ -sextet rings resulting in an increase in the aromatic character of the molecule.

Up to this point, all other compounds not fulfilling these criteria were considered non-aromatic until Breslow<sup>42,43</sup> introduced the term “antiaromaticity” in 1967 as “a situation in which a cyclic delocalization of electrons is destabilizing”. He also introduced examples of antiaromatic compounds, such as cyclobutadiene and cyclooctatetraene (COT). According to the crystallographic results, COTs tend to adopt a tub-shaped conformation belonging to  $D_{2d}$  point group to avoid antiaromaticity (Figure 4).<sup>10</sup>

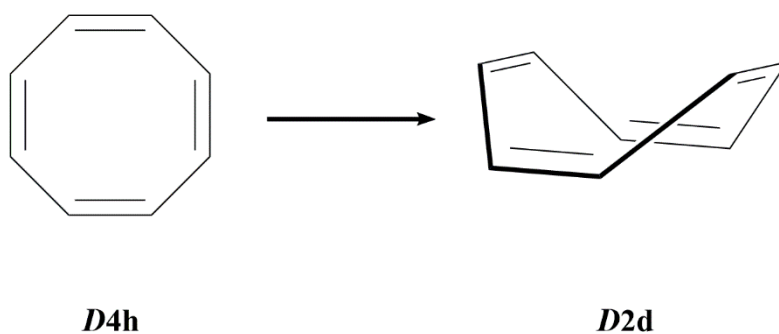


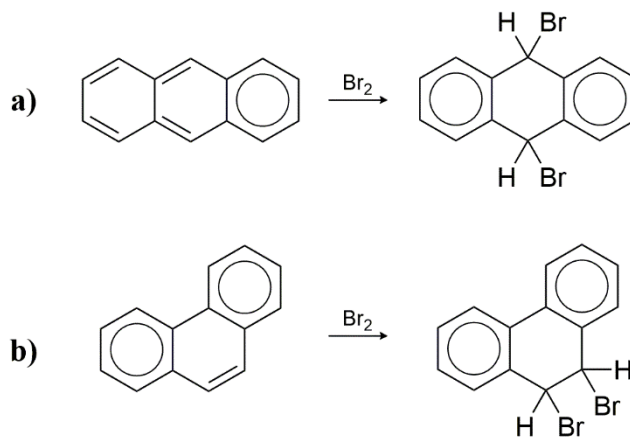
**Figure 4.** Cyclooctatetraene undergoes Jahn-Teller effect to avoid antiaromaticity.<sup>10</sup>

## 2.2 Criteria and measurement of aromaticity and antiaromaticity

During the past two decades, aromaticity has been extensively studied. In a recent review by Balaban,<sup>44</sup> five major criteria of aromaticity are explained: chemical reactivity, spectroscopic criteria, energetic criteria and magnetic and geometric properties.

### 2.2.1 Chemical reactivity

Following Labarre and Crasnier,<sup>45</sup> aromatic compounds are predisposed to substitution reactions in contrast to their olefinic analogues, which undergo addition reactions. Although aromatic compounds typically undergo electrophilic aromatic substitution, there are many exceptions, such as phenanthrene and anthracene, which undergo bromine addition like olefins (Figure 5).<sup>46</sup> Another example is a fullerene system, which undergoes addition reactions since it lacks any hydrogens.<sup>47</sup>

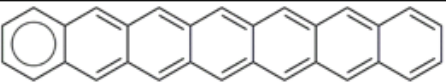
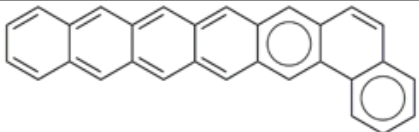
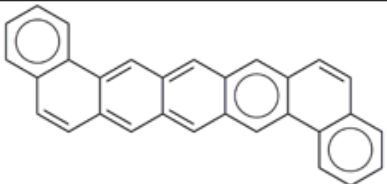
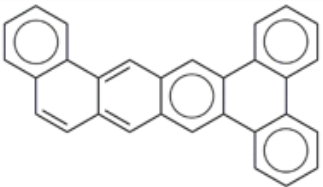
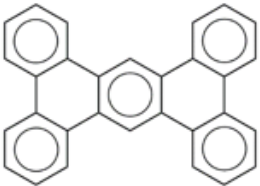


**Figure 5.** Anthracene (a) and phenanthrene (b) undergo addition reaction similar to olefins.<sup>46</sup>

## 2.2.2 Spectroscopic criteria

Spectroscopic criteria of aromaticity refer to the electronic absorption spectra of PAHs, which are classified based on their absorption bands. Lewis and Kasha<sup>48</sup> have studied and classified the absorption bands of this class of compounds, which are responsible for the color of various benzenoids. As an example, an isomeric catafusenes with seven benzenoid rings have been studied (Table 1). It was inferred that there is a direct correlation between the number of linearly condensed benzenoid rings (acenic portion), the number of Clar's sextets ( $C$ ) and the absorption wavelength ( $\lambda_{\max}$  in nm) corresponding to the colour.<sup>49</sup> The value of the absorption wavelength decreases by increasing the acenic portion. It depicts the higher the number of  $\pi$ -sextets, the more stable the benzenoid is due to the higher HOMO-LUMO gap.<sup>50</sup>

**Table 1.** Isomeric catafusenes and their correlation between the number  $C$  of Clar's sextets, absorption wavelength (nm) and color<sup>49</sup>

$\lambda_{\max}$	Colour	$C$	Clar sextet structures
840	Green	1	
651	Blue	2	
523	Red	3	
425	Yellow	4	
328	Colourless	5	

### 2.2.3 Energetic criteria

Among the most fundamental of all criteria are enhanced resonance energies (Res) and the aromatic stabilization energies (ASEs). The resonance energy, which can be measured experimentally, causes thermodynamic stability. According to Pauling and Sherman's<sup>51</sup> concept of resonance energy, delocalization of the  $\pi$ -electrons in a benzene ring makes it more stable than its non-aromatic counterpart. This phenomenon can be exhibited by the heat of hydrogenation of benzene towards cyclohexane. If the double bonds were localized in a benzene ring, the expected heat of hydrogenation of benzene to cyclohexane would be equal to the hydrogenation of three equivalents of cyclohexene (Figure 6). This theory is proved both computationally<sup>52</sup> and experimentally<sup>53</sup>.

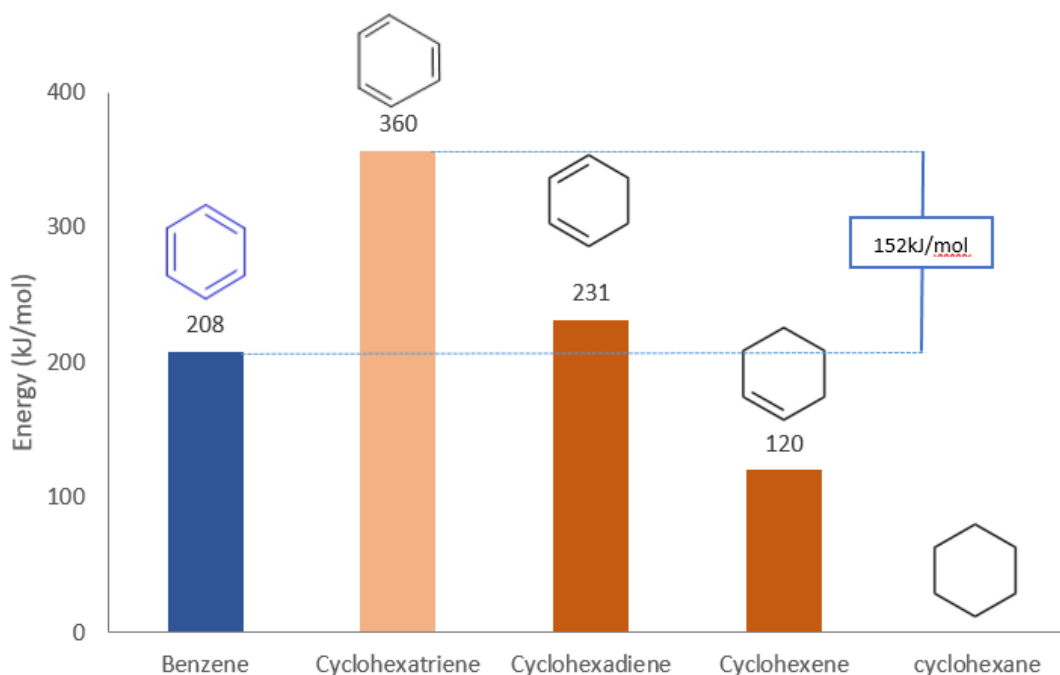


**Figure 6.** Resonance energy of benzene is lower than the hypothetical cyclohexatriene. Adapted from Ref.<sup>52</sup> with permission from the American Chemical Society (ACS) publication. Copyright © 2009, American Chemical Society.



## 2.2.4 Magnetic criteria

Assessing aromaticity through the magnetic properties of compounds is currently the most popular method. It includes various techniques, among which  $^1\text{H}$ -nuclear magnetic resonance (NMR) spectroscopy and the computational method of nuclear independent chemical shifts (NICS) have drawn more attention in this project.

The well-verified ring current model<sup>54</sup> (RCM) predicts that aromatic compounds show a diatropic ring current in the presence of an external magnetic field (Figure 6). In practice, the most direct method to visualize the effect of ring currents is NMR spectroscopy. The induced magnetic ring current affects the magnetic environment of the atoms. Therefore, it changes the chemical shift of the nuclei, observed by NMR spectroscopy. The change in the chemical shift can indicate the direction and magnitude of the induced magnetic field. For aromatic compounds, applying an external magnetic field perpendicular to the aromatic ring induces a ring current within the aromatic  $\pi$ -system. This ring current induces a secondary magnetic field, which affects the electrons in of the system. Thus, the protons of the ring are deshielded and therefore deshielded, which causes a downfield chemical shift. (Figure 7).<sup>54</sup>

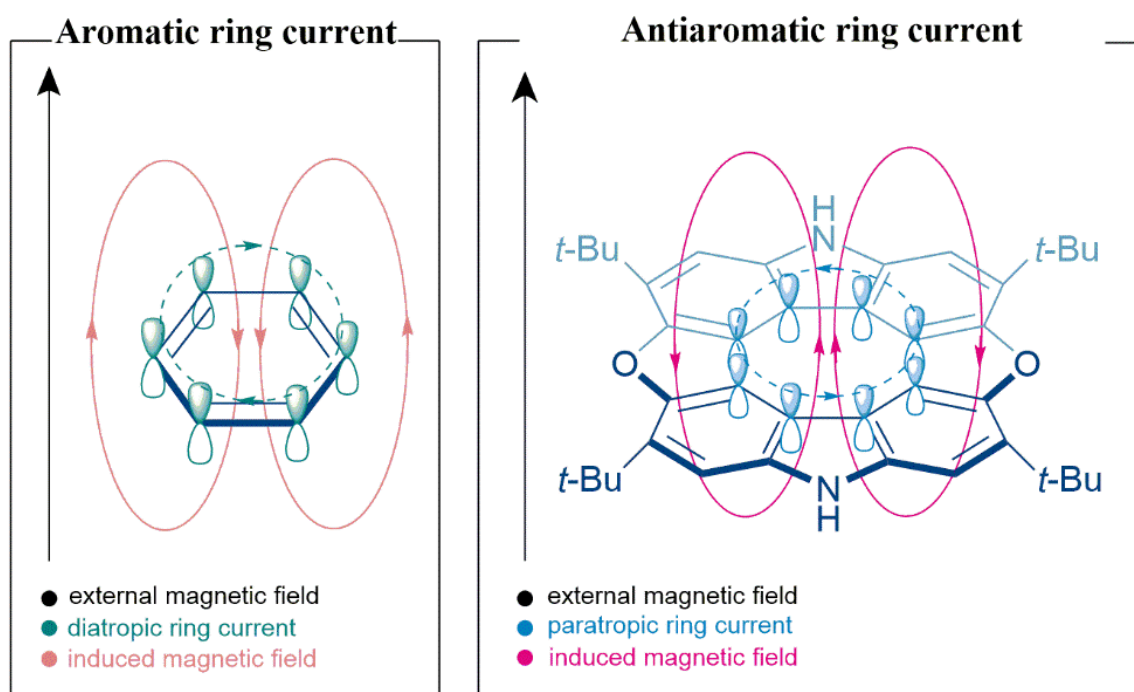


**Figure 7.** Ring current in aromatic and antiaromatic compounds.

For antiaromatic compounds, this effect is the opposite. The ring current is called paratropic, and it is diametric to the applied external field. Therefore, the nuclei at the inner face of the molecule show a downfield chemical shift. Meanwhile, the protons of the periphery of the ring experience further shielding, which reduces the effect of the external field and results in their upfield chemical shifts (Figure 8).

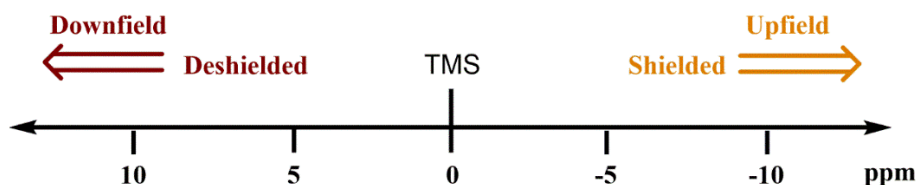


**Figure 8.** A schematic presentation of an NMR spectrum and terminology.

The unambiguous nature of aromaticity encouraged the researchers to develop a quantitative definition for aromaticity. In 1996, Shleyer and coworkers<sup>55</sup> used the resonance of  $^3\text{He}$  atoms to the proximity of the inner and outer surface of fullerenes as a criterion to measure aromaticity of cyclic  $[n]$ annulene systems. Soon after, they invented a computational method (the aforementioned NICS) to have general criteria for measuring aromaticity and antiaromaticity. NICS is nowadays a popular and easy-to-use method due to its simplicity and efficiency. NICS can be calculated using the standard quantum chemical programs such as Gaussian 98 and Gaussian 03. Since most aromatic rings are too small to accommodate atoms inside, the hydrogen atoms located on the bridge positions are used as probes.<sup>56</sup> This method uses a ghost atom with no protons and neutrons at any given location as a sensor for the magnetic environment of the molecule. In other words, it uses the absolute chemical shielding of a virtual nucleus to probe aromaticity. The NICS values are calculated at the ring centers, at points above, and as grids in and around the molecule. It is typically one ångström ( $\text{\AA}$ ) above the plane since it is reflecting the  $\pi$ -effect of the ring current in a better way, and there is less  $\sigma$ -bond effect compared to the ring plane.<sup>57,58</sup> The grid distribution values enable us to have a better understanding of the magnetic properties of the molecules (Figure 9).<sup>59</sup> In the grid plot, one can observe significantly negative NICS values corresponding to the diatropic ring current in aromatic compounds and positive NICS values corresponding to antiaromatic compounds.<sup>60</sup> It was observed that the number of  $\pi$  electrons affects the NICS values significantly in a way that systems bearing ten  $\pi$  electrons possess a higher value than those with six  $\pi$  electrons.<sup>60</sup>

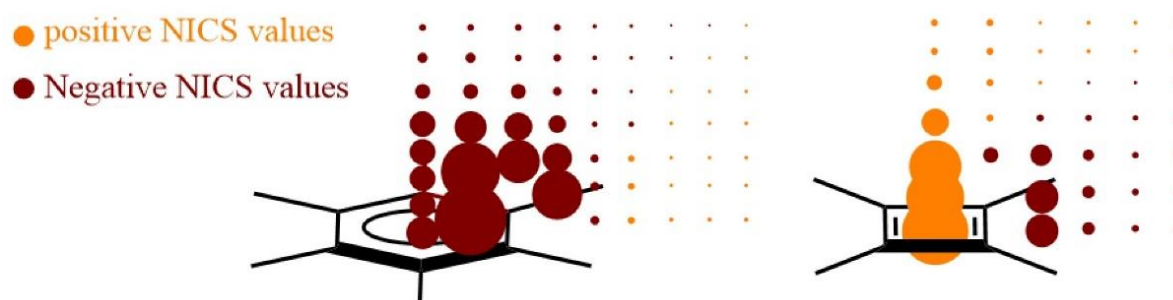


**Figure 9.** The NICS grid plot of benzene (left) and cyclobutadiene (right). The red and orange dots show negative and positive NICS values, which correspond to diatropic and paratropic ring currents, respectively. Adapted from Ref.<sup>59</sup> with permission from The American Chemical Society (ACS)

Publications. Copyright © 2001, American Chemical Society.

### 3 CIRCULENES

#### 3.1 Introduction to circulenes

Circulenes are a class of compounds consisting of a ring structure (circu-) and an unsaturated hydrocarbon moiety, such as one or more carbon-carbon double bonds (-ene).<sup>61</sup> Further,  $[n]$ circulenes, where  $n$  indicates the number of components forming the ring structure, are fully conjugated polycyclic compounds.<sup>62</sup> For example, [6]circulene can be considered as six *ortho*-fused benzene rings (Figure 9a) or to be derived from a [6]radialene<sup>63</sup> (Figure 9b) The radialene scaffold must undergo multiple Diels-Alder reactions with ethylene and consecutive oxidative coupling resulting in  $[n]$ circulenes (Figure 10).

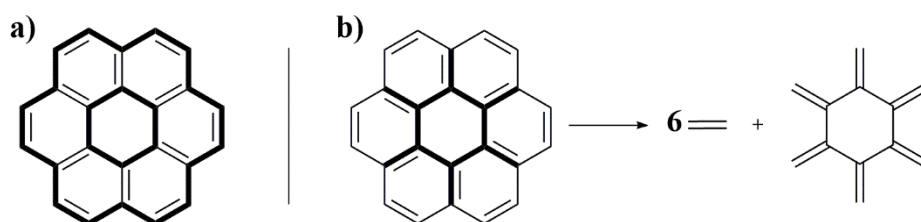


**Figure 10.** a) [6]Circulene as *ortho*-fused benzene motif: a band of benzene rings surrounds central benzene ring. b) Hypothetical retrosynthetic path of [6]circulene derived from [6]radialene. Adapted from Ref.<sup>63</sup> with permission from John Wiley and Sons and Copyright Clearance Center.

The largest  $[n]$ circulene is computationally predicted to be [20]circulene.<sup>2</sup> Experimentally, only [4]circulene,<sup>64,65</sup> [5]circulene,<sup>61</sup> [6]circulene,<sup>63</sup> [7]circulene<sup>66</sup> and [8]circulene<sup>67</sup> have been synthesized so far. [3]Circulene, however, is not synthetically feasible, and [4]circulene and [8]circulene have only been synthesized when surrounded by substituents. Density functional theory (DFT) calculations show that the larger circulenes tend to get saddle-shaped conformations due to strain energy compared to [6]circulene with a planar conformation (Figure 11). Historically, fullerenes and carbon nanotubes inspired the study of non-planar circulenes, as they are fully conjugated systems.<sup>68</sup>

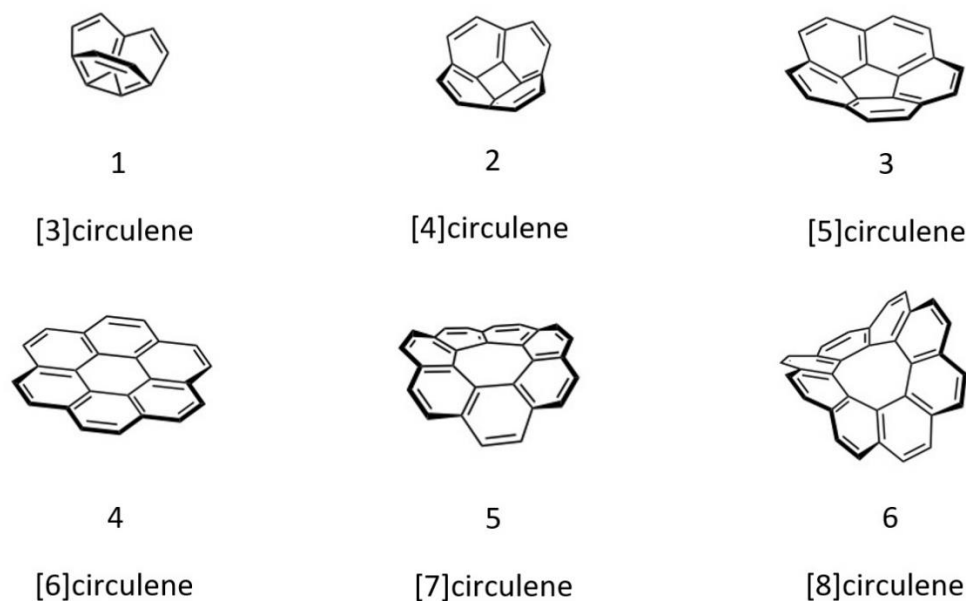


**Figure 11.** Geometries of  $[n]$ circulenes: hypothetical [3]circulene **1**, bowl-shaped [4]circulene or quadrannulene **2**, bowl-shaped [5]circulene or corannulene **3**, planar [6]circulene or coronene **4**, saddle-shaped [7]circulene or pleiadannulene **5**, saddle-shaped [8]circulene **6**.

### 3.1.1 Heterocirculenes

In the class of polycyclic aromatic compounds, heterocyclic circulenes with a heteroatom, such as O, N, S or Se, in the etheno-bridge(s) are an area of interest due to their different geometries and chemical and physical properties.<sup>63</sup> In this project, especially hetero[8]circulenes are of interest because they have eight  $\pi$ -electrons in their central ring. These compounds show antiaromatic properties when forced into planarity. Synthesizing a planar hetero[8]circulene can be challenging since they naturally tend to bend and form a tub-shaped conformation to avoid antiaromaticity. Otherwise, the structure does allow the COT core to be antiaromatic.<sup>69</sup>

Different five-membered heterocycles, such as furan, pyrrole, thiophene, or other heterocycles bearing six  $\pi$ -electrons, can affect the planarity of the hetero[8]circulenes compared to a hydrocarbon[8]circulene. This matter will be discussed in more detail in the next section. Some of the hetero[8]circulenes may contain alternating moieties of annulated benzene rings and a heterocyclic ring. On the other hand, in some hetero[8]circulenes the COT core can be surrounded only by heterocycles (Figure 12).<sup>70</sup>

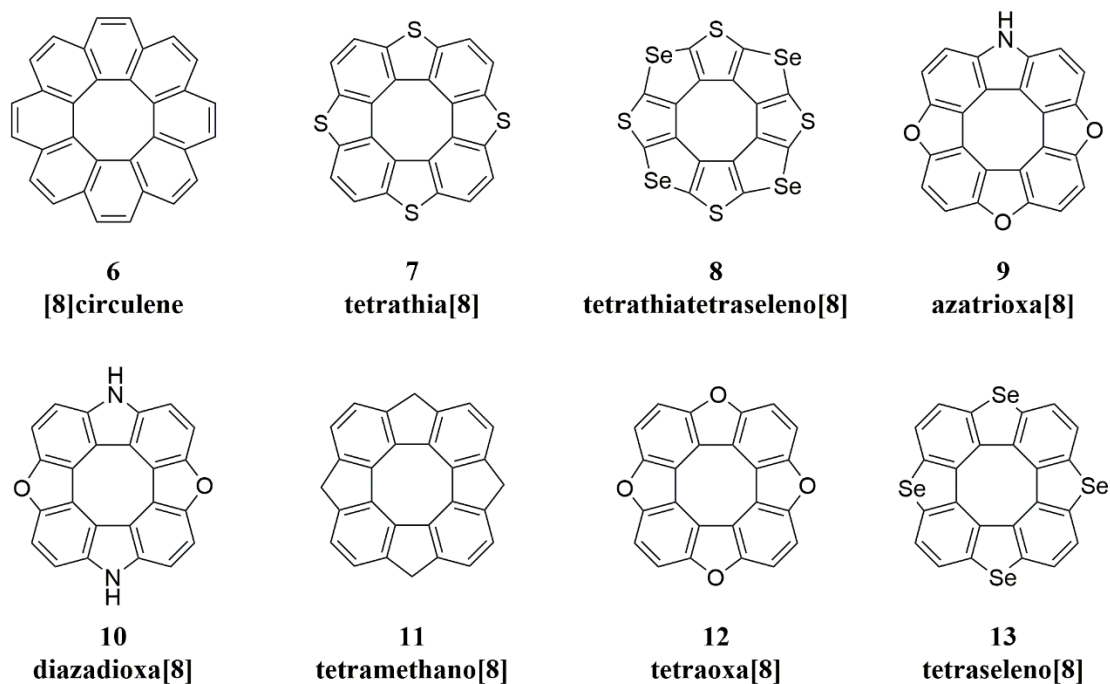


**Figure 12.** The core structure of synthesized hetero[8]circulenes without their substituents.

The *circulene* suffix is omitted for clarity.

In 2015, Wong *et al.*<sup>71</sup> published a paper explaining the synthesis of tetrathio[8]circulene **7** and tetraseleno[8]circulene **13**, showing antiaromatic properties based on NICS values. The studies on [8]circulene **6**, however, showed aromatic properties regarding its tub-shaped conformation due to  $D_{2d}$  symmetry.<sup>72,73</sup> Tetramethano[8]circulene **11**, synthesized by Helwinkell and Reiff in 1970,<sup>74,75</sup> is another example of planar, antiaromatic [8]circulenes.

Other tetraoxa[8]circulene<sup>76</sup> **12** derivatives and their planar analogues, azatrioxa[8]circulene<sup>77</sup> **9**, diazadioxa[8]circulene<sup>13</sup> **10**, and tetrathiatetraseleno[8]circulene<sup>78</sup> **8** have been synthesized. Computational and experimental analysis on these compounds suggest antiaromatic properties of the central core.<sup>79-80</sup>

Wu *et al.*<sup>5</sup> synthesized a [8]circulene **6** derivative through palladium-catalyzed annulation in a single step (Figure 12a). Meanwhile, Schaefer *et al.*<sup>81</sup> synthesized it by a Diels–Alder reaction and subsequently using palladium-catalyzed cross-coupling (Figure 13b).

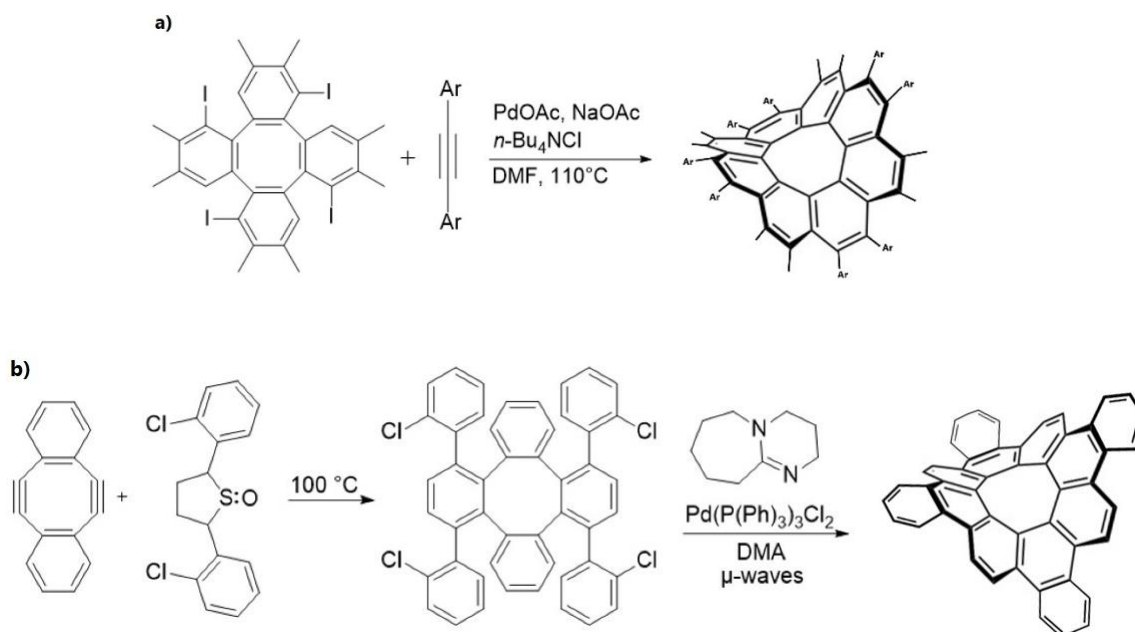


**Figure 13.** Palladium-catalyzed synthetic pathways of [8]circulene derivatives. **a)** Single step cross-coupling reaction using palladium as a catalyst. **b)** Diels-Alder reaction using palladium as catalyst combines the two starting compounds and palladium assists in closing the intermediate compound. Adapted from Ref.<sup>5</sup> with permission from John Wiley and Sons publication. Copyright © 2013 WILEY-VCH Verlag GmbH & Co. KGaA, Weinheim.

### 3.1.2 Modelling circulenes

Dopper and Wynberg<sup>82</sup> proposed a method to analyze the geometries of the circulenes by a mathematical method using the inner radius ( $r_1$ ), outer radius ( $r_2$ ), and the length of the spokes connecting the central ring to the outer edge ( $a$ ) of the circulene. These variables are schematically depicted for both planar and non-planar compounds (Figure 14). However, the method exhibits limited functions when studying saddle-shaped circulenes.

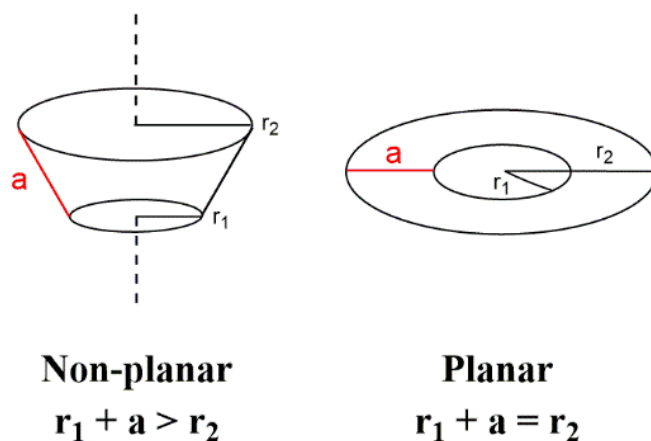


**Figure 14.** The structural differences between planarity (right) and non-planarity (left). One can assume the circles to have fixed diameters  $r_1$  and  $r_2$  where  $r_1 < r_2$ ; a line with length  $a$  connects the two circles. Therefore, the optimal geometry can be determined by the factors depicted in the figure. Adapted from Ref.<sup>82</sup> with permission from the publisher. Copyright © 1975, American Chemical Society.

To solve this issue, Pittelkow *et al.*<sup>14</sup> proposed an alternative model to determine the geometry of the circulene compounds. This model is somewhat inspired by Högberg's<sup>83</sup> work, and it is based on the summation of the wedge angles of the aromatic moieties of the compound (Figure 15). The wedge angles of heterocyclic moieties affect the geometry of the hetero[8]circulenes. Different heteroatoms create different bond angles in the ring depicted by an arc in the angle (Figure 15). Therefore, they shape into different geometries, which affect the planarity level of the compound. It has been found that the sum of wedge angles  $\Sigma \angle$  in planar circulenes is around  $360^\circ$ . From this value, one can estimate the geometry of the circulene, values less than  $360^\circ$  form bowl-shaped structures and values above  $360^\circ$  form a saddle-shaped structure. The angles are determined based on DFT calculations.<sup>84</sup>



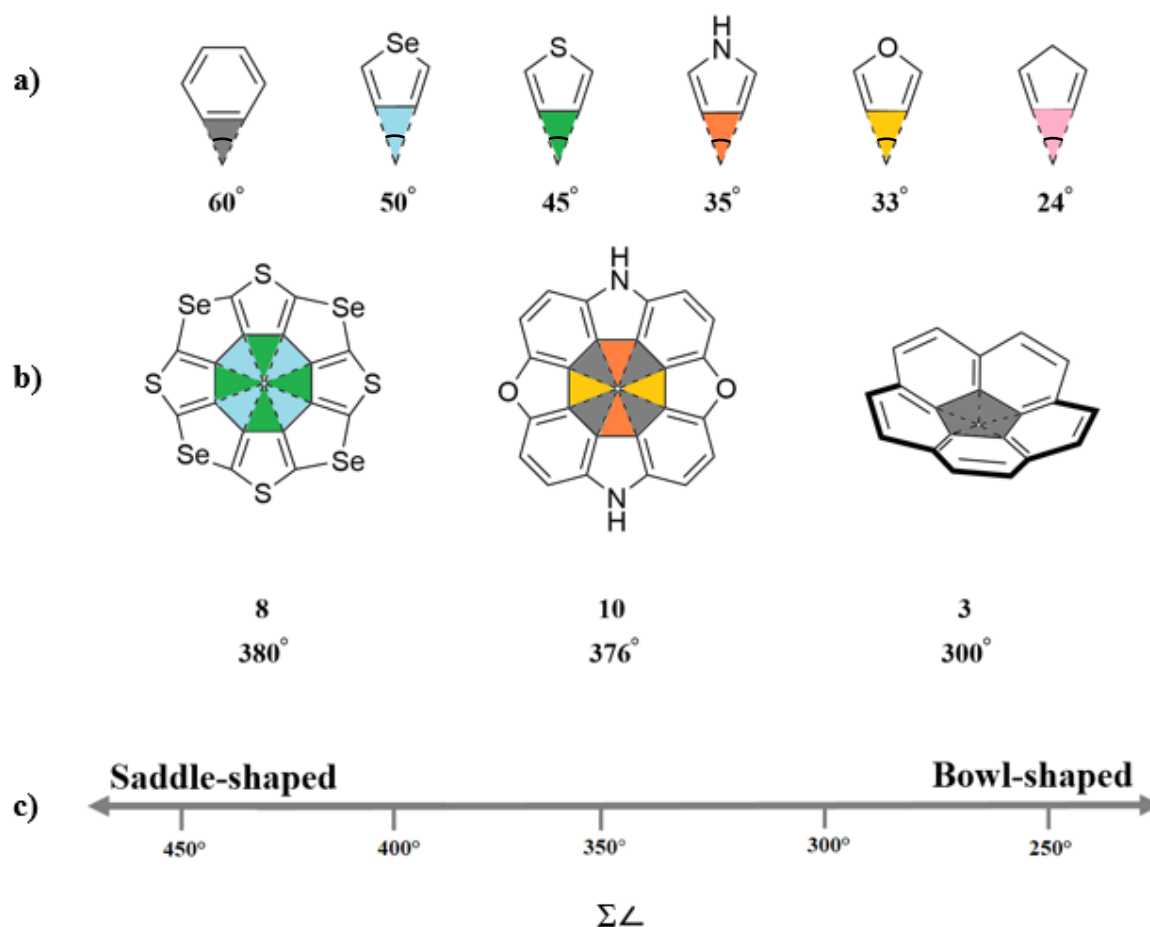


**Figure 15.** A computational model depicting the estimated geometry of different circulenes based on their heterocyclic moieties. **a)** Common aromatic rings, including cyclopentadiene and their wedge angles. **b)** A variety of circulenes and their geometries. **c)** A spectrum of  $\Sigma\angle$  with known circulenes showing their geometries. Adapted from Ref.<sup>14</sup> with permission from Georg Thieme

Verlag KG publication, from Copyright © 2016 Georg Thieme Verlag Stuttgart · New York.

### 3.1.3 Benzotetraoxa[8]circulene

The history of benzotetraoxa[8]circulene dates back to 1881 when Knapp and Schultz,<sup>7</sup> as well as Liebermann,<sup>85</sup> inadvertently synthesized an insoluble compound while reacting 1,4-naphthoquinones under acidic conditions. Later in 1933, Erdtman's<sup>76,86</sup> studies on quinones led to isolated products, which turned out to be tetraoxa[8]circulenes. The condensation of 2-methyl-1,4-benzoquinone could result in three possible structures (Figure 16). The product **14** has two furanic and two phenolic oxygen atoms. The trimeric structure **15** was later observed

to be unfeasible because of the high strain of the structure. Finally, in 1968 the tetrameric structure **16** was proposed based on the mass spectrometry results.<sup>8</sup>

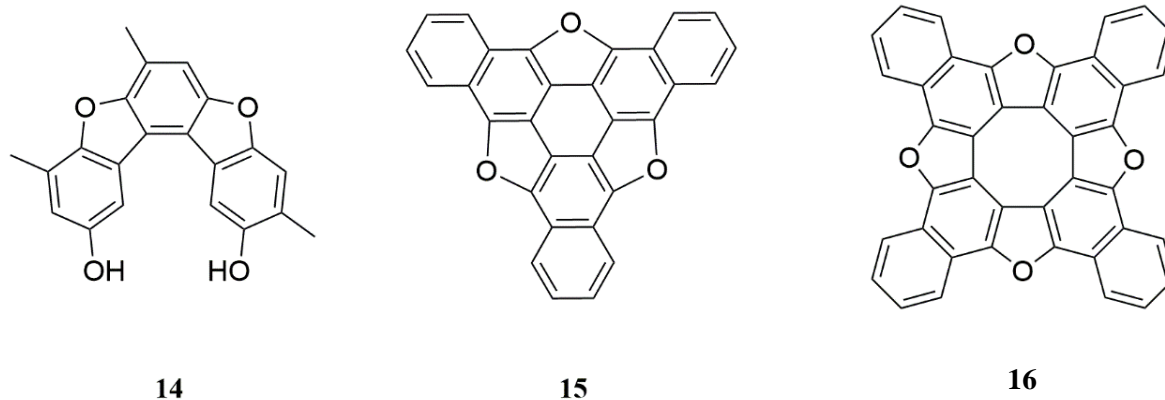


**Figure 16.** Proposed structures from Erdtman's work<sup>86</sup> on naphthoquinones. The product observed from the condensation of 2-methyl-1,4-benzoquinone **14**, proposed trimeric structure **15**, which was later established unlikely to happen. The correct structure of benzotetraoxa[8]circulene **16** produced by a condensation reaction of 1,4-naphthoquinone.

Synthesis of hetero[8]circulenes can take place in different ways. Erdtman and Högberg<sup>87,88</sup> reported a stepwise synthetic approach to tetraoxa[8]circulene. They suggested two different possibilities towards the formation of circulenes: sequential condensation of quinones and dimerization of two molecules (Figure 17).

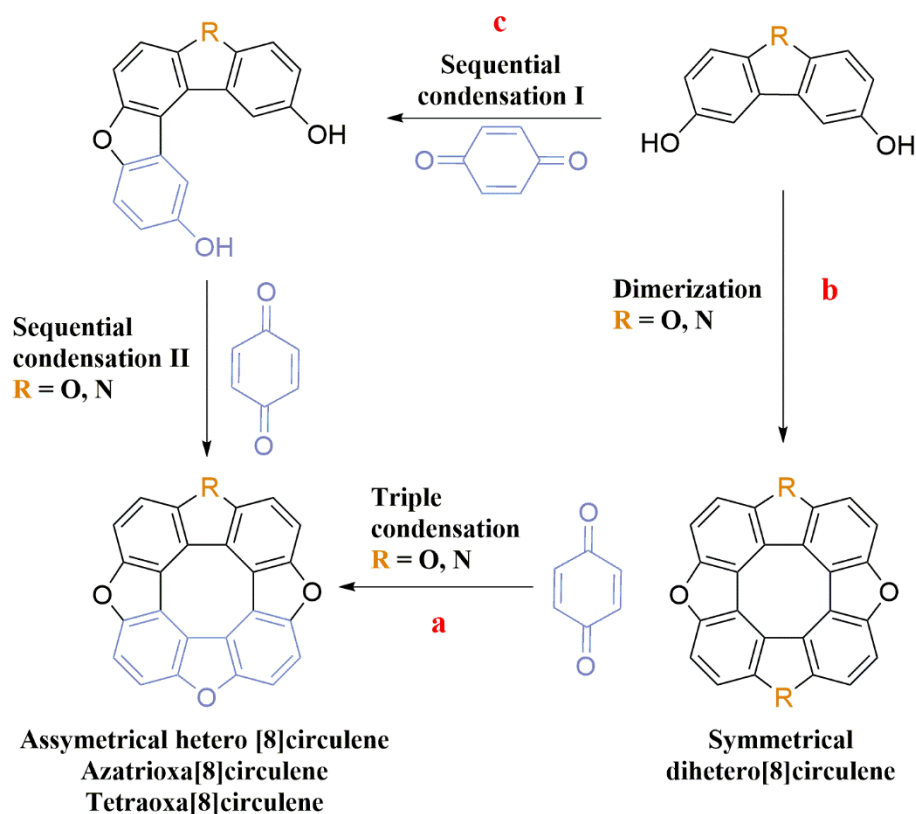


**Figure 17.** Different approaches to the synthesis of [8]circulenes. **a)** Triple condensation of 1,4-naphthoquinone, resulting in an asymmetrical hetero[8]circulene depending on the type of quinone used in the reaction. **b)** Dimerization of dihydroxydibenzofuran leads to a symmetrical hetero[8]circulene. **c)** A sequential condensation approach suggested by Erdtman<sup>87</sup>, where the trimeric product **17** as an intermediate was isolable.

Following these achievements, Högberg<sup>89</sup> noticed an increase in the yields following the addition of 2,8-dihydroxy-dibenzofuran in the reaction while oligomerizing  $p$ -benzoquinone. This indicates that 2,8-dihydroxy-dibenzofuran is an important intermediate in the formation of circulenes. Erdtman's and Högberg's<sup>90,91</sup> collaboration resulted in more achievements in 1977 when they obtained crystal structures of dihydroxydibenzofuran confirming the formation of circulenes.

In 2010, Pittelkow and Christensen<sup>12</sup> produced a series of tetraoxa[8]circulenes via condensation of 1,4-naphthoquinone and 2,3-undecyl-1,4-benzoquinone (Figure 18). This class of compounds show applicability in organic light-emitting diodes (OLEDs) due to their ability to emit blue light. The reason for this phenomenon is a smaller HOMO-LUMO gap compared with other planarized COT systems due to localization of double bonds in the antiaromatic core,

which is the result of the large  $\pi$ -electron system in these compounds. Alteration in the HOMO-LUMO gap will result in a series of consequences, such as a change in optical properties, which will lead to changes in electronic properties, and affects the absorption and emission spectra. These changing features are of interest in manufacturing organic semiconductors to produce OLEDs.<sup>55</sup>

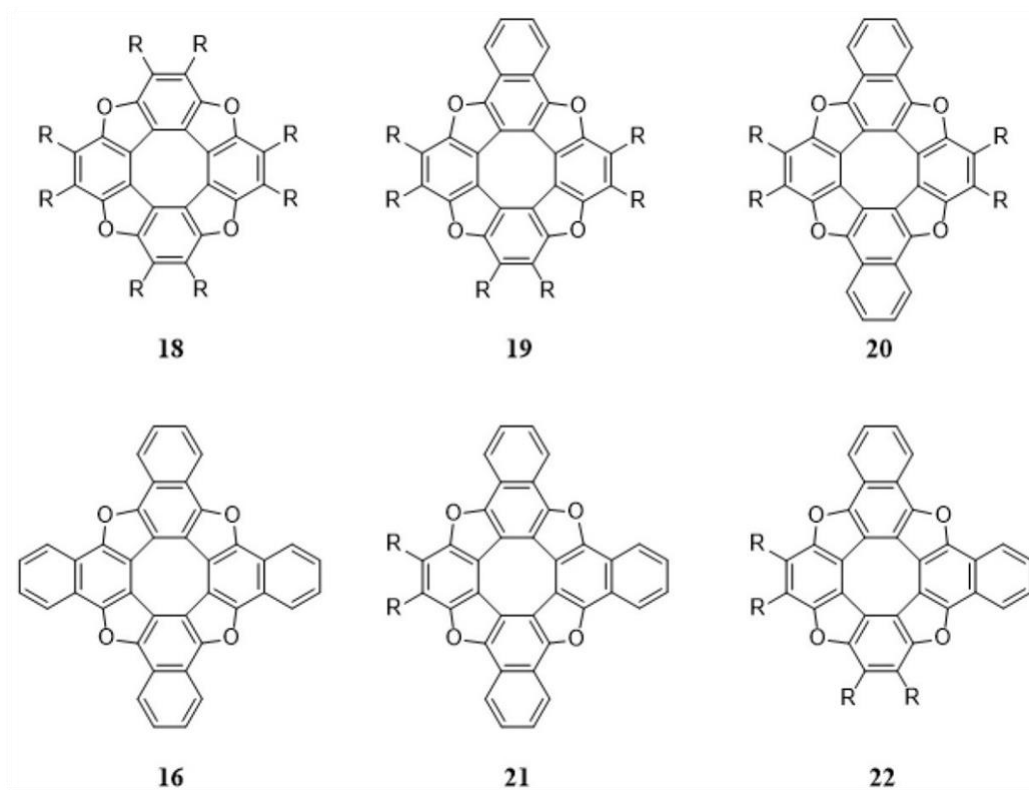


**Figure 18.** Different regioisomers isolated by Pittelkow's group from the condensation reaction of 1,4-naphthoquinone and 2,3-undecyl-1,4-benzoquinone ( $R = C_{11}H_{23}$ ). Adapted from Ref.<sup>90</sup> with the permission of Chemistry - A European Journal publication. Copyright © 2010 WILEY-VCH Verlag GmbH & Co. KGaA, Weinheim.

In 2013, Pittelkow and his group<sup>13</sup> used an oxidative coupling approach to synthesize diazadioxa[8]circulene, where two dihydroxydibenzofuran molecules are coupled together in two steps. The reason why dihydroxydibenzofuran was chosen refers to its importance as an intermediate in this reaction (Figure 19). The first step produces the COT core, and the following step forms the peripheral furan **24** rings with the help of a Lewis acid. What makes this approach preferable over the two other methods depicted in Figures 12 and 16 is the

elimination of side products, which raises the yield up to 75%. The final products **24** (R = benzyl, propyl) were crystallized and observed to be almost completely planar.

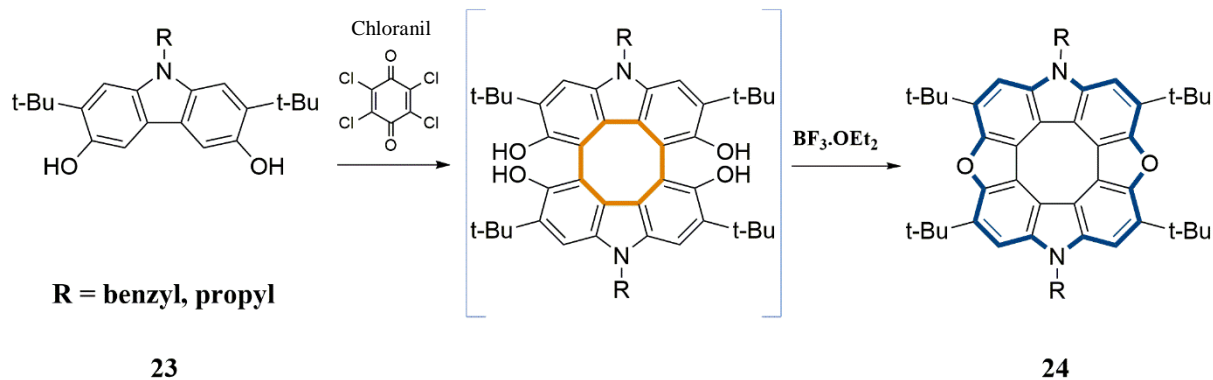


**Figure 19.** Oxidative dimerization pathway of 2,7-di-tert-butyl-3,6-dihydroxycarbazole **23** forming diazadioxa[8]circulene **24**. Chloranil in step 1 is necessary for this reaction to form the intermediate molecule for the formation of C-C bonds.

### 3.2 Other works regarding hetero[n]circulenes

Osuka and co-workers<sup>69</sup> introduced a different synthetic pathway for producing a tetrabenzatetraaza[8]circulene **28** in 2015 (Figure 20). This compound is the central moiety of a porphyrin sheet **29** (Figure 20), which was made to study antiaromaticity of the porphyrin sheets.<sup>79,92,93</sup> Porphyrins are important macrocyclic systems presenting excellent coordination chemistry. The system contains various metal ions, which are used in ligating organic molecules. This characteristic rises from the  $18\pi$ -conjugated electronic network in a square planar sheet, which causes a strong diatropic ring current beneficial in the field of host-guest chemistry. The central metal of porphyrin can be used for recognition of guest molecules.<sup>79</sup>

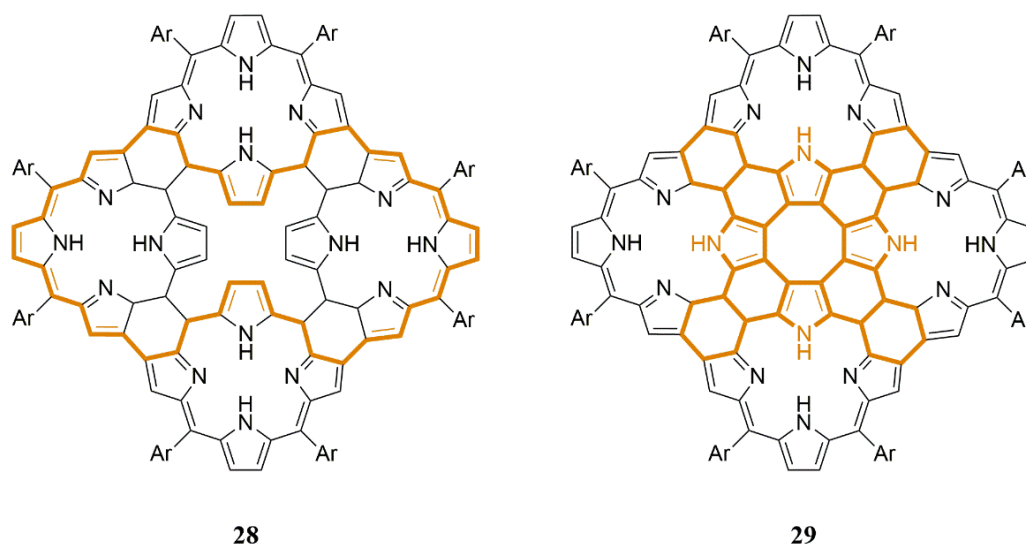


**Figure 20.** Transformation of a meso-meso-linked 5,10-porphyrin cyclic tetramer **28** by oxidative fusion reaction to synthesize porphyrin sheet **29** bearing a COT core by fold-in approach.

In the synthesis of tetrabenzotetraaza[8]circulene **27**, 1,2-di(pyrrol-2-yl)benzene **25** was brominated to obtain a dibromide.<sup>94,95</sup> A consequent coupling with 1,2-di(pinacolatoboryl)benzene resulted in 2-phenylene-bridged cyclic tetrapyrrole with 11% yield.<sup>96,97</sup> This tetrapyrrolic compound is non-aromatic according to its UV-Vis results and <sup>1</sup>H NMR analysis. The “fold-in” approach marked by arrows in Figure 21 on a tetrapyrrolic precursor **26** was applied to synthesize the central tetrabenzotetraaza[8]circulene **27** COT core, which is exhibiting antiaromatic properties on its central COT core. X-ray diffraction analysis on compound **27** depicted a planar square structure. Hetero[8]circulenes containing heteroatoms have attracted much attention due to their enforced planarity, the  $8\pi$  system and their potential application in OLEDs.<sup>69</sup> Tetrabenzotetraaza[8]circulene **27** could also pave the way to study the role of different segments in porphyrin sheet **29**.

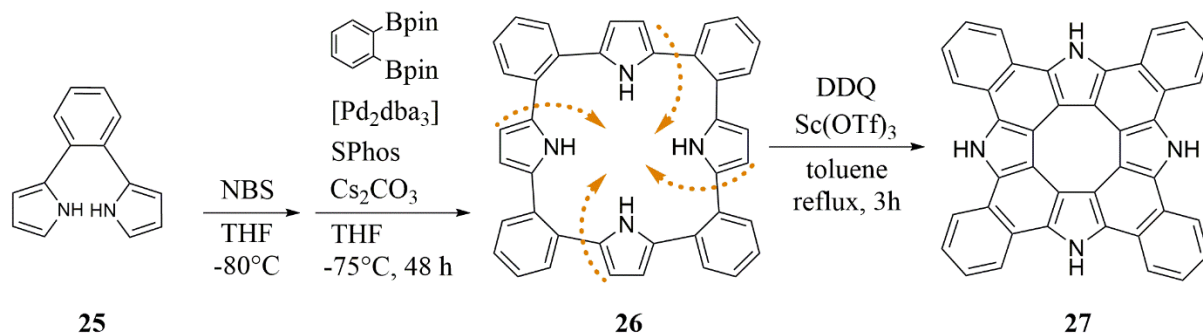


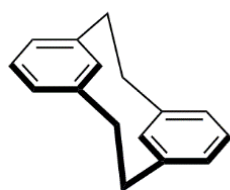
**Figure 21:** Synthesis of tetrabenzatetraaza[8]circulene **27**. Bpin: 4,4,5,5-tetramethyl-1,3,2-dioxaborolan-2-yl, dba: dibenzylideneacetone, NBS: *N*-bromosuccinimide. DDQ: 2,3-dichloro-5,6-dicyano-1,4-benzoquinone, Tf: trifluoromethanesulfonyl.

## 4 CYCLOPHANES AND RELATED SYSTEMS

### 4.1 Cyclophanes

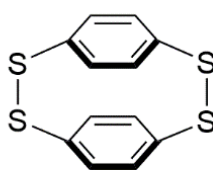
Another class of compounds used in this work is cyclophanes, which consist of benzene rings connected with a chain. A cavity is typically formed within the chain. Cyclophanes have been an interesting topic to study for decades due to their versatile facades and applications.<sup>98</sup>

Synthesis of cyclophanes dates back to Pellegrin's<sup>99</sup> work in 1899 as well as Parekh and Guha's<sup>100</sup> work in 1934. The cyclophane chemistry became more popular, however, by Brown and Farthing's<sup>101</sup> isolation of a [2.2]paracyclophane in 1949 and Cram's<sup>102</sup> subsequent synthesis of this compound in 1951 (Figure 22).



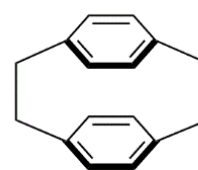
**30**

Pellegrin, 1899



**31**

Parekh and Guha, 1934



**32**

Brown and Farthing, 1949  
Cram, 1951

**Figure 22.** Early examples of cyclophanes.

Cyclophanes can be categorized according to which peripheral atoms are connected. Considering that there are six peripheral atoms in a benzene ring, a chain can connect in (1, 2), (1, 3), or (1, 4) positions of the ring creating an intra-ring bridging structure (Figure 23).<sup>103</sup> The chain concept can become more complex depending on the number and type of the systems used as a substrate creating an inter-ring bridging structure (see for example Figure 23d and e), as well as by introducing multiple bridging units connecting the peripheral atoms in the system. Anthracene and naphthalene (Figure 23) are simple examples of a more complex system compared to benzene. Anthracene contains ten peripheral atoms, but the quaternary carbons are excluded since their bridging will destroy the aromaticity.



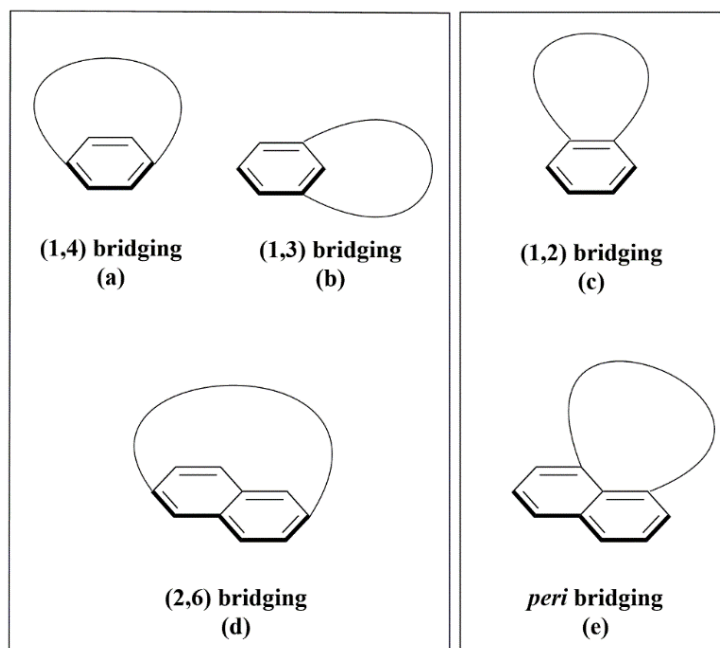


**Figure 23.** Typical cyclophane bridging motifs in benzene and naphthalene (**a**, **b** and **d**), Ring fusion-equivalent bridging motifs (**c** and **e**).

One of the unique applications of cyclophane systems is measuring the proximity of a proton to the ring and consequently measuring the NMR chemical shifts of the proton.<sup>15</sup> Several works towards this application have been done by Boekelheide and co-workers<sup>104</sup> who in 1973 synthesized [2.2]metaparacyclophane **33** and [2.2]metaparacyclophane-1,9-dienes **34** (Figure 24). Further work was performed by Pascal and co-workers<sup>105</sup> who worked with [7]metacyclophane (Figure 24) in 1987 and Vögtle *et al.*<sup>106</sup> in 1993, who synthesized adamantanoparacyclophane **35** (Figure 24). As it is observed in Figure 21, the proton **H** leaning above the benzene ring penetrates deep into the  $\pi$ -electron sphere of the ring resulting in up-field shifting of the  $^1\text{H}$  NMR values.

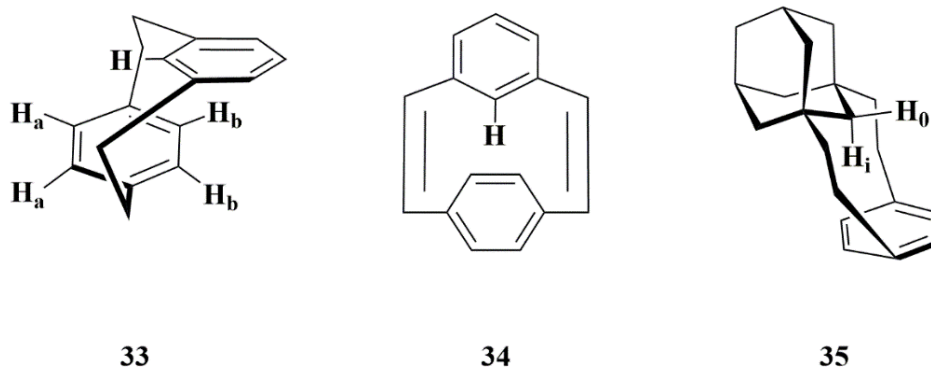


**Figure 24.** Early research on cyclophanes to measure the NMR chemical shift of the proton penetrating the  $\pi$ -electron sphere of the benzene ring. Boekelheide's [2.2]metaparacyclophane **33** and [2.2]metaparacyclophane-1,9-dienes **34**. Vögtle's adamantanoparacyclophane **35**.

An interesting observation on Boekelheide's [2.2]metaparacyclophane **33** and [2.2]metaparacyclophane-1,9-dienes **34** was that compound **33** needs to go through a transition state to pursue a conformational flipping of the meta-substituted benzene ring into the para-bridge.<sup>105</sup> This is due to the outweighing conformation effect of the  $sp^3$  carbon bridges of **33** compared to  $sp^2$  carbon bridges of **34**. Therefore, the effect of the bond angle is opposite to the bond length, and as a result, compound **33** needs a stronger force to afford conformational flipping. This has been confirmed by X-ray crystallography for both compounds. It was observed that the distance of the proton in **33** is 2.71 Å whereas in **34** the distance is only 2.16 Å. Cyclophane **33**, however, showed a higher up-field shift up to 5.24 ppm. It can be concluded that [2.2]metaparacyclophane derivatives are suitable compounds to study the interaction of a functional group to the aromatic  $\pi$ -electron cloud.

Furthermore, when comparing adamantane and its highly strained substituted derivative **35**, it was proven that the up-field shifted NMR signals are due to H<sub>i</sub> deeply forced into the  $\pi$  cloud of the benzene ring. The  $^1\text{H}$  NMR signal is highly shifted to -4.08 ppm at -65°C, while H<sub>0</sub> is less shielded at -1.01 ppm. H<sub>i</sub> has a distance of 1.84 Å to the centre of the ring. The bulky group in the adamantane derivative has forced the proton to orient towards the centre of the ring.<sup>106,107</sup>

Pascal and co-workers<sup>108,109</sup> were interested in synthesizing triple substituted benzene ring. The first synthesized compound **36** showed a short distance between the hydrogen and the ring without having a chemical bond (Figure 25).<sup>110</sup> Furthermore, they attempted to move the methine proton closer to the centre of the ring by removing the sulphones from compound **37**, resulting in the ring contraction of **38**. Calculations show that the proton should be 1.78 Å above the ring and resonance at -4.03 ppm was much higher, compared to compound **36**, which had a chemical shift of -1.68 ppm.

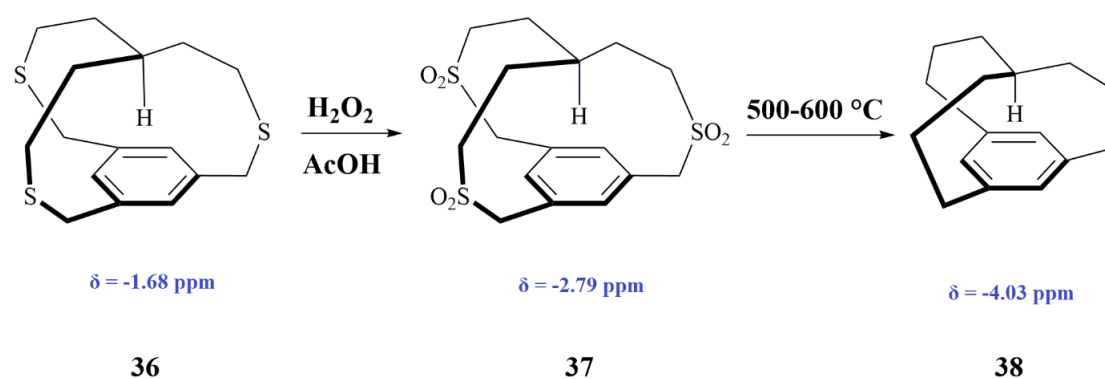
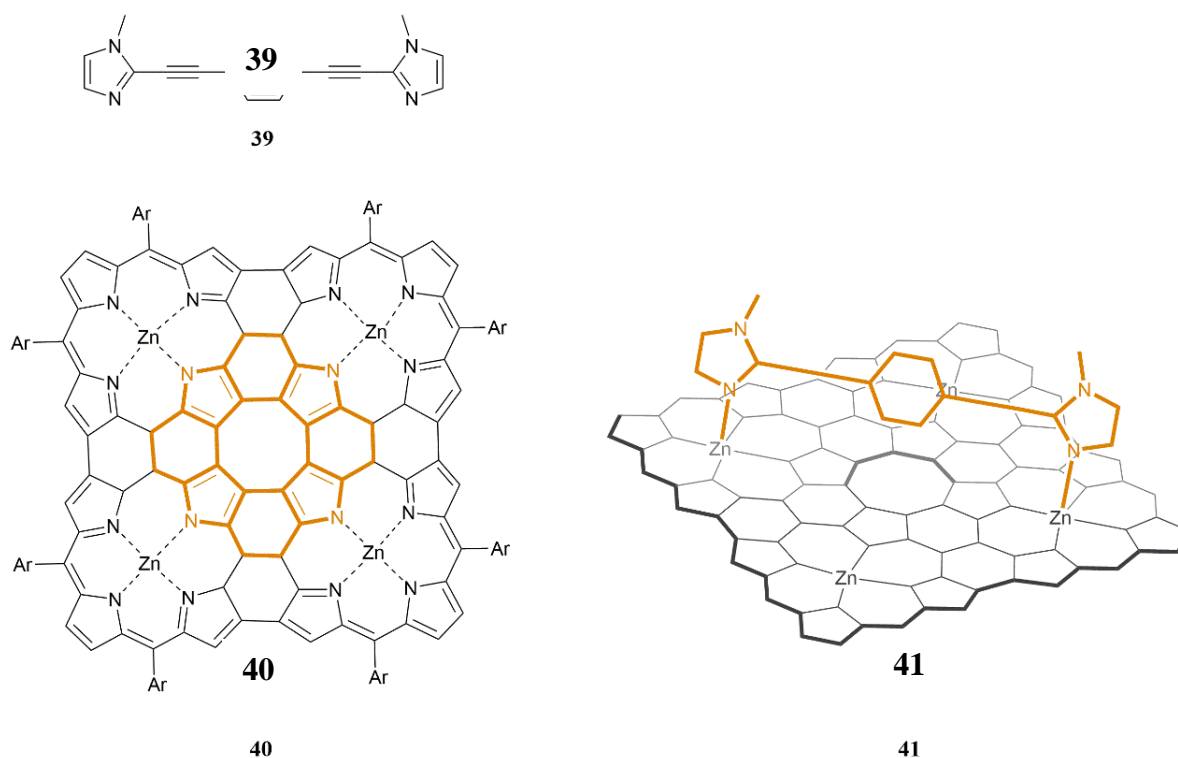


**Figure 25.** Pascal's macrocycles and projection of aliphatic hydrogen towards the center of the benzene ring. Adapted from Ref.<sup>110</sup> with permission from Copyright © 1987, American Chemical Society.

## 4.2 Planar cyclooctatetraene systems

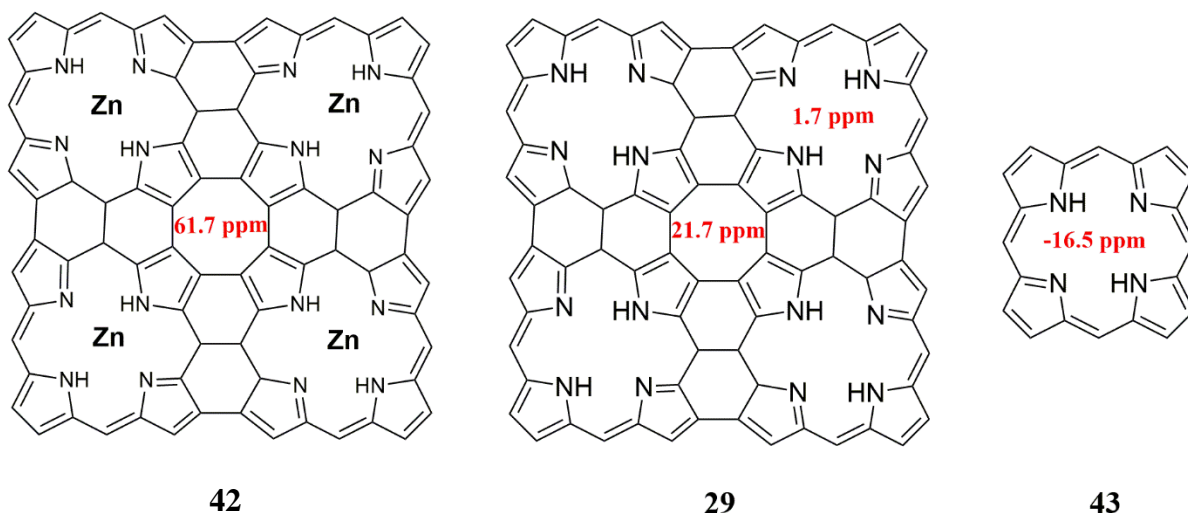
So far, it has been observed that antiaromatic compounds tend to form a non-planar conformation to avoid antiaromaticity. Therefore, studying antiaromatic compounds has become a challenge for scientists. Developing synthetic methods for a stable and planar antiaromatic compound has paved a way to analyse the properties of antiaromatic compounds in general.

Figure 26 presents a method by Osuka and co-workers<sup>79</sup> who synthesized a tetra annulated porphyrin sheet **40** having an [8]circulene in its centre. The idea was to coordinate (1,4-bis((1-methyl-1H-imidazol-2-yl)ethynyl)-benzene ligand **39** to zinc centres of the sheet **40** to enable the characterization of the paratropic ring current of the complex system **41**. The imidazoles are indeed diagonally coordinated to two zinc atoms in a 2:1 ratio. The ligand is located above the COT core, and the NICS values showed a significant downfield shift at 3.78 ppm.



**Figure 26.** Osuka's tetrameric porphyrin sheet **40**. 2:1 complexation **41** of the ligand **39** and tetrameric porphyrin sheet (The structure is simplified for clarity). Adapted with permission from Ref.<sup>79</sup> Copyright © 2006, American Chemical Society.

The structures of a zinc(II) porphyrin tetrameric sheet **42**, a porphyrin sheet without zinc(II) **29**, and a porphine **43** with calculated NICS values are shown in Figure 27. The NICS results indicated that the zinc complex showed stronger paratropic effects than the two other compounds. This suggests that the COT core is strongly antiaromatic and the paratropic ring current is affecting the  $18\pi$  aromatic systems surrounding the central core by weakening the aromatic values.



**Figure 27.** NICS(0) values (in ppm, shown in red) calculated on porphine **43** and its derivatives. The structures are simplified for clarity.<sup>79</sup>

Nishinaga *et al.*<sup>111</sup> synthesized compound **44** with a planar COT core which contained protons directly attached to the central core (Figure 28). Experimental and theoretical results confirmed the antiaromatic properties of the COT core. In addition to antiaromaticity, the synthesized molecule also showed narrow HOMO-LUMO gap, which can potentially be used in semiconductive materials.<sup>112</sup> <sup>1</sup>H NMR chemical shift for H<sub>a</sub> and H<sub>b</sub> protons were calculated to be 4.22 ppm and 4.00 ppm respectively, confirming the presence of a paratropic ring current in the core. Both protons showed slightly more up-field chemical shifts in the experimental data (4.71 and 4.41 ppm, respectively) depicting that H<sub>b</sub> protons are less affected by the ring current of the annulated thiophene ring.

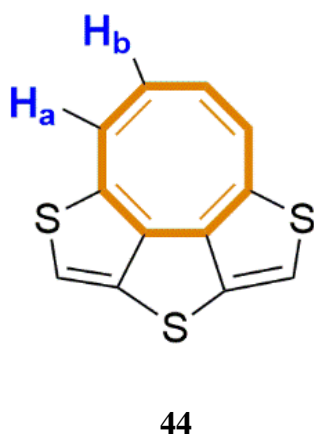


**Figure 28.** Structure of compound **44** and the position of the olefinic protons directly attached to the core. Adapted with permission from Ref.<sup>104</sup> Copyright © 2013, American Chemical Society.

### 4.3 Circulenophanes

By combining cyclophane and circulene chemistry, a new class of compounds called circulenophanes were designed by spanning hydrocarbon bridges over the circulene plane. Planarized annulated COT molecule can have a linker type bridge covalently bonded to its reactive centers, the pyrrole moieties (Figure 29).<sup>122</sup> As previously mentioned, this allows assessing the effect of the induced ring current of the core on the protons of the bridge to study antiaromaticity.

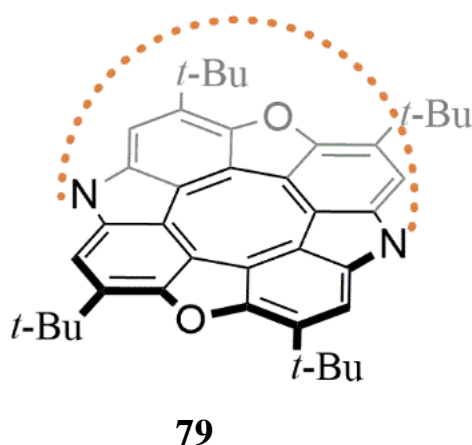


**Figure 29.** Planarized COT with a potential linker coupled to the pyrrole moieties.<sup>122</sup>

Several attempts were made regarding the formation of a circulenophane either by introducing a covalently bonded linker through the pyrrole moieties or by linking the linkers in advance to the dihydroxycarbazole **49** units and then perform the cyclization reaction.<sup>122,123</sup> The first attempts for synthesizing a circulenophane were made by reacting diazadioxo[8]circulene **10** with ortho-anilinyll groups in copper catalysed reaction conditions. This attempt resulted in obtaining *cis*- and *trans*-isomers. The same conditions were implemented on *ortho*-iodo-nitrobenzene groups with compound **10**. Both isomers were isolated, the *trans*-isomer **80** in 40 % and *cis*-isomer **81** in 12% yields and reduced to anilines directly. The *cis*-isomer **81** had two reactive centers on the aniline moieties, both facing each other above the circulene plane (Figure 30).

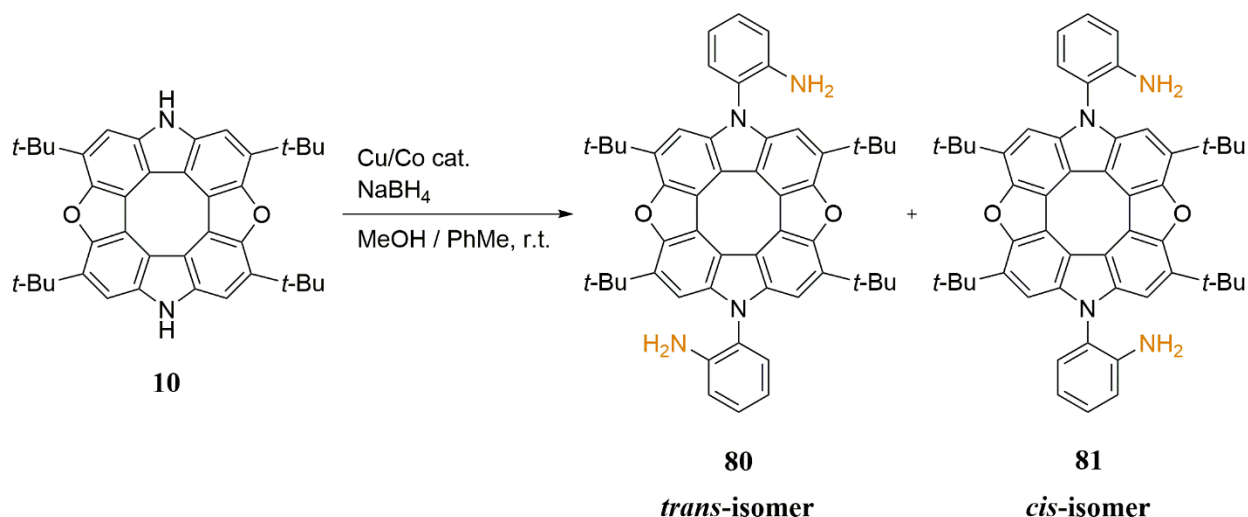


**Figure 30.** *Cis*- and *trans*-isomers of aniline containing substrate.<sup>122</sup>

Different reaction conditions and linker chains for the formation of a circulenophane were tried, however, they repeatedly failed (Figure 31). It was expected the *cis*-isomer **81** to form a circulenophane since the reactive centers are close to each other and it could favour intramolecular reaction. However, the attempts to introduce a linker in between the aniline moieties remained unsuccessful. In the approach I, different aliphatic chains were used in three different conditions, a, b and c. The reaction did not result in circulenophane **82**. In approach II, different reagents were used to couple the aniline groups, but the results suggested that the high reactivity of the acyl chloride groups did not allow the formation of the expected molecule **83**.

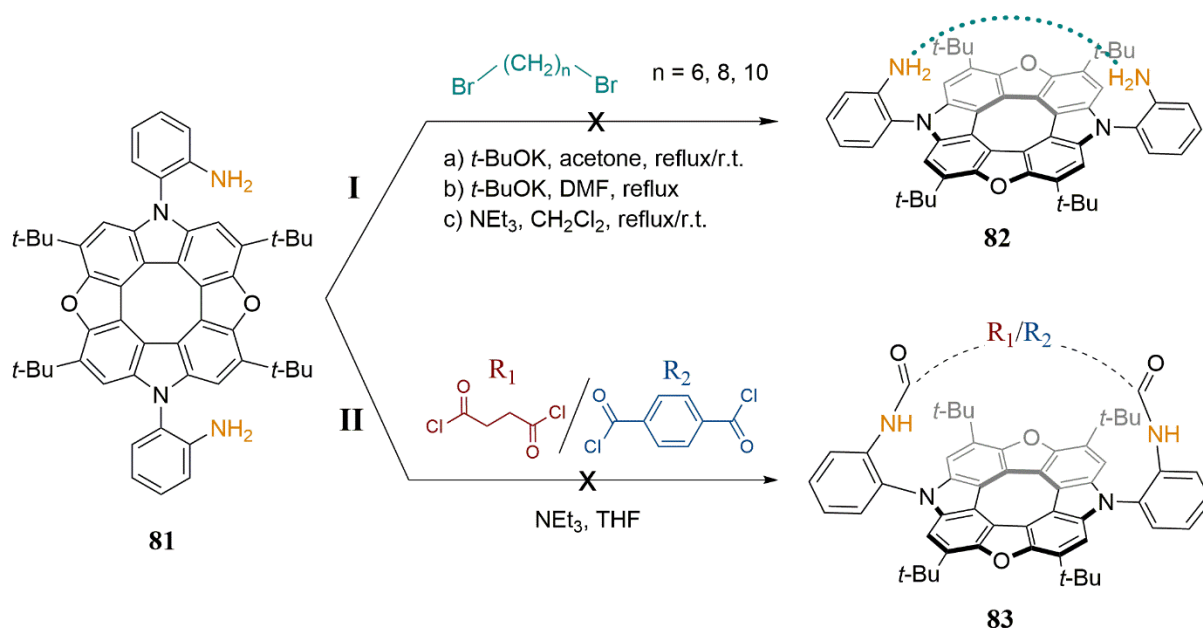


**Figure 31.** The *cis*-isomer underwent different reaction conditions.<sup>14</sup>

### 4.3.1 Forming a macrocycle

Formation of a circulenophane can be related to a macrocycle since it resembles the characteristics of a macrocycle. Macrocycles are molecules containing one or more rings with at least eight atoms. The formation of macrocycles depends on fundamental factors, of which the ring size is the primary factor to consider as it affects the ring's strain.<sup>113</sup> There are three types of strains associated with the planar cyclic conformations, which are easier to depict with the help of small rings.<sup>114</sup>

3- and 4- membered rings possess the highest ring strain associated with the first type of ring strain. Formation of these two rings is fast due to the proximity of the two ends. In heterocyclic systems, the formation of 5-membered rings are mostly fast, and the rings are affected by the second type of ring strain. 6-membered rings show almost no ring strain, and they are formed slower up to moderate rates. 7- and higher membered rings are formed slower due to the decrease in the proximity of the loose ends. These rings also depict the third type of rings strain, mostly because of the proximity of the hydrogen atoms in space. As macrocycles show less ring strain compared to smaller rings, they possess a higher number of degrees of freedom, and therefore they will adopt more conformations.

In 3- and 4-membered rings, high angle strain, called Baeyer strain or angular strain, is observed due to the competition between a tetrahedral configuration and the rigidity of the structure.<sup>115</sup> This type of strain arises from the distortion of the bond angles from the ideal tetrahedral conformation of the C-C bonds. A good example is cyclopropane ( $C_3H_6$ ), in which the C-C-C optimal bond angle would be  $109.5^\circ$  for an  $sp^3$  hybridized carbon atom according to the degree of hybridization, but instead, it is  $60^\circ$ . This leads to higher bending of the bonds between the carbon atoms and a change in the conformational structure (Figure 32a). There is a direct relation between the degree of distortion and the strain energy.<sup>116</sup>



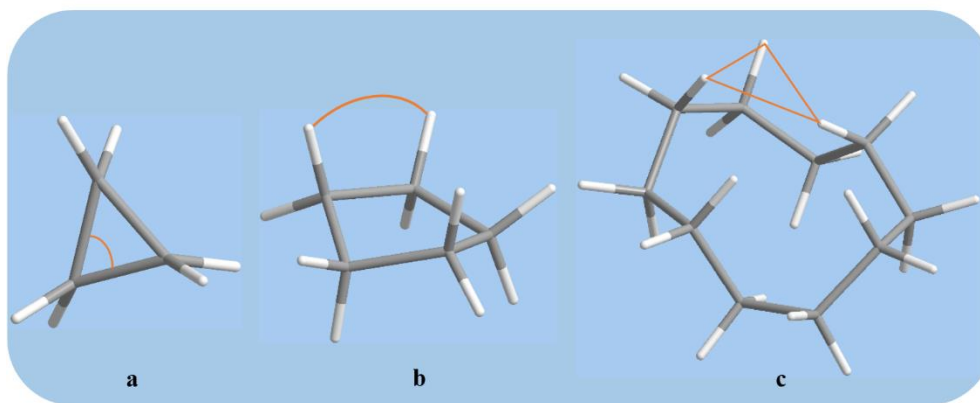


**Figure 32.** Different strain types: **a)** angle strain in cyclopropane, **b)** torsional strain in cyclopentane, and **c)** transannular strain between non-bonded atoms in cyclodecane.

5-membered rings, such as cyclopentane, experience strain by the vicinal hydrogen atoms known as torsional strain, or Pitzer strain (Figure 32b).<sup>117</sup> This type of strain is seen in atoms being separated over three covalent bonds, such as in eclipsed conformation, which brings the atoms into proximity of each other. This conformational change suppresses the transannular interactions between atoms and makes the conformation in any planar cyclic alkane unstable and with higher energy.

7- and more membered rings depict transannular interactions known as Prelog strain, which arises from the interaction between the non-bonded atoms in a cyclic system (Figure 32c).<sup>118</sup> This occurs when the atoms at non-adjacent locations can affect each other due to their proximity and repulsive interactions. Transannular strain plays a crucial role in the regioselectivity, thermodynamics and kinetics of synthesizing cyclic compounds.

The conformational restriction for ring closure in large macrocycles is a challenge. It has been observed that by dilution of the reaction mixture to  $10^{-3}$  M or less the reaction favours intramolecular cyclization. This phenomenon is known as the Ziegler and Ruggli dilution principle.<sup>119</sup> The diluted solution prevents the molecule from going through an intermolecular coupling and favours intramolecular ring closure.<sup>120</sup> It was observed that adding the reagents slowly, rather than consuming a high volume of solvent, using low temperatures, and having pre-organised compounds as the linker, could be used for the synthesis of the desired circulenophane.<sup>121</sup>

## 4.4 Bridge-type linkers

Different types of pre-organized hydrocarbon linkers **88**, including different lengths and building blocks, were synthesized in Pittelkow's group.<sup>122</sup> In the case of an aliphatic hydrocarbon chain, in between two *meta*-substituted halide moieties, the attempt to attach both ends to the circulene *via* the Ullmann coupling remained unsuccessful. The reason could be the variety of conformations around the aliphatic chain of the linker, making it hard to couple the halide moieties to the pyrrolic nitrogen atoms in the desired conformation.<sup>122</sup> Thus, the synthesis plan was changed, and the halide moieties were placed at the *ortho* positions, which led to a successful coupling (Figure 33). Different aliphatic chain lengths were tried to identify the optimum length for the linker.<sup>122</sup> A chain containing nine carbon atoms appeared to be the right length compared to chains containing eight or ten carbon atoms, which showed strain or required to have the right conformation before coupling, respectively.

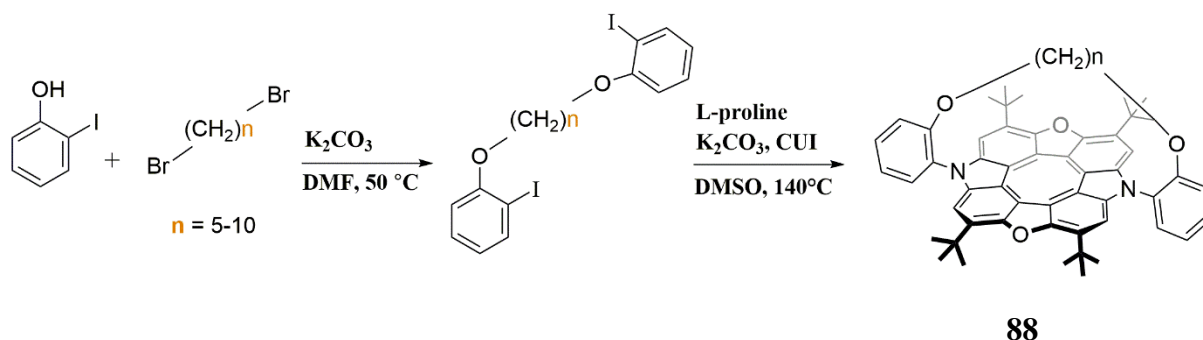
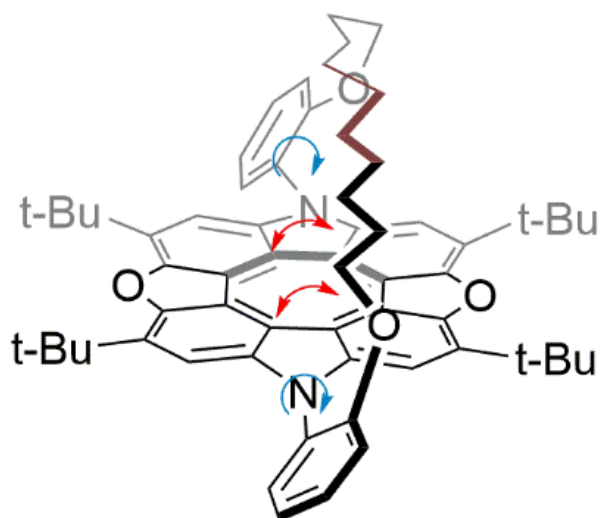


**Figure 33.** Synthesis of a variety of aliphatic chains for spanning over the circulene plane.<sup>122</sup>

The synthesized hydrocarbon chain, however, did not show an upfield shift of the protons according to the NMR results. The reason could be that a) there was no paratropic ring current in the molecule, b) the high distance of the methylene protons from the centre of the circulene, c) the linker flipped in between different conformations and did not stay above the ring (Figure 34), or d) the hydrogen atoms on the chain were pointing outward; thus they were not to the proximity of the centre of the COT core.<sup>122</sup> The system with a 10 carbon atom chain **63** is shown in Figure 34.



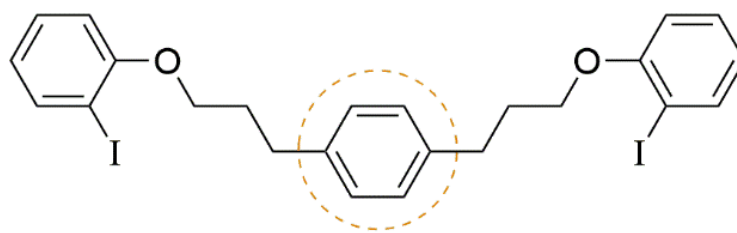
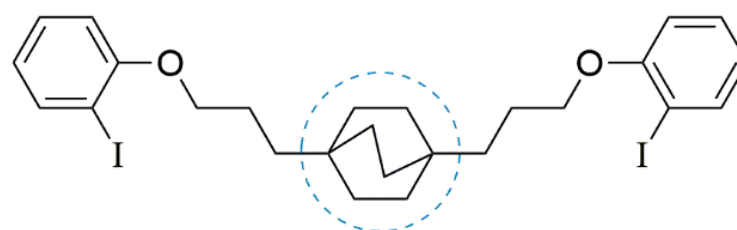
63

**Figure 34.** It is suggested that the linker is flipping into different conformations preventing the methylene protons from remaining above the COT core.<sup>123</sup>

Functionalized linker **50** containing a phenylene group in the middle was synthesized (Figure 35).<sup>123</sup> However, the results suggested that the structure was not rigid enough. The crystal structure and NMR results suggested that the linker had the same problems depicted in Figure 34; flipping into different conformations and rotating around the linker's axis.

The results also suggested that the linker tilts into aromatic and antiaromatic regions. Relatively small upfield shifts suggest that the bridge spent more time swapping in between the aromatic and antiaromatic region and did not stay in one state. This observation was noted upon cooling experiments. Further upfield shifts were observed in addition to the broadening peaks, which was a sign of having different conformations.

Moreover, the protons were not pointing to the center or were too far from the core. This supported the idea that the phenylene group was not bulky enough to restrict the movement. Thus, a new approach towards a bulkier linker **51** was designed. The synthesis was not, however, completed during the time allocated for the project.

**50****51**

**Figure 35.** Linker **50** containing a benzene ring in the middle to point the protons towards the circulene core. Linker **51** containing a bicyclo moiety in the chain for bulkier centre.<sup>123</sup>

**EXPERIMENTAL PART: TOWARDS THE SYNTHESIS OF A  
CIRCULENOPHANE**

## 5 MOTIVATION

Antiaromatic compounds are of high interest due to their instability.<sup>14</sup> However, compounds containing more than six-membered central ring form a saddle-shaped conformation. A planarized cyclooctatetraene (COT) was previously synthesized to study the antiaromatic properties of the COT core in Pittelkow's group.<sup>13</sup>

The purpose of this work was to synthesize a circulenophane **72** with a bridged diazadioxa[8]circulene **10**. This compound would allow proving of the antiaromaticity of the 8-membered central ring of the COT core using NMR. In this approach, the chemical shift of the protons on the central DABCO unit (shown by dotted lines in Figure 36) could be investigated due to their proximity to the center of the circulene ring.

During the summer of 2017, the synthesis of previously reported diazadioxa[8]circulene **10** was repeated.<sup>13</sup> Furthermore, the synthesis of a bridge-type linker containing bicyclo[2.2.2]octane moiety in its centre was initiated. The synthesis, however, was not successful due to the failure in purification and no conversion was observed in step four.

During the summer and autumn of 2018 the synthesis of a new linker **60**, which contained protons that can be covalently bonded to the diazadioxa[8]circulene **10** through the pyrrole nitrogens, was done. However, the attempts for coupling both arms of the linker to the circulene were unsuccessful probably due to steric hindrance.

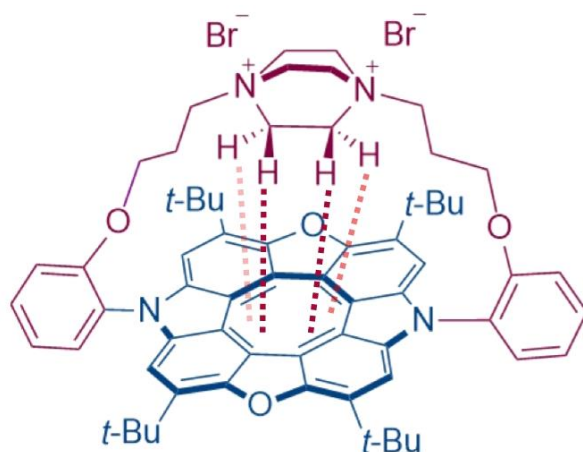


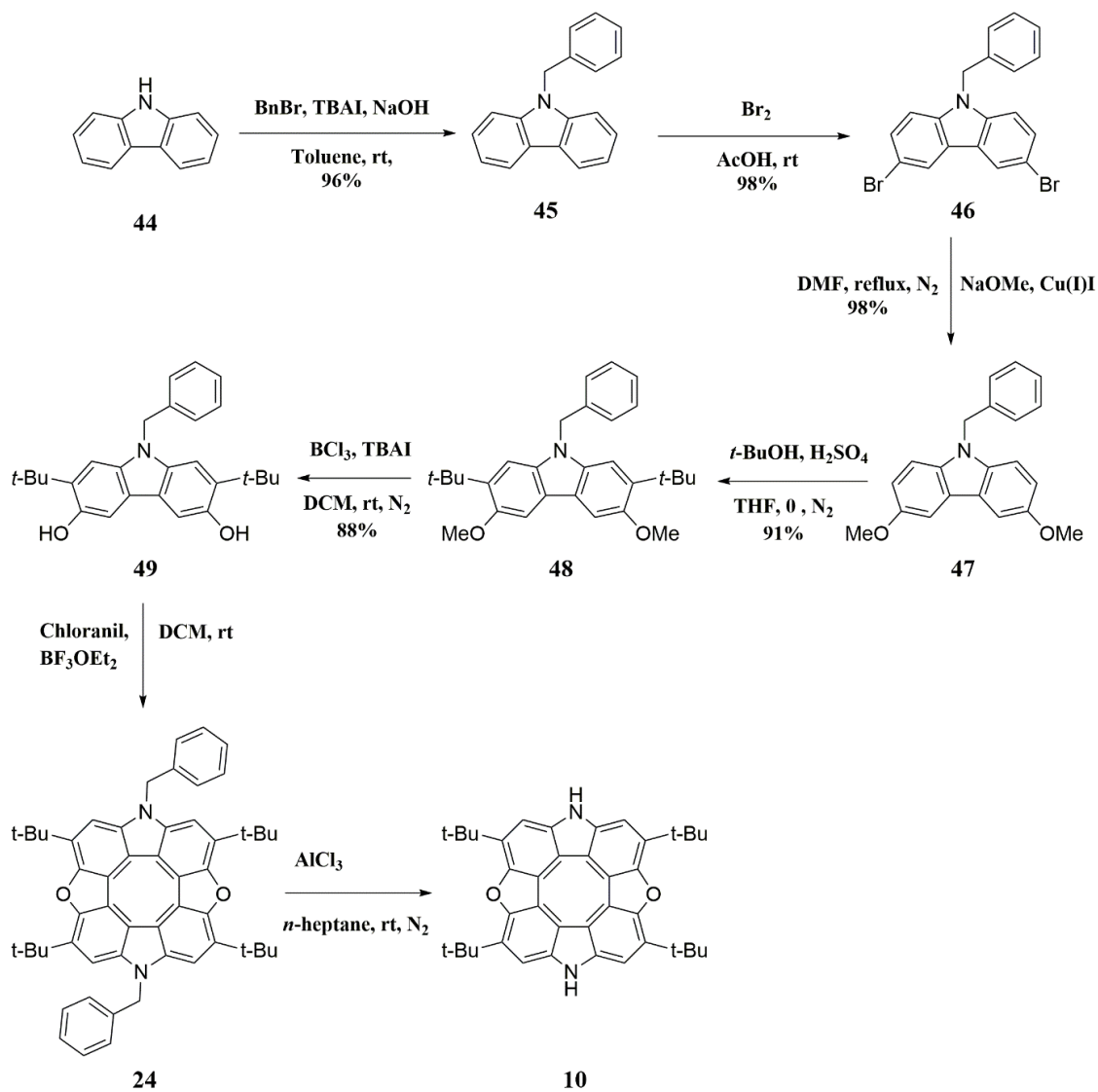
**Figure 36.** An ideal structure of the target circulenophane **72** containing the synthesized linker **60** coupled to diazadioxa[8]circulene **10** for studying the antiaromaticity properties of the central 8-membered ring through measuring the NMR chemical shift of the protons on DABCO.

## 6 SYNTHESIS APPROACH

### 6.1 Synthesis of diazadioxa[8]circulene **10**

The synthesis of diazadioxa[8]circulene **10** was repeated according to the literature by using commercially available 9*H*-carbazole **44** (Figure 37).<sup>13</sup> The synthesis in this project was initiated by using previously synthesized 9-benzyl-3,6-dimethoxy-9*H*-carbazole. For compound **48**, Friedel-Crafts *tert*-butylation was carried out to increase the solubility and prevent the aggregation of the final diazadioxa[8]circulene **10**.<sup>124</sup> This was an important adjustment since compound **10** contains a large  $\pi$ -system, which drives the compound into  $\pi$ -stacking. *Tert*-butyl groups also block *ortho*-positions of the hydroxy groups, which prevented the polymerization of compound **49** and increased the probability of dimerization towards a cyclic compound **24** by reacting on 4- and 5-positions. Compound **49** was dimerized to give **24** by oxidative dimerization using chloranil as an oxidative agent and BF<sub>3</sub>OEt<sub>2</sub> as a Lewis acid. Compound **24** was deprotected by AlCl<sub>3</sub> and diazadioxa[8]circulene **10** was obtained.<sup>111</sup>

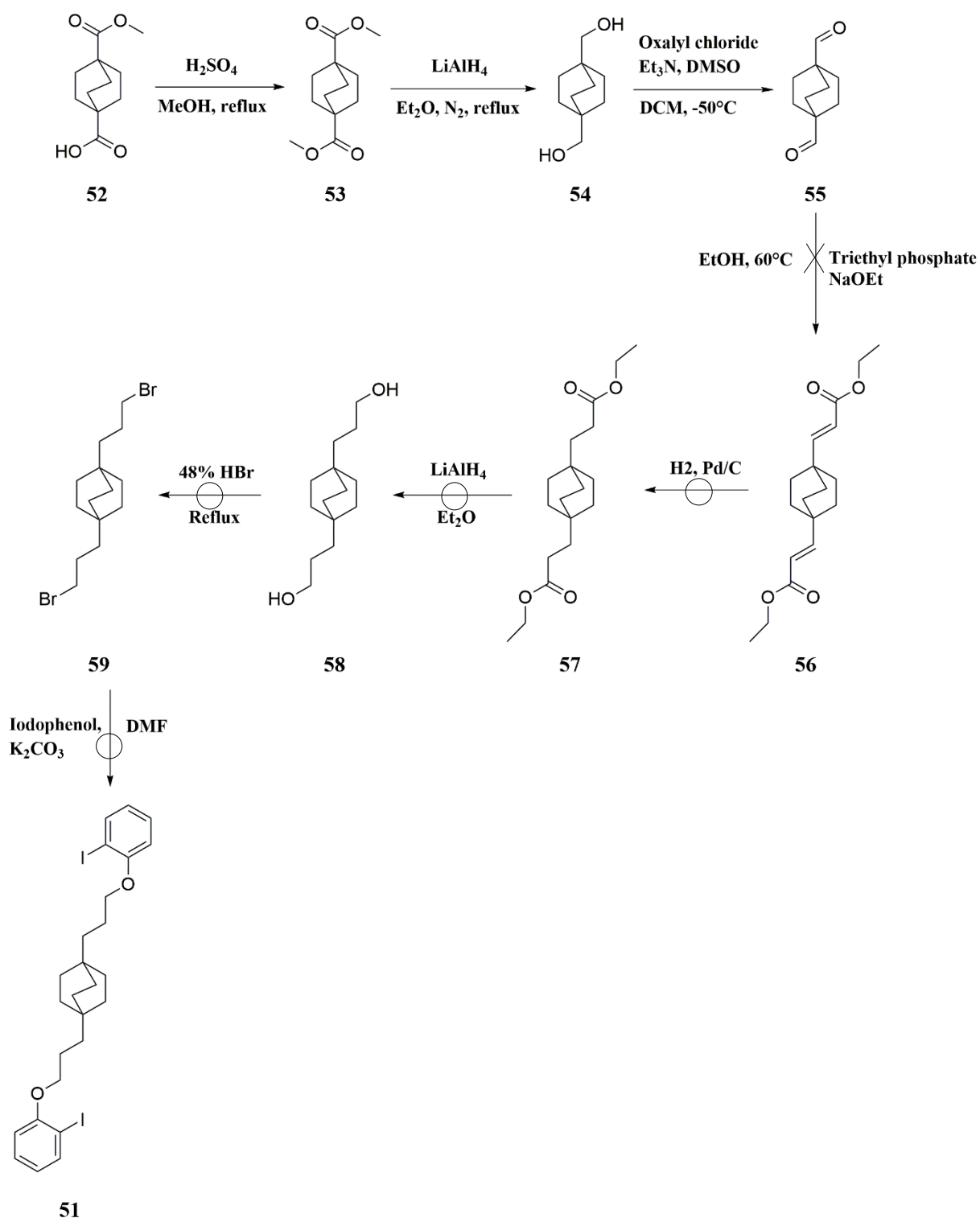
40

Figure 37. Synthesis of a diazadioxo[8]circulene **10**.



## 6.2 Synthesis of bicyclo[2.2.2]octane containing linker **51**

In favor of creating a circulenophane, the synthetic pathway towards linker **51** containing a bicyclo[2.2.2]octane moiety is depicted (Figure 38). The bicyclic moiety was used in the center of the linker to obtain a rigid chain for better proximity of the bicyclo protons to the COT core. The synthesis towards linker **51** was initiated with commercially available compound **52**. The monoester **52** underwent an esterification reaction with sulfuric acid to obtain diester **53**.<sup>125,126</sup> Concentrated sulfuric acid was used as a catalyst for the formation of the ester from the carboxylic acid. By use of lithium aluminium hydride on the carbonyl groups, one can achieve the formation of diol compound **54**.<sup>125,126</sup> Compound **55** was obtained by the Swern oxidation.<sup>126,127</sup> However, the following reaction step towards compound **56** was unsuccessful.<sup>125</sup> The purification of compound **56** as well as repeating the reaction of esterification of bicyclo[2.2.2]octane-1,4-dicarboxaldehyde **55** to 1,4-Bis[2-(ethoxycarbonyl)ethen-1-yl]bicyclo[2.2.2]octane **56** proved to be rather difficult; the compound was lost during the dry column purification, and repeated reactions were unsuccessful. Therefore, ligand **51** could not be synthesized according to the presented plan (Figure 38).



**Figure 38.** Bicyclo[2.2.2]octane approach for the synthesis of the linker **51**.

### 6.3 Synthesis of linker **60**

A different approach was considered for synthesizing a bridge-type linker using a DABCO moiety. The new approach was far less challenging, cheaper, with fewer synthetic steps and better yields. 1,4-Bis(3-(2-hydroxyphenoxy)propyl)-1,4-diazabicyclo[2.2.2]octane-1,4-dium **60** was synthesized using DABCO and 2-(3-bromopropoxy)phenol **62** (Figure 39).<sup>128</sup> The synthesis started by the reaction of commercially available 2-iodophenol **64** with an excess amount of dibromopropane in acetone. The reaction resulted in 1-(3-bromopropoxy)-2-iodobenzene **62**. Compound **62** reacted thereafter with DABCO in 2:1 ratio as to react both nitrogen atoms on DABCO.<sup>129</sup> In the first attempt THF was used as a solvent, which resulted in early precipitation of the monosubstituted DABCO moiety shortly after the addition of the reagents.

The conditions were changed, and during the second attempt, DMF was used instead of THF. In addition, the reaction was heated under reflux. Changing the reaction conditions appeared successful and resulted in both nitrogen atoms being involved and reacting with linker **60**.

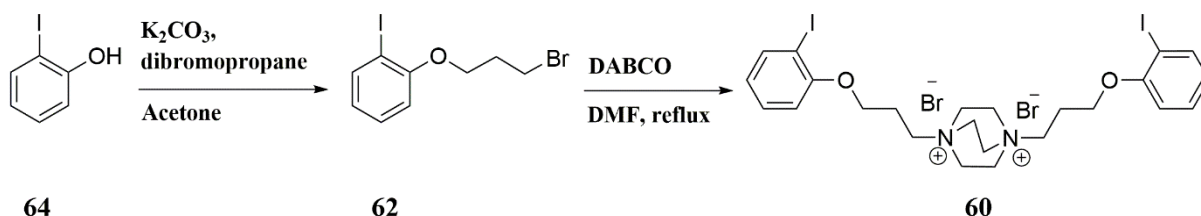


**Figure 39.** Synthesis of a bridge-like linker **60** using DABCO moiety in the centre of the linker.

## 6.4 Synthesis of a circulenophane

Several attempts were made to couple both arms of linker **60** to the nitrogen atoms of diazadioxo[8]circulene **10**. The LC/MS data showed a full conversion after 24 hours of stirring, but no product was attained.<sup>130</sup> It was suggested based on the NMR and mass spectrometry results that only one arm of the linker coupled to diazadioxo[8]circulene **68** (Figure 40). The reaction was therefore repeated at higher temperatures to force the second arm into coupling, but the reaction was not successful. A possible explanation could be steric hindrance due to the bulky moiety in the center of the linker, making it difficult to connect the second arm to the pyrrole nitrogen. An alternative suggestion could be that the bulky *tert*-butyl groups make the second coupling less favourable.

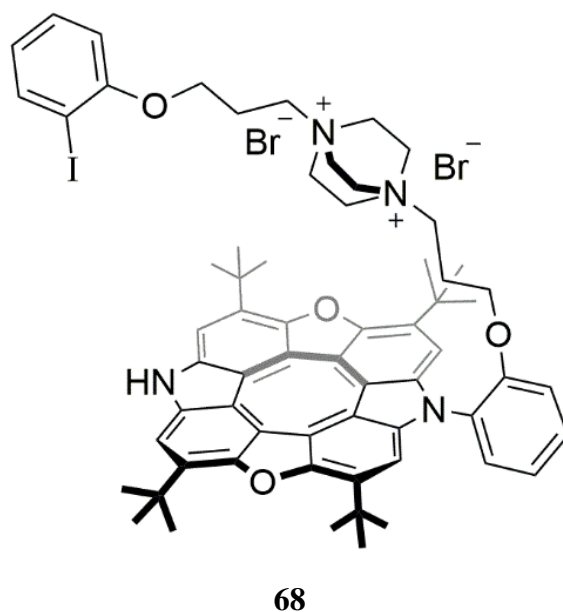


**Figure 40.** Suggested structure of **68**. The linker coupled to one nitrogen atom of circulene **10**.

Another approach was attempted to achieve coupling. In this attempt, the linker **60** could couple to the dimethoxy carbazole moieties of **48** after deprotonation of the pyrrole moiety to obtain compound **70**. Furthermore, the methoxy groups could be converted to hydroxyl groups after which the cyclization of the carbazole units could lead to the circulenophane **72** (Figure 41). However, the reaction failed, and the plan seemed to be ineffective as the units could

polymerize instead of achieving cyclization. Figure 41 suggests another synthesis pathway to achieve the target circulenophane.

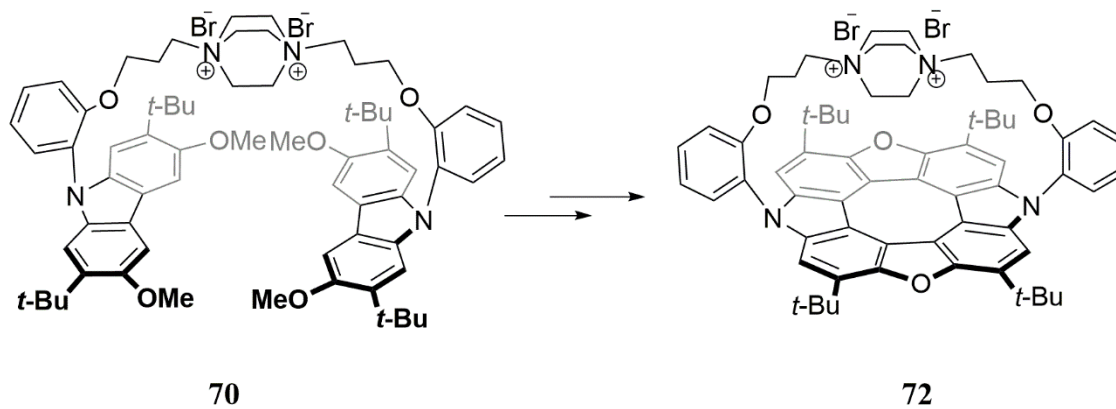


**Figure 41.** Suggested synthesis pathway for achieving circulenophane **72** from dimethoxycarbazole **48** and linker **60**.

## 7 REACTION MECHANISMS

### 7.1 Diazadioxa[8]circulene

It is possible to synthesize diazadioxa[8]circulene **10** by the oxidative dimerization of 3,6-dihydroxycarbazole **49**. Chloranil acts as an oxidative agent and boron trifluoride diethyl etherate as a Lewis acid. The reaction mechanism of the dimerization is presented in Figure 42.

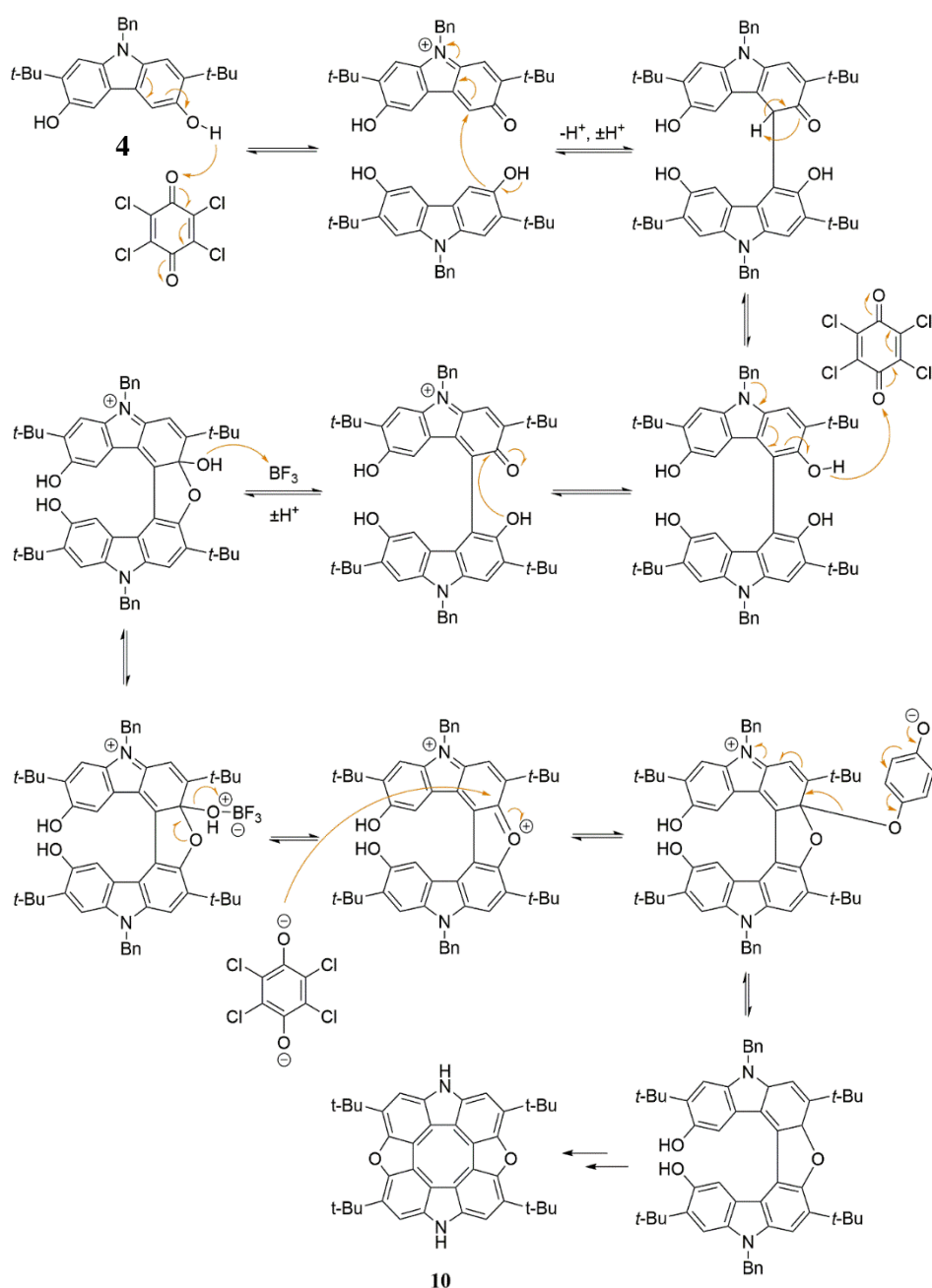


**Figure 42.** The reaction mechanism of the dimerization toward the synthesis of diazadioxa[8]circulene.

## 7.2 Synthesis of the bicyclo containing linker **51**

Synthesis of linker **51** initiated by commercially available compound **52**. Addition of concentrated sulphuric acid as a catalyst assisted in the esterification of the carboxylic acid moiety. Sulphuric acid also acted as a dehydrating agent to force the equilibrium to the right. When the diester **53** was obtained, it was reduced to alcohol by  $\text{LiAlH}_4$ . This reaction required two hydrides to be added to the carbonyl carbon (Figure 43).

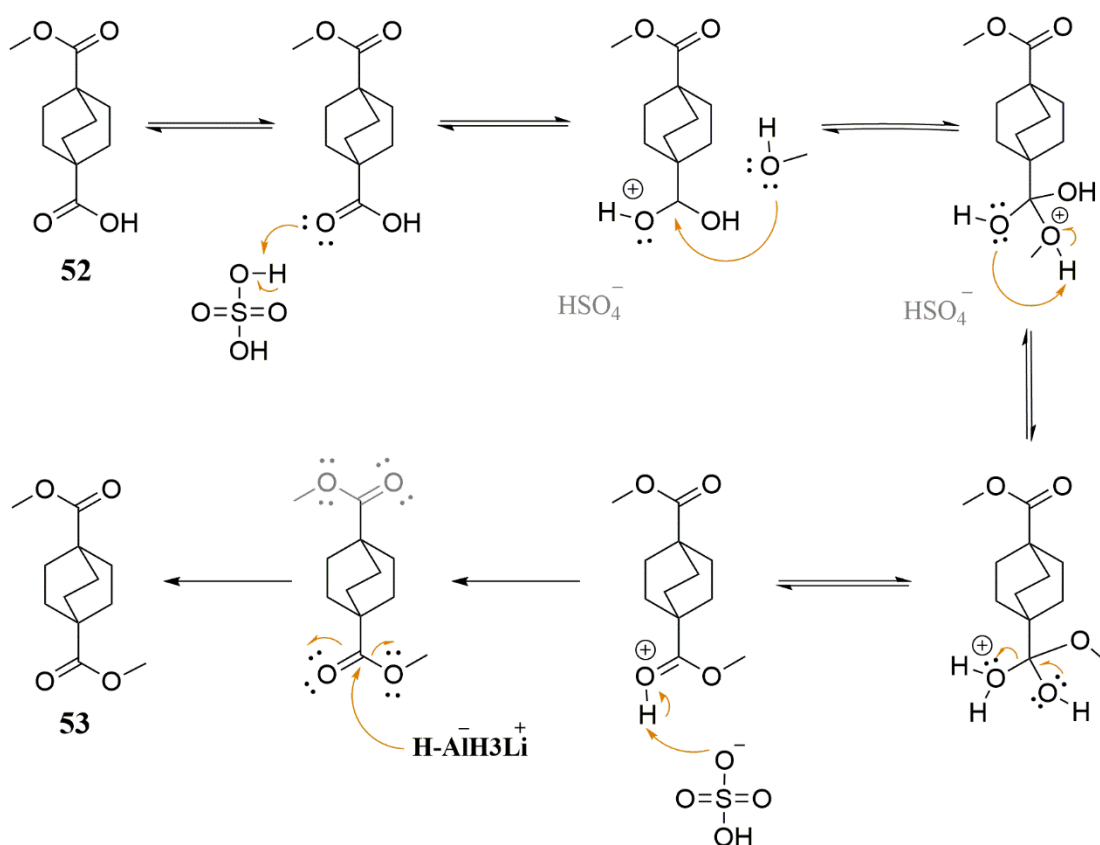


**Figure 43.** The reaction mechanism of dimethyl bicyclo[2.2.2]octane-1,4-dicarboxylate **53**.

The nucleophilic H from the reagent attacked the electrophilic carbonyl carbon of **53**, forcing the electrons to move towards the electronegative oxygen atom. This transfer created a tetrahedral complex, which made the alcohol portion of the ester to act as a leaving group, an alkoxide, and produced an aldehyde as an intermediate. Afterwards, the nucleophilic H from the reagent attacked the carbonyl group and made the electrons move to the electronegative oxygen creating a metal alkoxide complex. At last, protonation of the alkoxide oxygen created a primary alcohol **54** from the complex (Figure 44).

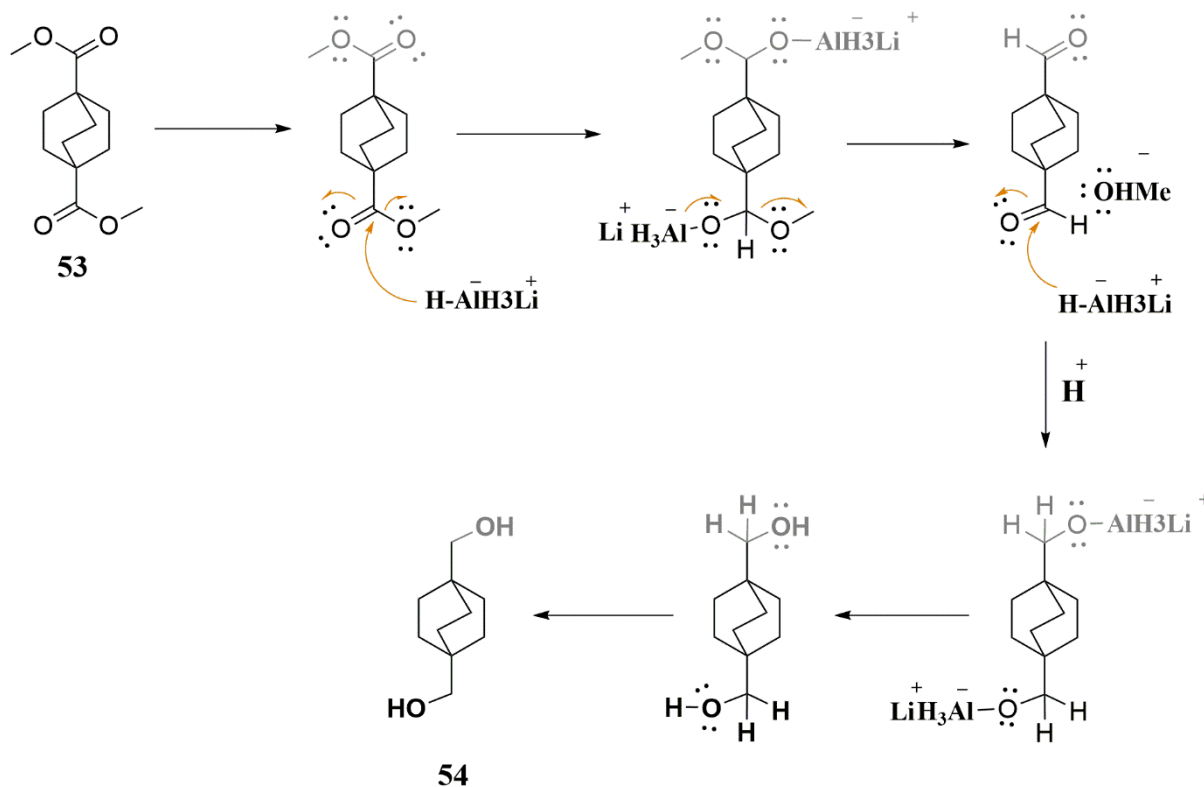


**Figure 44.** The reaction mechanism of bicyclo[2.2.2]octane-1,4-dimethanol **54**.

To avoid consuming toxic metals, the Swern oxidation was used to obtain the aldehyde from the 1° (primary) alcohol. The only drawback of this reaction was the production of the malodorous gas dimethyl sulfide (DMS). As shown in Figure 45 in the blue box, the reaction initiated by the activation of DMSO using oxalyl chloride towards the dimethyl chlorosulfonium ion. The ion deprotonated the alcohol **54** to produce an alkoxy-sulfonium ion.

The reaction continued *via* intramolecular deprotonation to produce the target aldehyde **55** and malodorous DMS. The reaction took place in dry ice and acetone bath to inhibit the formation of thioacetals (Figure 45).



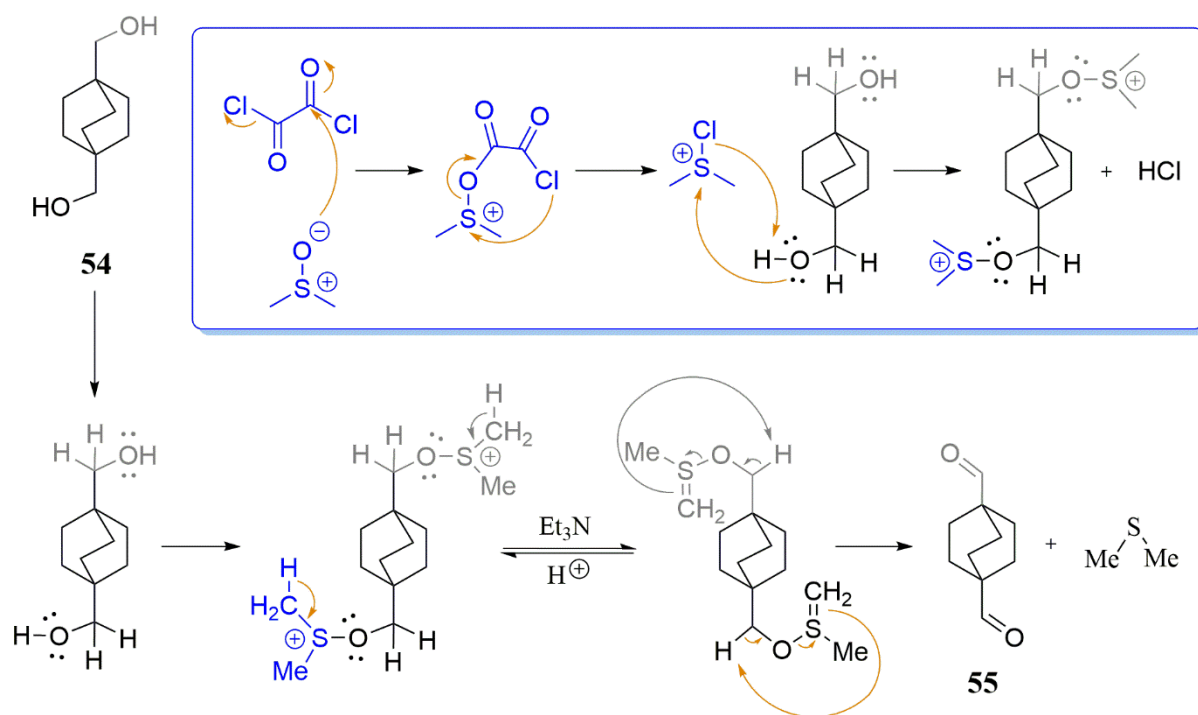


**Figure 45.** The reaction mechanism of bicyclo[2.2.2]octane-1,4-dicarboxaldehyde **55**.

Horner-Wadsworth-Emmons (HWE) reaction is similar to a Wittig reaction frequently used to produce olefins from aldehydes and ketones. The advantage of this approach is the control of the stereochemistry as the *E*-isomer is obtained over *Z* when modifying the conditions. By reacting phosphonate esters with a base, a stabilized phosphonium anion is produced which reacts with the desired aldehyde or ketone. The phosphonate by-products are easily removed by extraction with water.<sup>131</sup> The reaction started by deprotonation of the phosphonate and produced a phosphonate carbanion (Figure 46). Then the nucleophilic addition of the carbanion onto the aldehyde **55** produced an intermediate, which converted to the target compound **56** by the final elimination using NaOEt as a base.

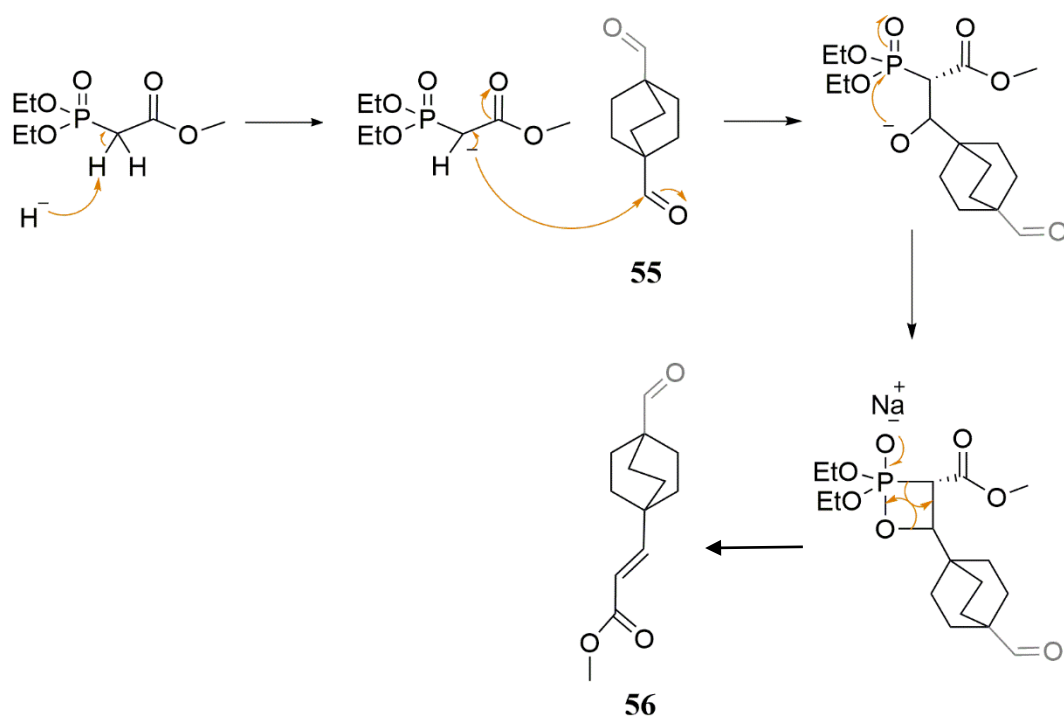


**Figure 46.** The reaction mechanism towards compound **56**. Only one arm is shown for clarity.

### 7.3 Mechanistic view towards the synthesis of DABCO containing linker **60**

For the synthesis of linker **60**, 2-iodophenol was used for a Williamson etherification step. This is a popular method for obtaining ethers from alkyl halides and alcohols by the formation of an alkoxide intermediate.<sup>132</sup>  $K_2CO_3$  was used as a base to deprotonate the alcohol **64** for the formation of the corresponding alkoxide. Then the alkyl halide was added. The halogen was partially negative compared to the carbon due to the difference in electronegativity. The carbon acted as an electrophile. The alkoxide attacked the alkyl halide as a nucleophile from the back to produce an ether *via* a nucleophilic substitution reaction ( $S_N2$ ). In this step cleavage and formation of a bond happens simultaneously. The halide ion acted as a leaving group producing KBr as side product while the ether **62** was formed (Figure 47).

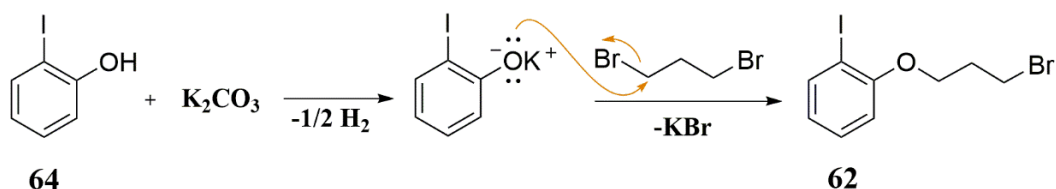


**Figure 47.** The Williamson etherification reaction towards the formation of compound **62**.

During the next step, compound **62** reacted with DABCO in DMF in a 2:1 ratio to substitute both nitrogen atoms and obtain linker **60** (Figure 48). The reaction follows a nucleophilic substitution mechanism, in which the DABCO unit acts as a nucleophile and compound **62** as an electrophile. In **62** the difference in the electronegativity of bromine and carbon creates a dipole, in which the electron density at the carbon-halogen bond is attracted towards the halogen making the carbon possess a partially positive charge and the bromine a partially negative. This made the carbon atom (an electron-deficient unit) susceptible to a nucleophile attack. An important factor in this type of reactions was to select the right solvent; polar aprotic solvents create a medium in which the stabilization of the nucleophile is decreased, and thus the reaction can take place.

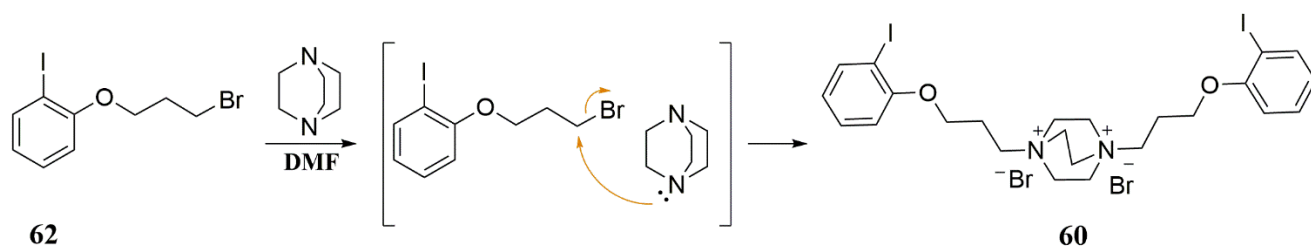


**Figure 48.** The synthesis mechanism of compound **60**.

## 8 MATERIAL AND INSTRUMENTATION

All chemicals and solvents were purchased from commercial suppliers and used without further purification. HPLC grade solvents were used for synthesizing the compounds whereas technical grade solvents were used for purification. When needed, solvents were dried over molecular sieves of 4 Å before use.

TLC was performed using Merck TLC Silica gel 60 F<sub>254</sub> 0.2 mm thick. Pre-coated TLC plates were developed in a specific solvent system, and when stained, the spots were visible under UV irradiation using a Konrad Benda UV lamp at 254 and 366 nm.

NMR experiments were performed using a Bruker Ultrashield Plus 500 MHz spectrometer. <sup>1</sup>H-NMR spectra were recorded at 500 MHz. Solvents were used as purchased, and the data was analysed using MestReNova 11.0.4. No <sup>13</sup>C-NMR was measured.

DCVC was performed using ROCC S. A. Silica gel 60 Å, 15-40 μm, SI 1722 using technical grade solvents. The celite was Hyflo Super Cel® diatomaceous earth.

MALDI-TOF-HRMS measurements were performed on a Solarix ESI/MALDI FTMS spectrometer using dithranol as a matrix made by Annette Anderson.

GC-MS analysis was performed on an Agilent 6890 series GC system, coupled to an Agilent 5973 Network Mass Selective Detector.

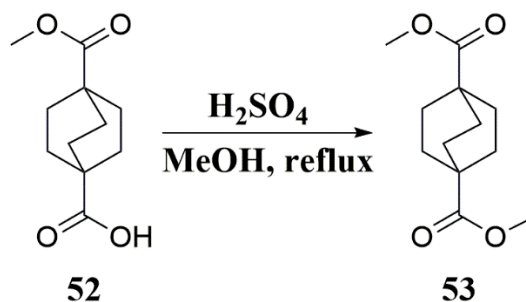
Standard HPLC analysis was performed using a Dionex Ultimate 3000 system coupled to an Ultimate 3000 diode array UV/Vis detector. The column used for the separation was a Dionex Acclaim RSLC 120 C18 2.2 μm 120 Å 2.1x50 mm, and it was maintained at 20 °C or 40 °C. The mobile phase solutions were prepared with 0.1% HCOOH in the solvents. The water used as eluent was purified by a Millipore system. Bruker MicroTOF-GII-system with an ESI-source with nebulizer, 1.2 bar, dry gas: 8.0 L/min, dry temperature: 200°C, capillary: -4500 V, endplate offset: -500 V, funnel 1 RF: 200.0 Vpp, ISCID energy: 0.0 eV, funnel 2 RF: 200.0 Vpp, hexapole RF: 100.0 Vpp, quadrupole ion energy: 5.0 eV, low mass: 100.00 *m/z*, collision energy: 8.0 eV, collision RF: 100.0 Vpp, transfer time: 80.0 μs and pre-plus storage: 1.0 μs.

All GC-MS, MALDI-TOF-HRMS and HPLC analyses were performed for confirming the presence of the product after observation with <sup>1</sup>H NMR. Unfortunately, the results were lost due to miscarrying the data.

Boiling points were measured with a Büchi melting point apparatus.

## 9 SYNTHESIS

### 9.1 Synthesis of dimethyl bicyclo[2.2.2]octane-1,4-dicarboxylate **53**



First, 4-(methoxycarbonyl)bicyclo[2.2.2]octane-1-carboxylic acid **52** (5.00 g, 23.56 mmol) was dissolved in methanol (70 ml, 23.56 mmol) in a 250 ml round bottom flask. Then one drop of  $\text{H}_2\text{SO}_4$  (95 % w/w) was added to the mixture, and it was refluxed overnight at  $80^\circ\text{C}$ .

On the next day, analysis of NMR, GC-MS and TLC stained by  $\text{KMnO}_4$  solution showed full conversion. The solution was quenched with water ( $3 \times 100$  ml), giving a white mixture and precipitates. DCM was added. The organic layer was separated, and the water phase was washed with DCM. The organic phase was dried over  $\text{Na}_2\text{SO}_4$ . The solvent was removed by rotary evaporator to give dimethyl bicyclo[2.2.2]octane-1,4-dicarboxylate **53** as a white solid.

**Molecular formula:**  $\text{C}_{12}\text{H}_{18}\text{O}_4$ . **Yield:** 5.2 g, 97 %. **MP:**  $98\text{--}99^\circ\text{C}$ . **TLC:**  $R_f = 0.7$  (heptane/ethyl acetate, 1:2).  **$^1\text{H}$  NMR** (500 MHz,  $\text{CDCl}_3$ )  $\delta$  1.81 (s, 12 H), 3.65 (s, 6H) ppm.  **$^{13}\text{C}$  NMR** was not measured.

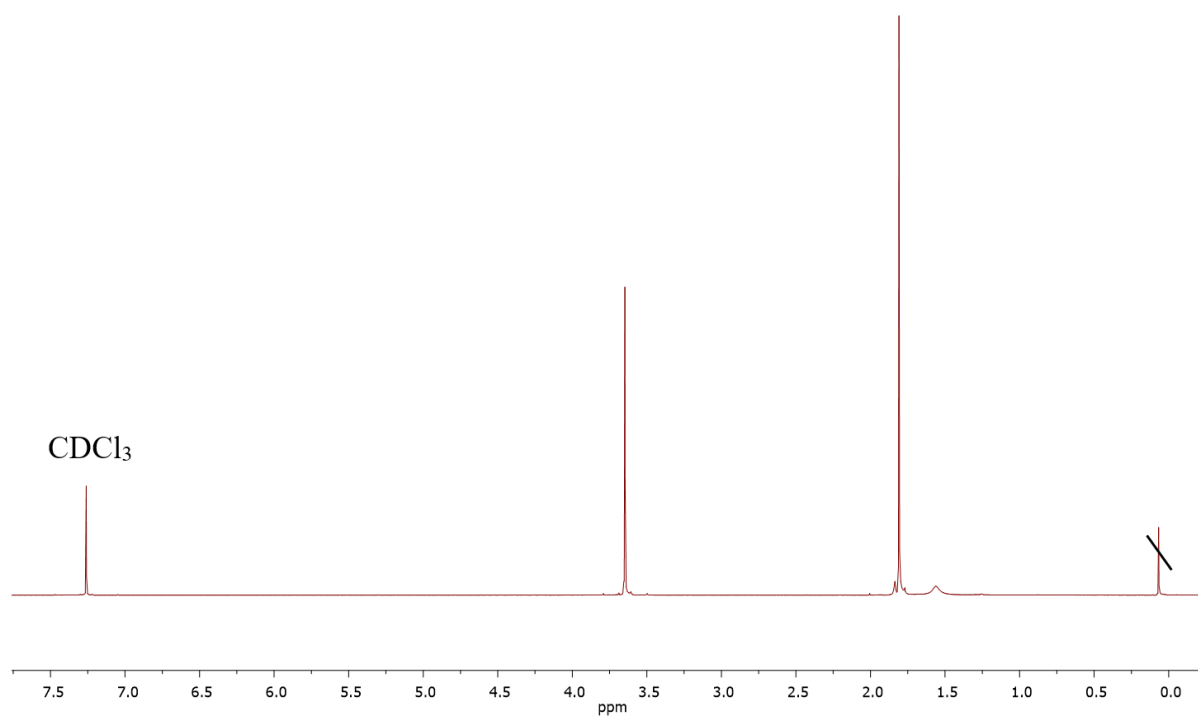
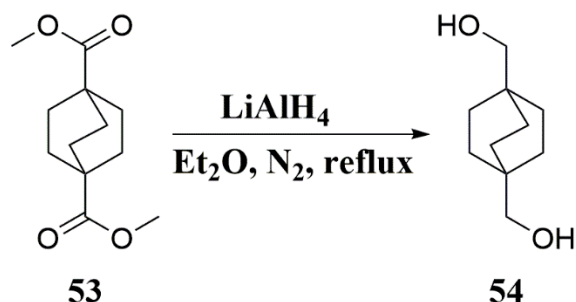


**Figure 49.**  $^1\text{H}$  NMR spectra of compound **53**.

## 9.2 Synthesis of bicyclo[2.2.2]octane-1,4-dimethanol **54**



A 250-ml three-necked flask was equipped with a reflux condenser, magnetic stirrer and nitrogen inlet. The flask was charged with 20 ml of diethyl ether and LiAlH<sub>4</sub> (2.47 g, 64.97 mmol). Dimethyl bicyclo[2.2.2]octane-1,4-dicarboxylate **53** [APF-01-B] (4.90 g, 21.66 mmol) was dissolved in 30 ml dry ether. The solution was added dropwise to the flask while stirring for 1,5 hours. Subsequently, the flask was heated and refluxed for five hours.

The reaction was quenched by dropwise addition of water (8.5 ml), 2.5 ml of NaOH (15 %, 2 M) and 25 ml of water. The mixture was filtered, and the salts were washed with ether. The organic layer was dried with Na<sub>2</sub>SO<sub>4</sub>, and the solvent was removed with a rotary evaporator. The product was obtained as a bright yellow solid.

**Molecular formula:** C<sub>10</sub>H<sub>18</sub>O<sub>2</sub>. **Yield:** 2.65g, 72 %. **MP:** 105°C. **TLC:** R<sub>f</sub>= 0.30 (heptane:ethyl acetate, 1:2). **<sup>1</sup>H NMR** (500 MHz, CDCl<sub>3</sub>) δ 1.30 (broad s, 2H), δ = 1.43 (s, 12H), 3.27 (s, 4H) ppm. **<sup>13</sup>C NMR** was not measured.



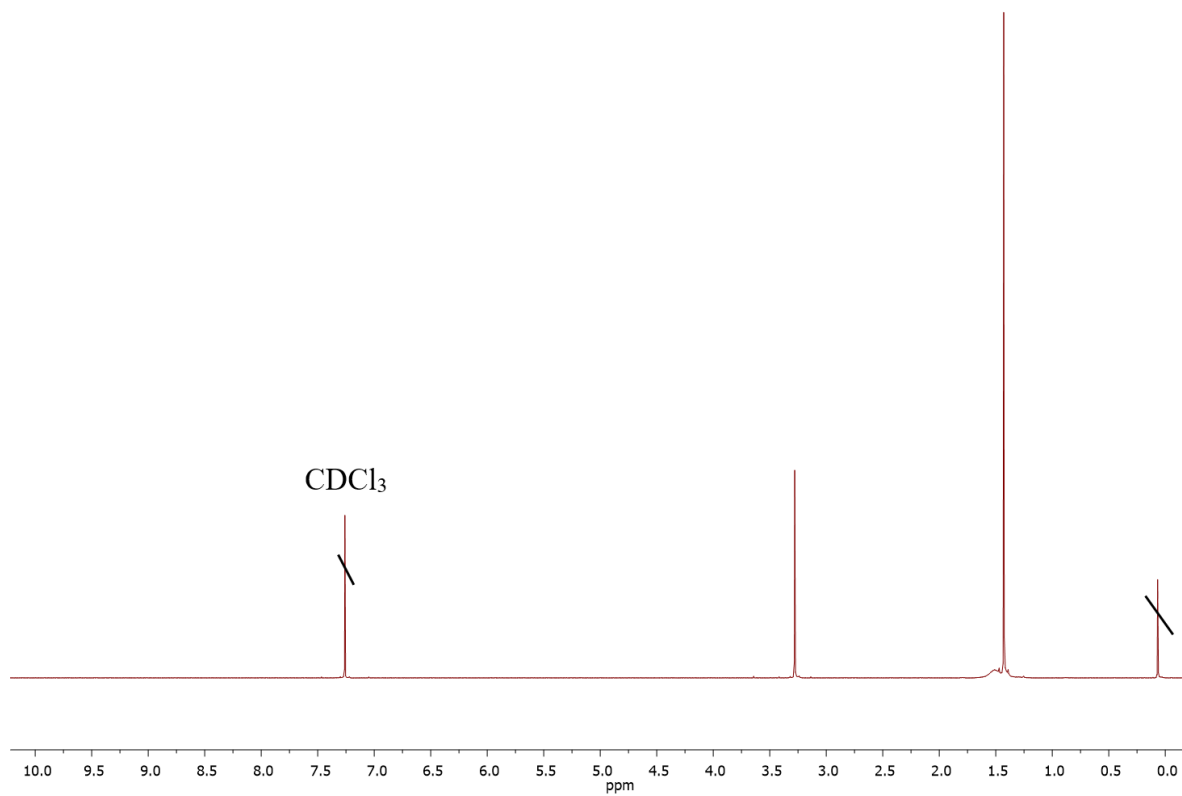
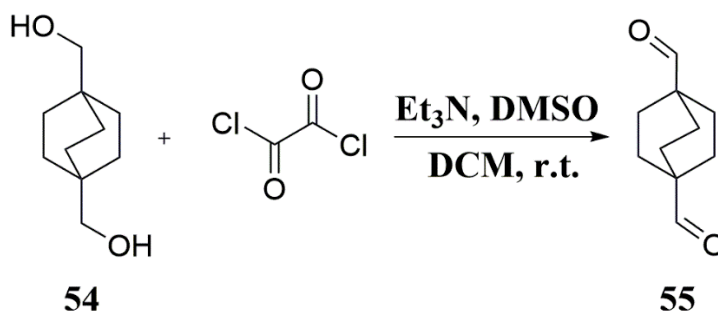


**Figure 50.**  $^1\text{H}$  NMR spectra of compound 54.

### 9.3 Synthesis of bicyclo[2.2.2]octane-1,4-dicarboxaldehyde **55**



A 250 ml round bottom flask was flame dried and flushed with nitrogen. The flask was put in acetone dry ice bath. Oxalyl chloride (1.43 ml, 16.69 mmol) and DCM (40 ml) solution was added to the flask. DMSO (2.75 ml, 38.65 mmol) mixed with DCM (15 ml) was added dropwise while stirring and the mixture was let to stir for five minutes. Bicyclo[2.2.2]octane-1,4-dimethanol **54** [APF-02-B] (1.40 g, 8.22 mmol), DCM (5 ml) and DMSO (1.25 ml) were added dropwise, and stirring was continued for fifteen minutes.

The reaction mixture was warmed to -10 °C, triethylamine was added, and the mixture was stirred for one hour. Water (80 ml) was added, and DCM layer separated. The water layer was extracted with DCM. Organic layers were combined and washed with HCl 1%, Na<sub>2</sub>CO<sub>3</sub> 5%, brine and dried over Na<sub>2</sub>SO<sub>4</sub>. The solvent was removed under vacuum. Sticky dark orange product was obtained. DNPH was used for TLC stain.

**Molecular formula:** C<sub>10</sub>H<sub>14</sub>O<sub>2</sub>. **Yield:** 1.11 g, 82%. **MP:** 103-104 °C. **TLC:** R<sub>f</sub> = 0.7 (Heptane:EtOAc, 1:2). **<sup>1</sup>H NMR** (500 MHz, CDCl<sub>3</sub>) δ 1.72 (s, 12H), 9.44 (s, 2H) ppm. **<sup>13</sup>C NMR** was not measured.

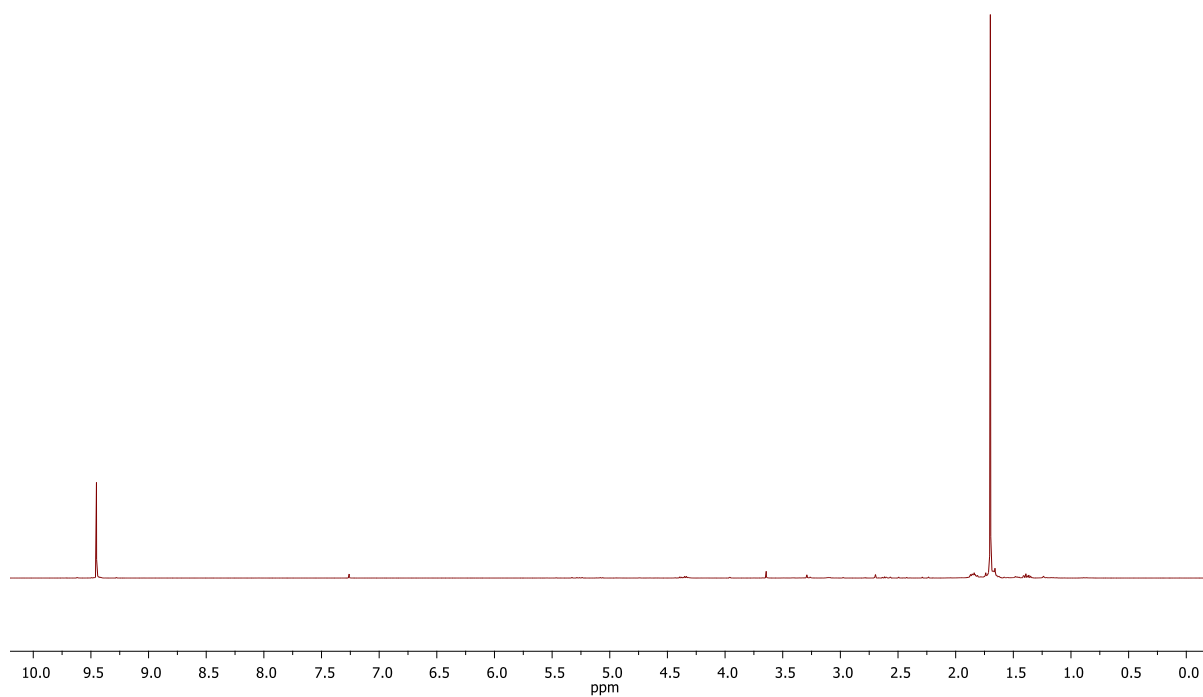
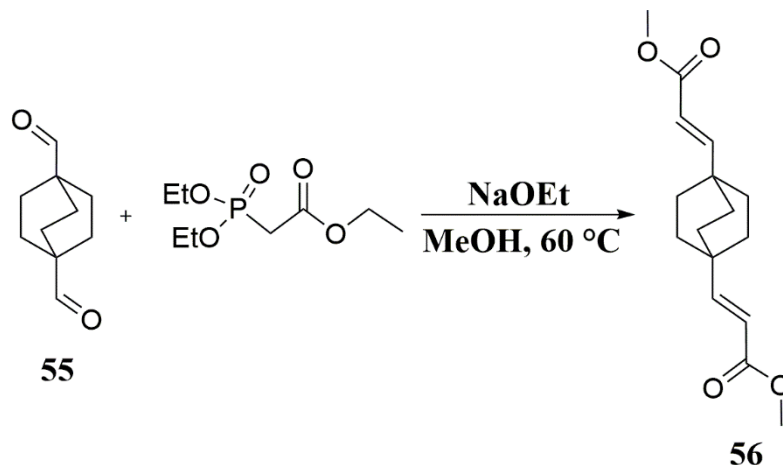


**Figure 51.**  $^1\text{H}$  NMR spectra of compound **55**.

### 9.4 Synthesis of 1,4-bis[2-(ethoxycarbonyl)ethen-1-yl]bicyclo[2.2.2]octane **56**



Bicyclo[2.2.2]octane-1,4-dicarboxaldehyde **55** (470 mg, 2.83 mmol) and ethyl 2-(diethoxyphosphoryl)acetate (2.24 ml, 11.31 mmol) were added to a 250 ml round-bottomed flask at 60 °C. Sodium ethoxide (15 ml, 1N) was added by syringe, and the mixture was stirred overnight.

Next day the solvent was removed by rotary evaporator, petrol ether was added, and the mixture was refluxed for 2 hours. The solution was filtered, and the product was evaporated onto celite. The product was subjected to DCVC. White sticky product was obtained. DCM:Hep, 2:3.

**Molecular formula:** C<sub>18</sub>H<sub>26</sub>O<sub>4</sub>. **Yield:** 183 mg, 23 %. **TLC:** R<sub>f</sub> = 0.5 (heptane/ethyl acetate, 4:1). **<sup>1</sup>H NMR** (500 MHz, CDCl<sub>3</sub>) δ 1.28 (t, 6H), 1.59 (s, 12H), 4.16 (q, 4H), 5.66 (d, 2H), 6.85 (d, 2H). **<sup>13</sup>C NMR** was not measured.

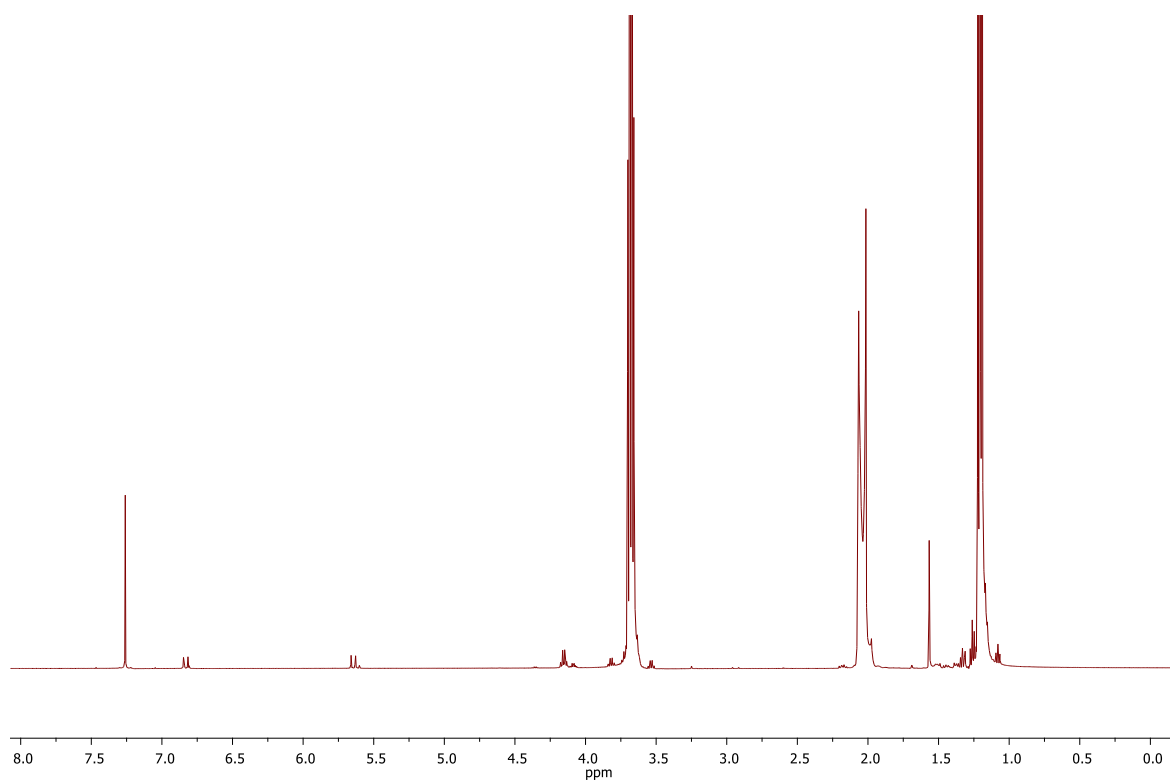
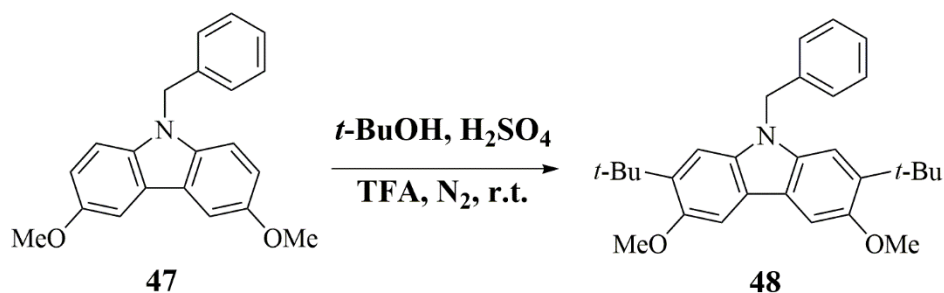


**Figure 52.**  $^1\text{H}$  NMR spectra of compound 56.

### 9.5 Synthesis of *N*-benzyl-2,7-di-*tert*-butyl-3,6-dimethoxy-9*H*-carbazole **48**



3,6-dimethoxy-9-propyl-9*H*-carbazole **47** (2.00 g, 6.30 mmol) was dissolved in trifluoroacetic acid (TFA) (9.15 ml 119.49 mmol). Then *tert*-butanol (*t*-BuOH), (7.74 ml, 81 mmol) was added. The mixture was cooled down in an ice bucket, and sulfuric acid (158  $\mu$ l, 2.84 mmol) was added slowly. The mixture was left to stir overnight.

The next day white sediments were observed. Some water was added, and immediately more white sediments precipitated. The mixture was filtered and dried under vacuum line. A white solid was obtained.

**Molecular formula:** C<sub>29</sub>H<sub>35</sub>NO<sub>2</sub>. **Yield:** 2.49 g, 92%. **MP:** 168-170°C. **TLC:** R<sub>f</sub> = 0.64 (heptane/ethyl acetate, 4:1). **<sup>1</sup>H NMR** (500 MHz, CDCl<sub>3</sub>)  $\delta$  1.53 (s, 18H), 3.93 (s, 6H), 5.45 (s, 2H), 7.21-7.26 (m, 3H), 7.28 (t, 2H), 7.23 (s, 2H), 7.56 (s, 2H) ppm. **<sup>13</sup>C NMR** was not measured.

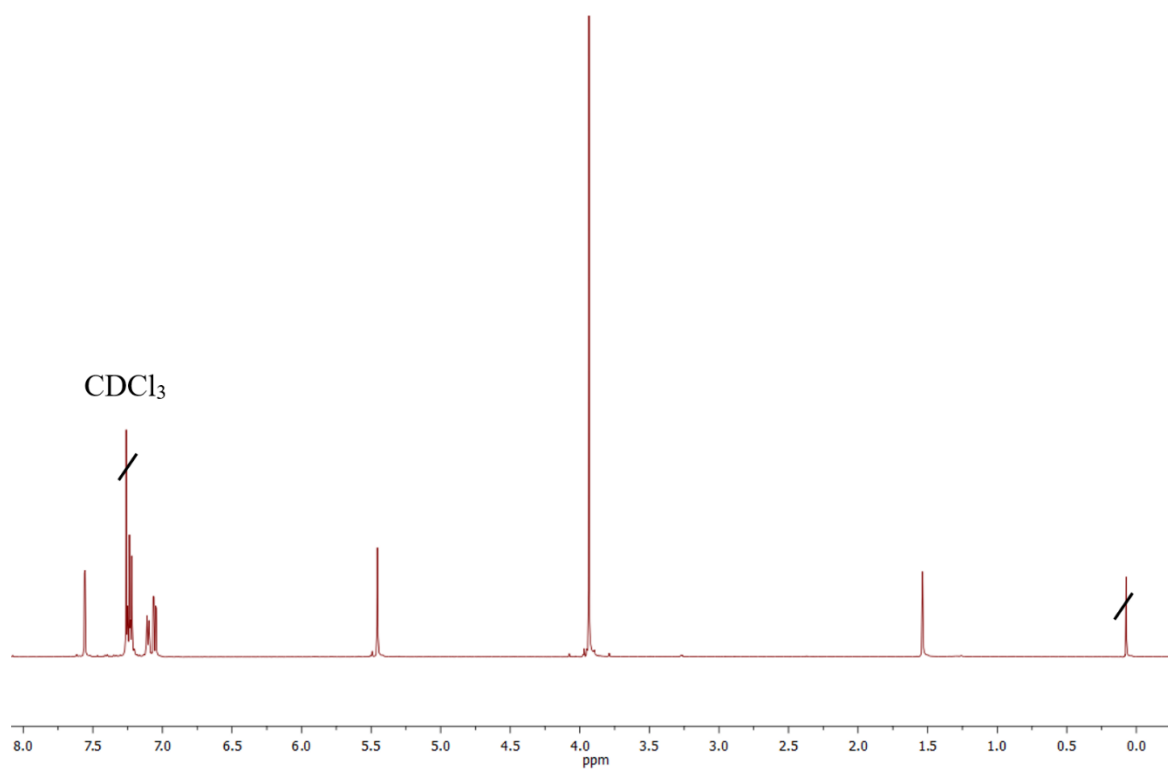
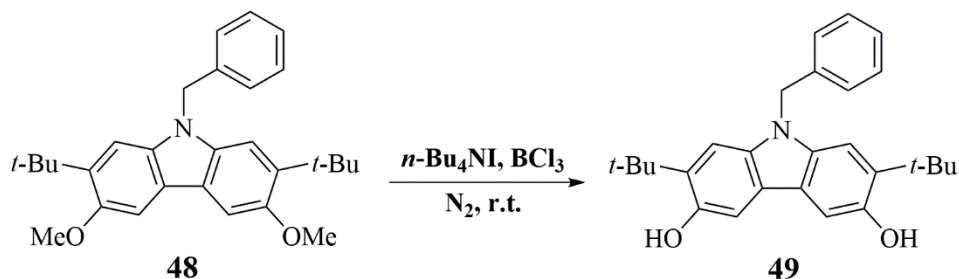


**Figure 53.**  $^1\text{H}$  NMR spectra of compound 48.

## 9.6 Synthesis of 9-benzyl-2,7-di-tert-butyl-9H-carbazole-3,6-diol **49**



9-benzyl-2,7-di-*tert*-butyl-3,6-dimethoxy-9H-carbazole **48** (2.00 g, 4.66 mmol) and *tert*-butylammonium iodide (3.5 g, 9.53 mmol) were mixed in a 500 ml round bottom flask and closed with a sealing rubber. Boron trichloride (40 ml, 452.71 mmol) was added slowly to the mixture under N<sub>2</sub>, and the mixture was left to stir for 75 minutes. The solution turned dark red. After full conversion, the solution was slowly quenched with HCl (1M, 200 ml), then washed with DCM (4x60ml) and dried over Na<sub>2</sub>SO<sub>4</sub>. The mixture was purified using a dry column with acetonitrile:toluene v/v %, 12 % gradient in 2 % increments. A white powder was obtained.

**Molecular formula:** C<sub>27</sub>H<sub>31</sub>NO<sub>2</sub>. **Yield:** 1.34 g (72%). **MP:** ≈ 240 ° (With decomposition). **TLC:** R<sub>f</sub> = 0.3 (Heptane:EtOAc, 2:1). **<sup>1</sup>H NMR** (500 MHz, DMSO-*d*<sub>6</sub>) δ 1.40 (s, 18H), 5.47, (s, 2H), 7.18-7.21 (m, 5H), 7.24 (d, 2H), 7.28 (d, 2H), 8.87 (s, 2H) ppm. **<sup>13</sup>C NMR** was not measured.



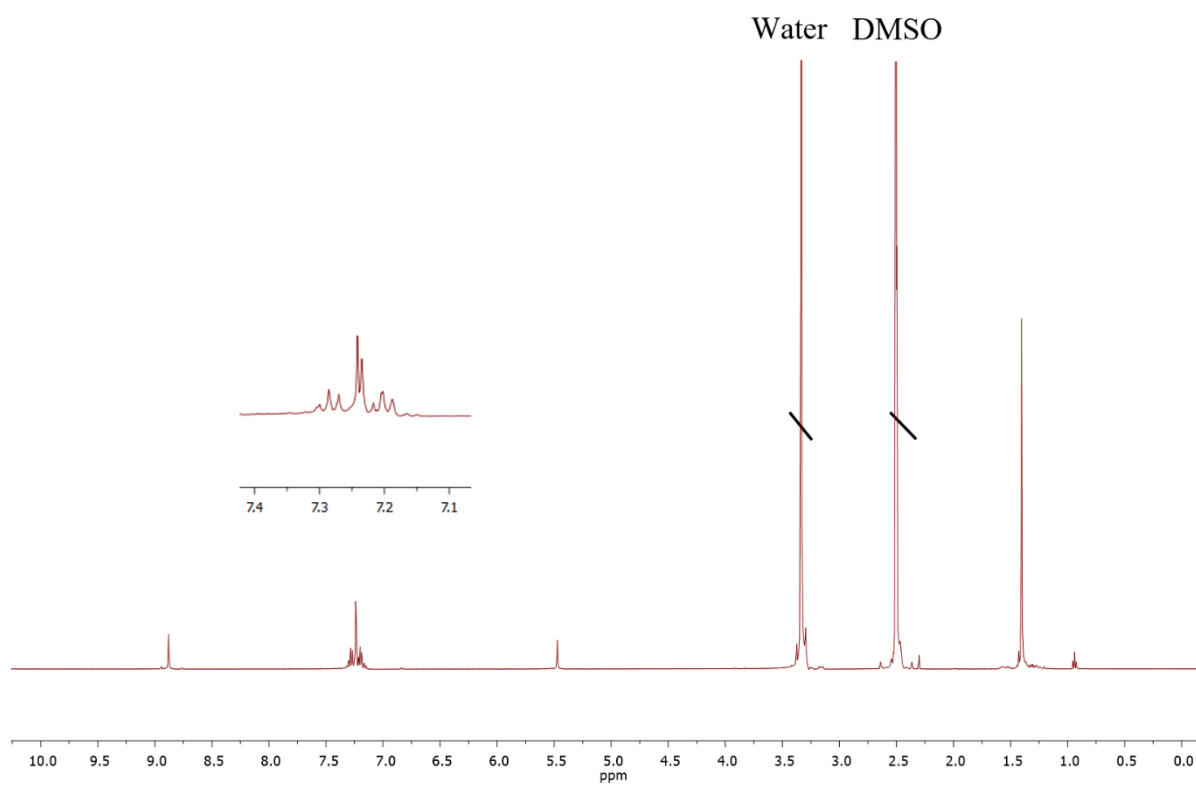
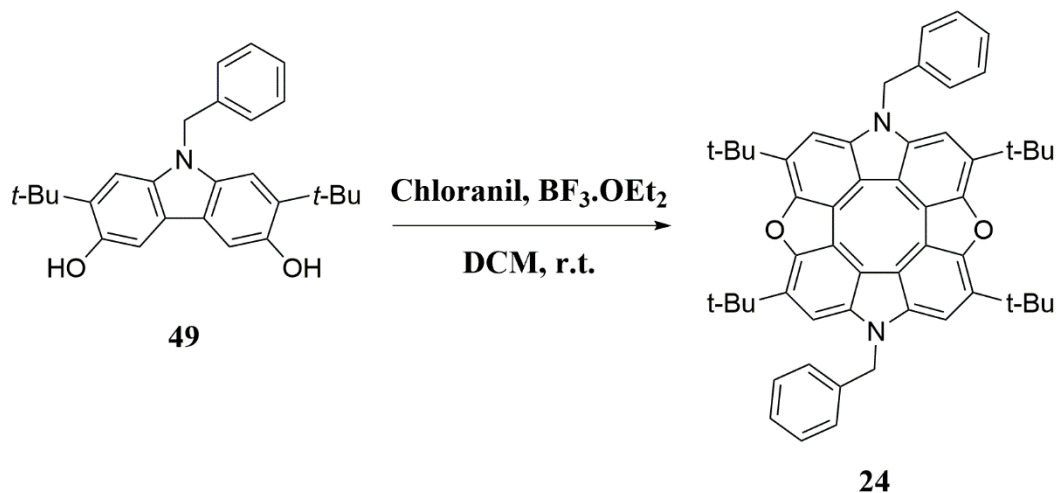


**Figure 54.**  $^1\text{H}$  NMR spectra of compound **49**.

## 9.7 Synthesis of 9,11-bis(*N*-benzyl)-2,3,6,7-tetra-*tert*-butyl diazadioxa[8]circulene **24**



9-benzyl-2,7-di-*tert*-butyl-9H-carbazole-3,6-diol **49** (1.40 g, 3.49 mmol) and 2,3,5,6-tetrachloro-1,4-benzoquinone (chloranil; 944 mg, 3.84 mmol) were dissolved in 200 ml DCM in a 250 ml round bottom flask and stirred for 3 hours at room temperature. Subsequently, boron trifluoride diethyl etherate (0.47 ml, 3.84 mmol) was added to the mixture, and the mixture was left to stir overnight.

Full conversion of the starting material was observed the next day by TLC. The mixture was then quenched with KOH (2 M, 50 ml) and let to stir for 10 minutes. The mixture was extracted with DCM (4x70 ml) and dried over  $\text{Na}_2\text{SO}_4$ . The solvent was removed by rotary evaporator. The crude compound was purified using a dry column. (heptane:toluene v/v%, 12% gradient in 5% increments). The product was a yellow solid.

**Molecular formula:**  $\text{C}_{54}\text{H}_{54}\text{N}_2\text{O}_2$ . **Yield:** 650 mg (48%). **MP:**  $\approx 240^\circ$  (With decomposition).

**TLC:**  $R_f = 0.3$  (Heptane/EtOAc 2:1).  **$^1\text{H}$  NMR** (500 MHz,  $\text{DMSO}-d_6$ )  $\delta$  1.72 (s, 36H), 6.02 (s, 4H), 7.32 (m, 5H), 7.75 (s, 2H) ppm.  **$^{13}\text{C}$  NMR** was not measured.

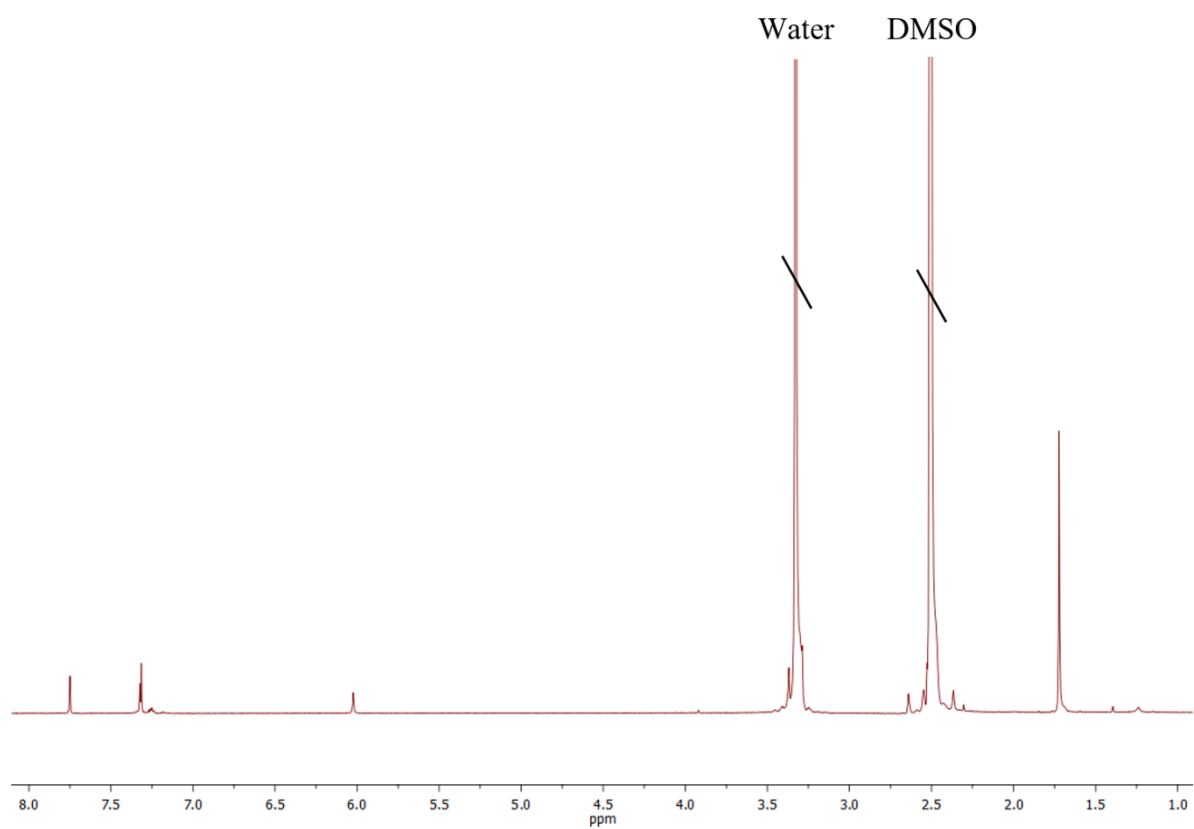
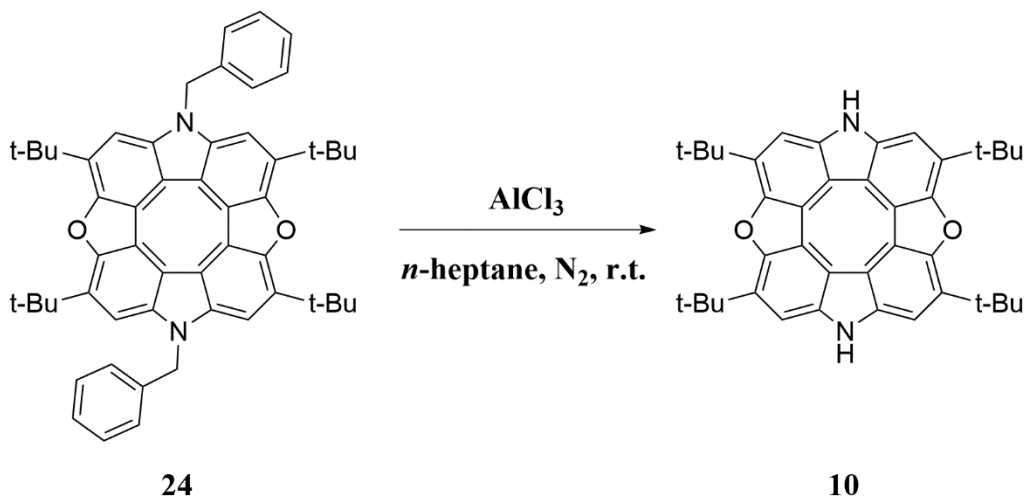


**Figure 55.**  $^1\text{H}$  NMR spectra of compound 24.

## 9.8 Synthesis of 9,11*H*-2,3,6,7-tetra-*tert*-butyl-diazadioxa[8]circulene **10**



9,11-bis(*N*-benzyl)-2,3,6,7-tetra-*tert*-butyl-diazadioxa[8]circulene **24** (APF-03-C) (245 mg, 321,08  $\mu\text{mol}$ ) and aluminium chloride (866.6 mg, 6.5 mmol) were dissolved in *n*-heptane (25 ml) in a round-bottomed flask under  $\text{N}_2$ . The reaction mixture was stirred overnight at room temperature and later quenched with 2 M HCl (8 ml) which resulted in a two-phase system. The product was extracted by adding DCM (5 x 30 ml). The organic phase was dried over  $\text{Na}_2\text{SO}_4$  and filtered. The solvent was then removed under reduced pressure, and the crude product was purified by trituration in 96 % EtOH (30 ml). 140 mg yellow powder in 75 % yield was obtained.

**Molecular formula:**  $\text{C}_{29}\text{H}_{35}\text{NO}_2$ . **Yield:** 140 mg, 75%. **MP:** 168-170°C. **TLC:**  $R_f = 0.8$  (heptane/toluene, 1:2).  **$^1\text{H NMR}$**  (500 MHz,  $\text{DMSO-}d_6$ )  $\delta$  1.76 (s, 36H), 7.64 (s, 4H), 11.61 (s, 2H) ppm.  **$^{13}\text{C NMR}$**  was not measured.

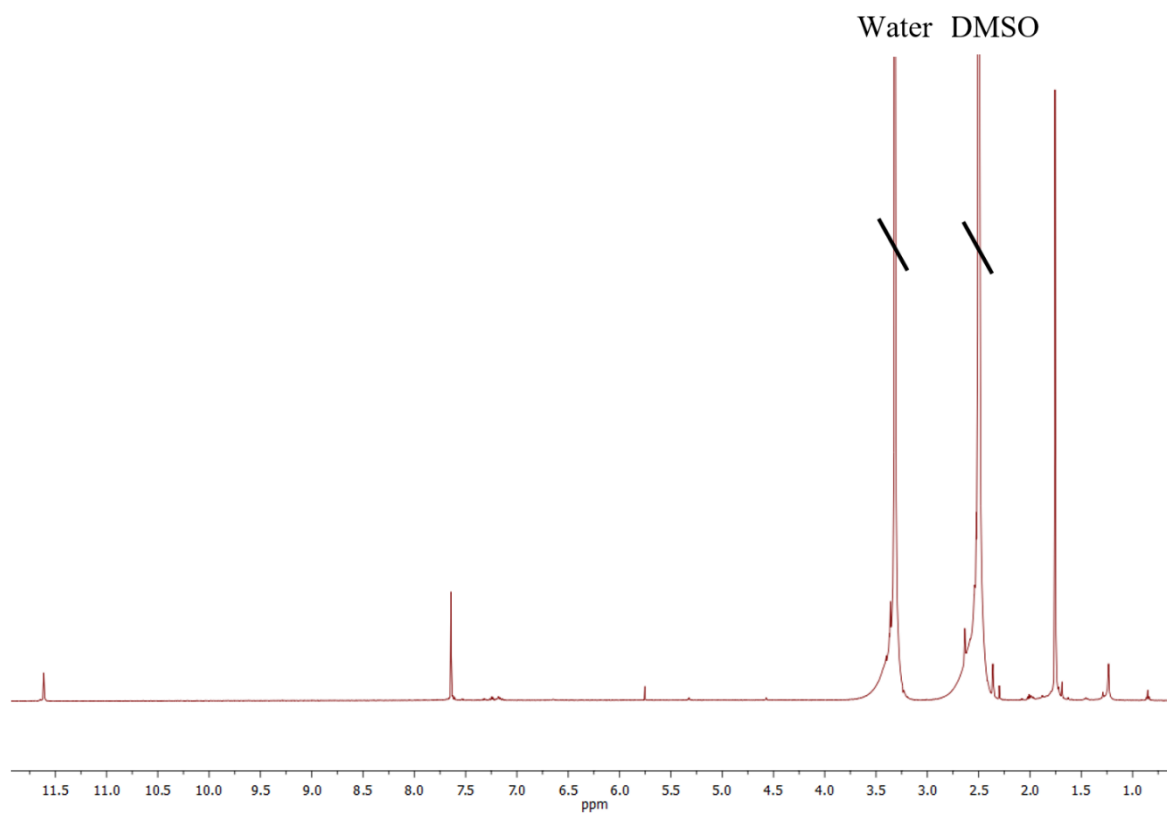
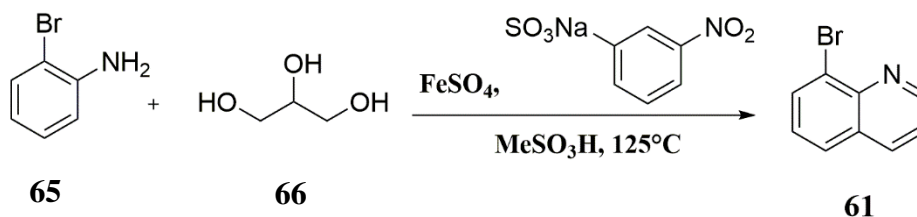


**Figure 56.**  $^1\text{H}$  NMR spectra of compound 10.

## 9.9 Synthesis of 8-bromoquinoline 61



In a 500 ml round bottom flask, methanesulfonic acid (32 ml) was warmed while stirring up to 125 °C. 2-Bromoaniline (10 g, 60 mmol) was added followed by iron sulfate heptahydrate (0.5 g, 1.80 mmol). Glycerol (13 ml, 180 mmol) was added dropwise, and the brown solution was stirred overnight.

The next day the solution was let to reach room temperature, and water (40 ml) was added. The black-brown solution was transferred to a beaker, which was placed in an ice bath. An aqueous NaOH solution (50% m/v) was added while stirring until the solution was basified up to pH 14. The heterogeneous mixture was extracted with Et<sub>2</sub>O, and the emulsion was let to rest for 10 minutes. The organic extracts were washed with brine (200 ml), dried over Na<sub>2</sub>SO<sub>4</sub> and filtered through celite. The expected product, 8-bromoquinoline, was obtained as a viscous brown oil.

**Molecular formula:** C<sub>9</sub>H<sub>6</sub>BrN. **Yield:** 8.82 g (73%). **MP:** ≈ 240 ° (With decomposition). **TLC:** R<sub>f</sub> = 0.30 (heptane:dichloromethane, 1:1). **<sup>1</sup>H NMR** (500 MHz, CDCl<sub>3</sub>) δ 7.41 (t, 1H) 7.47 (dd, 1H), 7.80 (dd, 1H), 8.06 (dd, 1H), 8.18 (dd, 1H), 9.06 (dd, 1H) ppm. **<sup>13</sup>C NMR** was not measured.

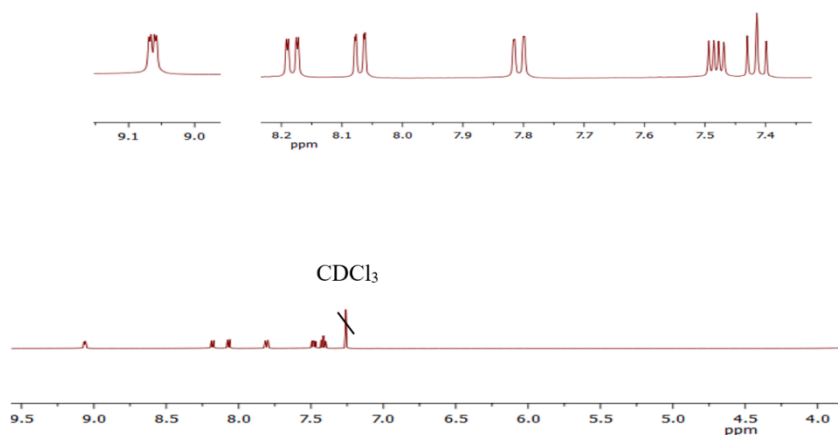
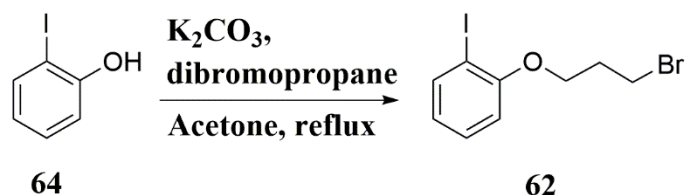


**Figure 57.** <sup>1</sup>H NMR spectra of compound **61**.

### 9.10 Synthesis of 1-(3-bromopropoxy)-2-iodobenzene 62



2-iodophenol (3.5 g, 15.91 mmol), potassium carbonate (11 g, 79.5 mmol) and an excess amount of dibromopropane (23 ml, 227 mmol) were added in a 250 ml round bottom flask. Subsequently, acetone (150 ml) was added as a solvent. The mixture was stirred for 48 hours under reflux.

The acetone was removed by rotary evaporator. Water and ether were added, and the organic layer was separated, dried over  $\text{MgSO}_4$  and filtered. The flask contained a white solid. Flash column with heptane was used for purification. The product was obtained as a yellow liquid.

**Molecular formula:**  $\text{C}_9\text{H}_9\text{BrIO}$ . **Yield:** 4.95 ml, 91 %. **TLC:** Heptane,  $R_f = 0.3$ .  **$^1\text{H NMR}$**  (500 MHz,  $\text{DMSO}-d_6$ )  $\delta$  2.37 (tt, 2H), 3.72 (t, 2H), 4.16 (t, 2H), 6.72 (td, 1H), 6.84 (dd, 1H), 7.27-7.33 (m, 1H), 7.77 (dd, 1H).  **$^{13}\text{C NMR}$**  was not measured.

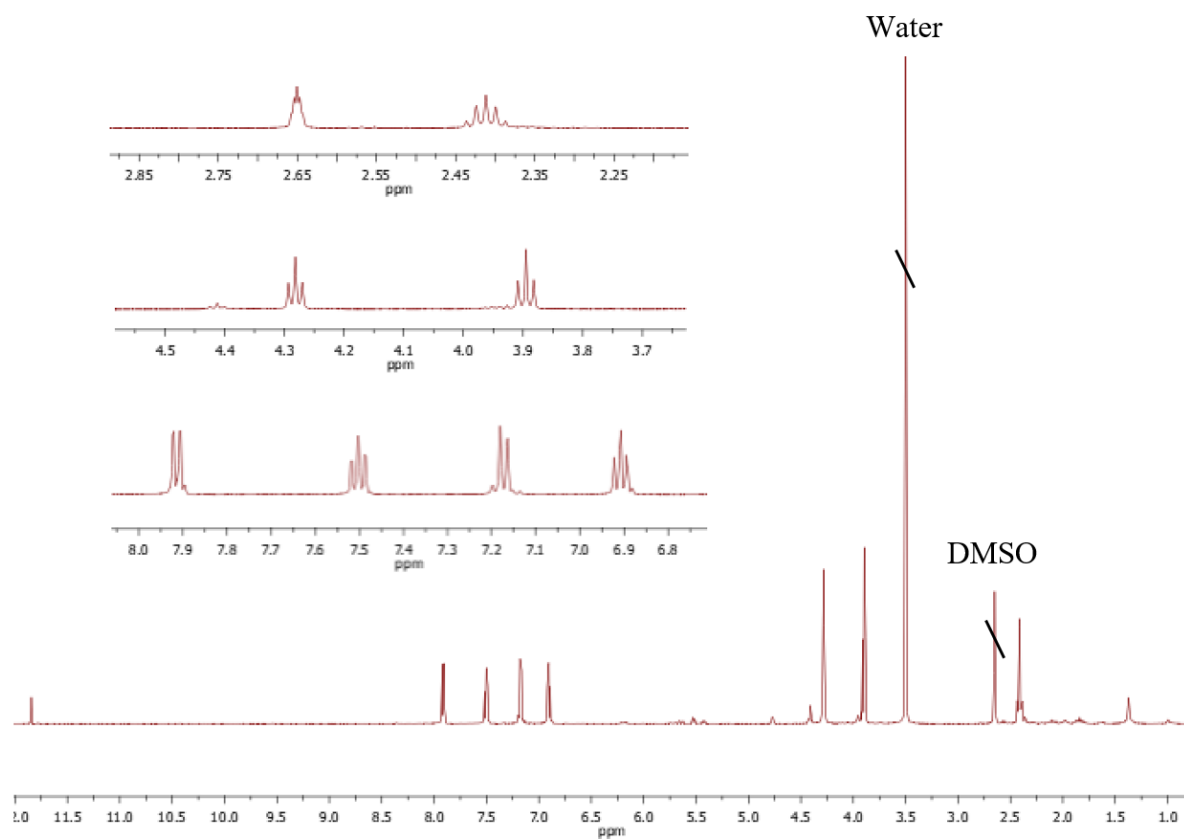
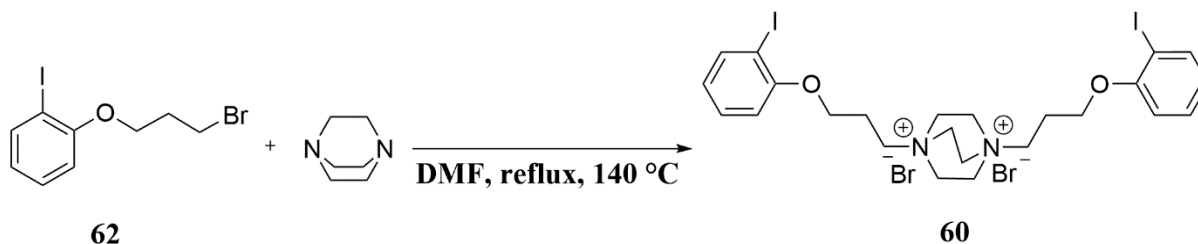


**Figure 58.**  $^1\text{H}$  NMR spectra of compound **62**.



### 9.11 Synthesis of DABCO with 1-(3-bromopropoxy)-2-iodobenzene **62**



A mixture of 1,4-Diazabicyclo[2.2.2]octane (DABCO) (560 mg, 5 mmol) and 1-(3-bromopropoxy)-2-iodobenzene **62** (3.41 g, 10 mmol) in DMF (10 ml) was stirred in a 50 ml round bottom flask for 1 hour at room temperature, then let to stir overnight at 140 °C.

The next day absolute ethanol (20 ml) was added to precipitate the quaternary ammonium salt. The mixture was let stand at room temperature for 5 hours, and the solid **60** was filtered and washed with cold ethanol, after which it was dried.

**Molecular formula:** C<sub>24</sub>H<sub>32</sub>Br<sub>2</sub>I<sub>2</sub>N<sub>2</sub>O<sub>2</sub>. **Yield:** 2.3 g, 34 %. **MP:** ≈ 205 °C. **TLC:** DCM:MeOH, 1:4, R<sub>f</sub> = 0.4. **<sup>1</sup>H NMR** (500 MHz, DMSO-*d*<sub>6</sub>) δ 2.27 (tt, 4H), 3.73 (t, 4H), 3.95 (t, 12H), 4.16 (td, 4H), 6.80 (dd, 2H), 6.78-6.82 (m, 2H), 7.05-7.07 (dd, 2H), 7.37-7.41 (dd, 2H), 7.79-7.81 (dd, 2H). **<sup>13</sup>C NMR** was not measured.

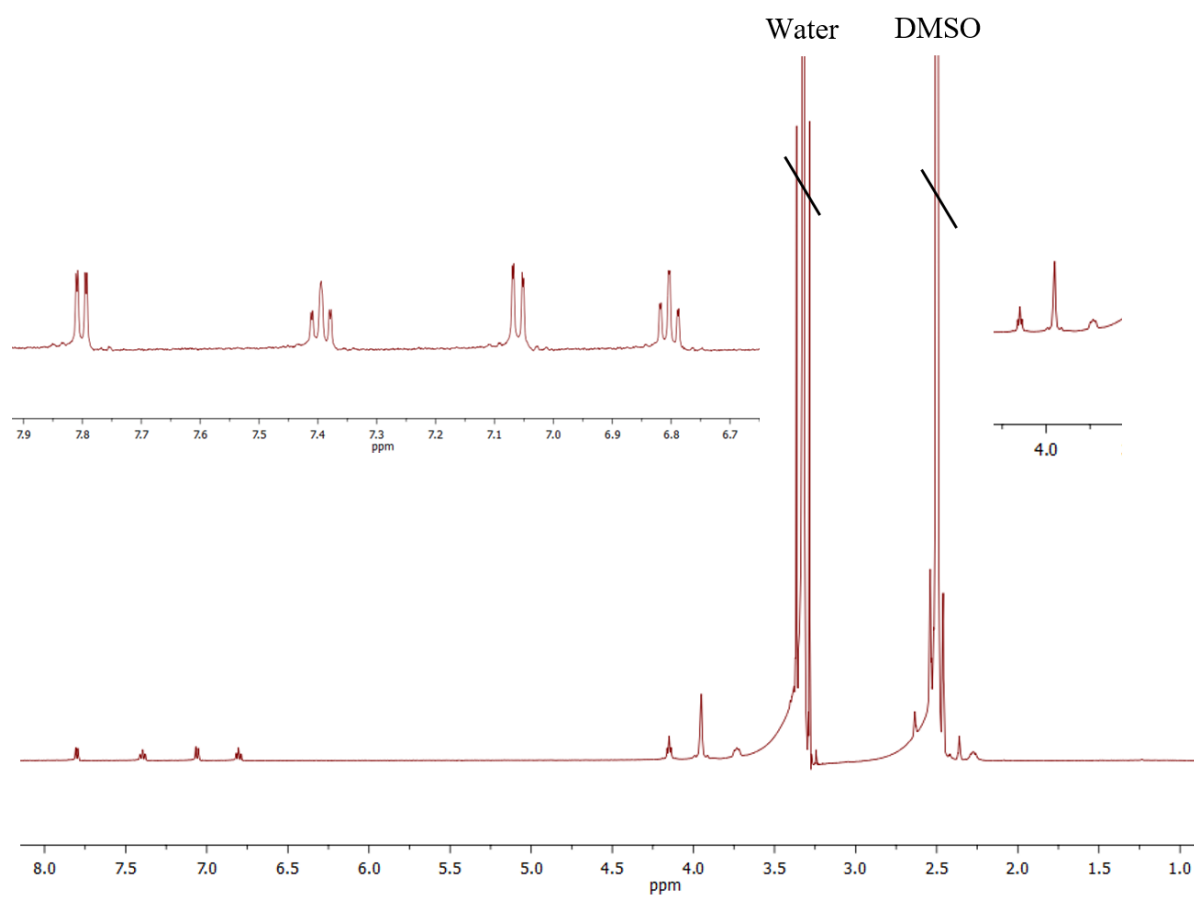
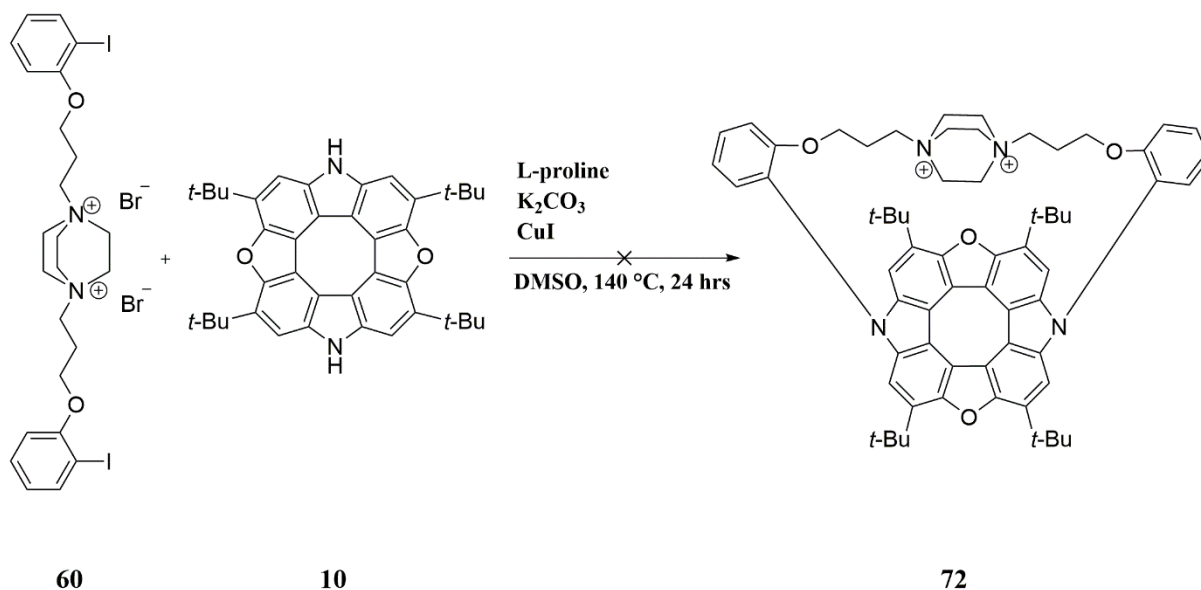


**Figure 59.**  $^1\text{H}$  NMR spectra of compound **60**.

## 9.12 Synthesis of a circulenophane: Approach I 72

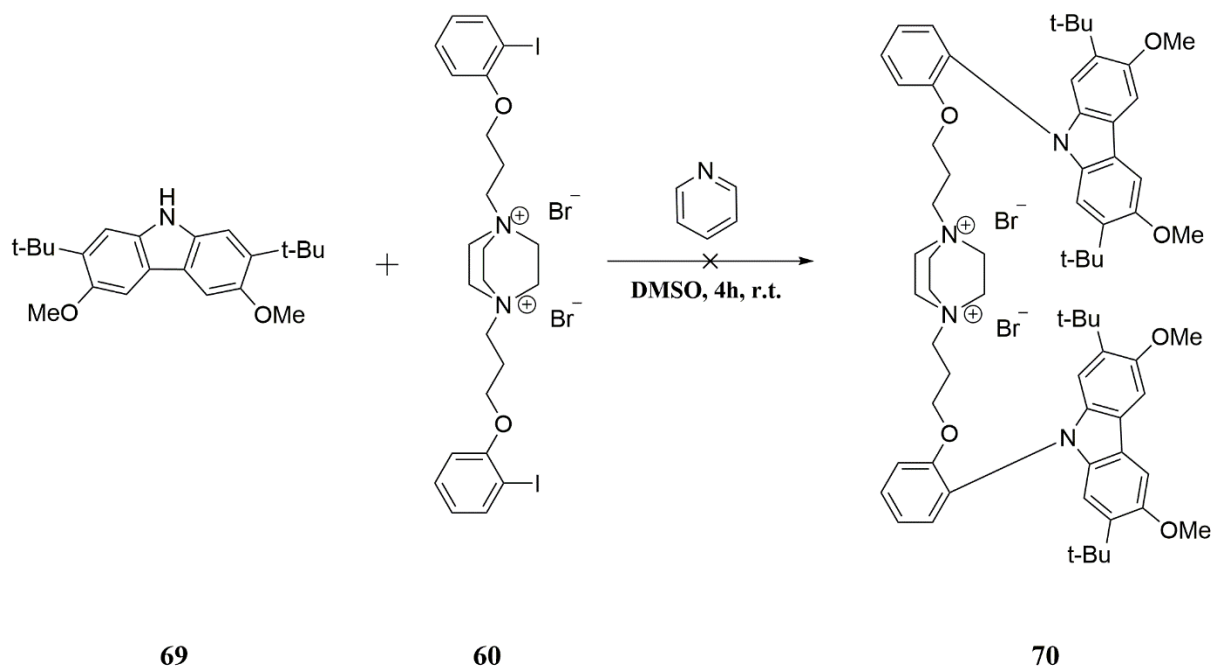


Linker **60** (10 mg, 18.81  $\mu\text{mol}$ ) and diazadioxo[8]circulene **10** (50 mg, 62.96  $\mu\text{mol}$ ) were placed in a 25 ml flask.  $\text{K}_2\text{CO}_3$  (9.2 mg, 66.57  $\mu\text{mol}$ ),  $\text{CuI}$  (4.40 mg, 23.10  $\mu\text{mol}$ ) and L-proline (2.02 mg, 17.55  $\mu\text{mol}$ ) were added. 4 ml DMSO as solvent was added to the flask. The solution was stirred for 24 hours at 140  $^\circ\text{C}$ .

10 ml of water was added for the workup. The solution turned bright with precipitation. Copper slats could be seen in brown color. A mixture of  $\text{EtOAc}:\text{Cyclohexane}$ , 1:2 (3x30 ml) was added to the solution. The organic phase was separated, and the copper salt was filtered. Organic layer was quenched with brine and dried over  $\text{MgSO}_4$ . The solvent was removed by rotary evaporator.

**Molecular formula:**  $\text{C}_{64}\text{H}_{72}\text{N}_4\text{O}_4^{2+}$ . **TLC:**  $\text{DCM}:\text{Hep}$ , 1:1,  $R_f = 0.6$ .

### 9.13 Synthesis of a circulenophane: Approach II 72



Compound **69** (50 mg, 147.28  $\mu\text{mol}$ ) was dissolved in 50 ml DMSO. Pyridine (11.88  $\mu\text{l}$ , 147.47  $\mu\text{mol}$ ) was added. Then linker **60** (58.48 mg, 73.64  $\mu\text{mol}$ ) was added. The mixture was stirred at room temperature for 4 hours.

The mixture was poured on 100 ml ice water and extracted with cyclohexane:EtOAc (2x50 ml, 1:2). Organic extracts were washed with brine 50 ml and water 50 ml, a pink foggy mixture appeared. The organic phase dried over  $\text{MgSO}_4$ . The solvent was removed by rotary evaporator.

**Molecular formula:**  $\text{C}_{68}\text{H}_{88}\text{Br}_2\text{N}_4\text{O}_6$ . **TLC:** DCM:Hep, 1:1,  $R_f = 0.6$ .

## 10 CONCLUSIONS AND OUTLOOK

Cyclooctatetraene (COT) compounds are versatile building blocks and easy to synthesize. They form a saddle-shaped conformation, however, which makes them hard to study. A hetero[8]circulene is one option containing aromatic  $\pi$ -system with different bond angles to overcome the non-planar conformation. Different heterocycles affect the geometry of the circulenes creating a smaller bond angle, therefore resulting in a planar diazadioxo[8]circulene. To defeat this obstacle substituents containing heteroatoms have been added around the core. This approach allowed investigating antiaromatic properties of the COT core.

To study the property of the planarized circulene, cyclophane-chemistry has been applied to create a system in which the circulene substrate holds a bridge-type linker containing protons in its centre. The linker is covalently bonded through the pyrrole nitrogens of the circulene system. Creating this system enables further study of the antiaromaticity of the circulenophane compound.

This project focused on synthesizing the linker **51** containing a bicyclo moiety for the bulkier center. However, the synthesis remained unsuccessful due to the challenging synthetic path and purification. Step 4 toward synthesizing a bulkier linker failed, and very low yield was obtained. The reaction is known as Horner-Wadsworth-Emmons, using aldehydes or ketones as starting material and converting them to olefinic products by utilising a phosphonate catalyst. Repeating the reaction was unsuccessful. The reason could be the poor reaction conditions since the reagents were highly unstable.

Nevertheless, a new approach to synthesizing a linker was designed. A linker containing a DABCO moiety in the middle was suggested to be a more promising bulky unit to maximize the protons proximity to the center of the COT core.

The new linker **60** was synthesized in two steps with satisfactory yields. However, the attempt for coupling the linker to the circulene substrate remained incomplete. The NMR and mass spectrometry measurements showed coupling of one arm of the linker to the pyrrole moiety of diazadioxo[8]circulene **24**. This could be due to steric hindrance and the bulkiness of the linker. To overcome this barrier, it was suggested to repeat the reaction in higher temperature to create a force for the second arm to couple. As a second solution, a catalyst could be used to facilitate the Ullman-type coupling. However, within the period allocated for the project, the solutions mentioned above could not be performed.

For the future investigation, a circulenophane having the diazadioxo[8]circulene **24** unit can be obtained using different synthetic approaches. Two of the possible pathways are described here; however, no attempts could be pursued due to the limited time designated to this project.

The synthesis toward the circulenophane **72** can possibly be achieved by different synthesis pathways. A helicene unit **73** can be used instead of diazadioxo[8]circulene **24** to couple to the linker **60** and subsequently go through the formation of the second furan ring within two steps (Figure 60).

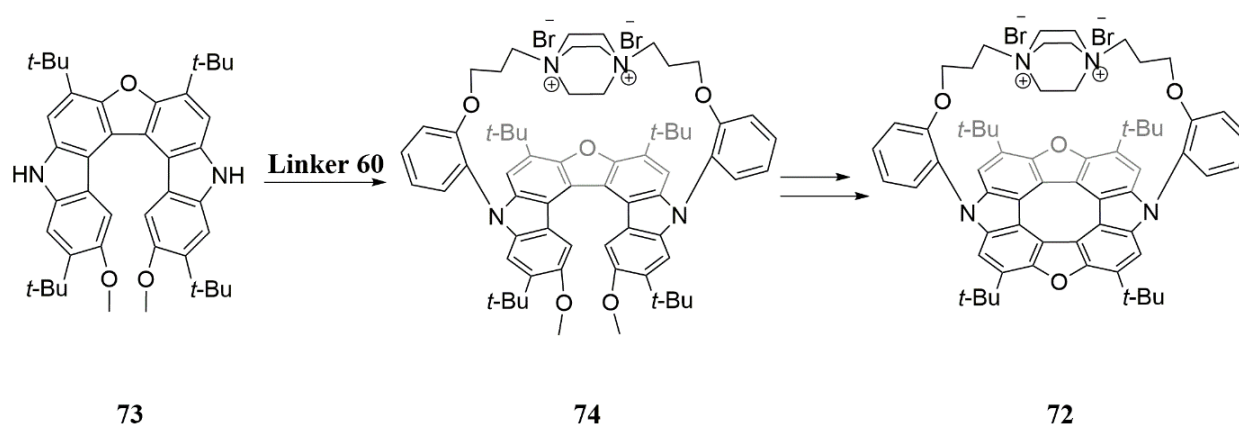


**Figure 60.** Proposed synthetic pathway for future work regarding the formation of a circulenophane **72** using a helicene **73**.

Another suggestion could be having the helicene unit with substituted aliphatic arms **76** in advance. Furthermore, the formation of linker could take place by introducing the DABCO moiety in the following step a creating compound **77**. The formation of the furan ring can be conducted in step b to achieve the circulenophane **78** (Figure 61).

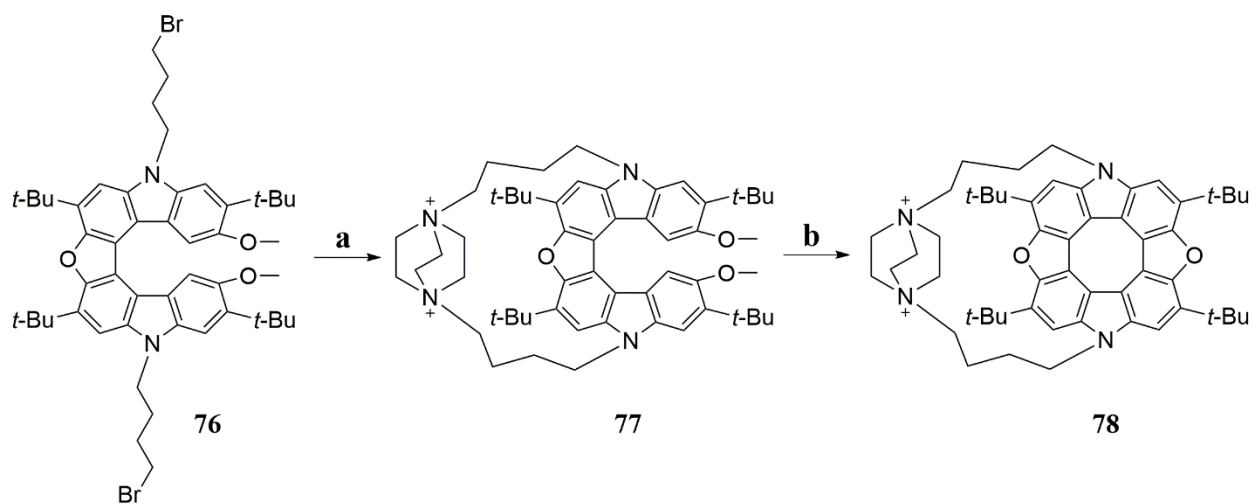


**Figure 61.** Proposed synthetic pathway for future work regarding the formation of a circulenophane **78** using a functionalized helicene **76** and DABCO.

## LITERATURE REFERENCES

1. Dopfer, J. H.; Wynberg, H., Heterocirculenes a new class of polycyclic aromatic hydrocarbons, *Tetrahedron Lett.*, **1972**, *13*, 763-766. [https://doi.org/10.1016/S0040-4039\(01\)84432-4](https://doi.org/10.1016/S0040-4039(01)84432-4).
2. Christoph, H.; Grunenberg, J.; Hopf, H.; Dix, I.; Jones, P. G.; Scholtissek, M. and Maier, G., MP2 and DFT calculations on circulenes and an attempt to prepare the second lowest benzolog, [4]circulene, *Chem. -Eur. J.*, **2008**, *14*, 5604-5616. <https://doi.org/10.1002/chem.200701837>.
3. Miller, R. W.; Averill, S. E.; Van Wyck, S. J. and Whalley, A. C.; General method for the synthesis of functionalized tetrabenzo[8]circulenes, *J. Org. Chem.*, **2016**, *81*, 12001-12005. <https://doi.org/10.1021/acs.joc.6b02244>.
4. Vaughan, D. J., Anthony, J. W., Bideaux, R. A., Bladh, K. W., Nichols, M. C., *Handbook of Mineralogy: Volume I; Elements, Sulfides, Sulfosalts*, Tucson, Arizona, 1991, 146-147. <https://doi.org/10.1180/minmag.1991.055.378.20>.
5. Feng, C. N.; Kuo, M. Y.; Wu, Y. T., Synthesis, structural analysis, and properties of [8]circulenes, *Angew. Chem. Int. Ed. Engl.*, **2013**, *52*, 7791-7794. <https://doi.org/10.1002/anie.201303875>.
6. Miller, R. W.; Duncan, A. K.; Schneebeli, S. T.; Gray, D. L.; Whalley, A. C., Synthesis and structural data of tetrabenzo[8]circulene, *Chem. -Eur. J.*, **2014**, *20*, 3705-3711. <https://doi.org/10.1002/chem.201304657>.
7. Hermann, K., 2. Über die einwirkung von ammoniak und aminbasen auf gechlorte chinone, *Justus Liebigs Ann. Chem.*, **1881**, *210*, 164-191. <https://doi.org/10.1002/jlac.18812100203>.
8. Erdtman, H.; Högberg, H.-E. H., Tetranaphthocyclo-octatetraene tetra-oxide, a cyclisation product from  $\alpha$ -naphthoquinone, *Chem. Commun.*, **1968**, *14*, 773-774. <https://doi.org/10.1039/C19680000773>.
9. Kumar, B.; King, B. T., Synthesis of 1,8,9,16-tetrakis(Trimethylsilyl)tetra-cata-tetrabenzoquadrannulene, *J. Org. Chem.*, **2012**, *77*, 10617-10622. <https://doi.org/10.1021/jo3015648>.
10. Kaufman, H. S.; Fankuchen, I.; Mark, H., Structure of cyclo-octatetraene, *Nature*, **1948**, *161*, 165. <https://doi.org/10.1038/161165a0>.
11. Kulkarni, A. P.; Tonzola, C. J.; Babel, A.; Jenekhe, S. A., Electron transport materials for organic light-emitting diodes, *Chem. Mater.*, **2004**, *16*, 4556-4573. <https://doi.org/10.1021/cm049473l>.
12. Nielsen, C. B.; Brock-Nannestad, T.; Reenberg, T. K.; Hammershøj, P.; Christensen, J. B.; Stouwdam, J. W.; Pittelkow, M., Organic light-emitting diodes from symmetrical and unsymmetrical  $\pi$ -extended tetraoxa[8]circulenes, *Chem. -Eur. J.*, **2010**, *16*, 13030-13034. <https://doi.org/10.1002/chem.201002261>.
13. Hensel, T.; Trpcevski, D.; Lind, C.; Grosjean, R.; Hammershøj, P.; Nielsen, C. B.; Brock-Nannestad, T.; Nielsen, B. E.; Schau-Magnussen, M.; Minaev, B.; Baryshnikov, G. V.; Pittelkow, M., Diazadioxa[8]circulenes: planar antiaromatic cyclooctatetraenes, *Chem. -Eur. J.*, **2013**, *19*, 17097-17102. <https://doi.org/10.1002/chem.201303194>.
14. Hensel, T.; Andersen, N. N.; Plesner, M.; Pittelkow, M., Synthesis of heterocyclic



- [8]circulenes and related structures, *Synlett.*, **2016**, 27, 498-525.  
<https://doi.org/10.1055/s-0035-1560524>.
15. Zhang, B.; Manning, G. P.; Dobrowolski, M. A.; Cyrański, M. K.; Bodwell, G. J., Nonplanar aromatic compounds. 9. synthesis, structure, and aromaticity of 1:2,13:14-dibenzo[2]paracyclo[2](2,7)-pyrenophane-1,13-diene, *Org. Lett.*, **2007**, 10, 273-276.  
<https://doi.org/10.1021/ol702703b>.
  16. Krygowski, T. M.; Cyrański, M. K.; Czarnocki, Z.; Häfelinger, G.; Katritzky, A. R., Aromaticity: a theoretical concept of immense practical importance, *Tetrahedron*, **2000**, 56, 1783-1796. [https://doi.org/10.1016/S0040-4020\(99\)00979-5](https://doi.org/10.1016/S0040-4020(99)00979-5).
  17. Balaban, A. T.; Schleyer, P. v. R.; Rzepa, H. S., Crocker, not Armit and Robinson, begat the six aromatic electrons, *Chem. Rev.*, **2005**, 105, 3436-3447.  
<https://doi.org/10.1021/cr0300946>.
  18. Kaiser, R., "Bicarburet of hydrogen". Reappraisal of the discovery of benzene in 1825 with the analytical methods of 1968, *Angew. Chem. Int. Ed. Engl.*, **1968**, 7, 345-350.  
<https://doi.org/10.1002/anie.196803451>.
  19. Kekulé, A., Untersuchungen über aromatische verbindungen ueber die constitution der aromatischen verbindungen. I. ueber die constitution der aromatischen verbindungen. *Justus Liebigs Ann. Chem.*, **1866**, 137, 129-196.  
<https://doi.org/10.1002/jlac.18661370202>.
  20. Hofmann, A. W. V., I. On insolinic acid, *Proc. R. Soc. London*, **1857**, 8, 1-3.  
<https://doi.org/10.1098/rspl.1856.0002>.
  21. Ladenburg, A., Bemerkungen zur aromatischen theorie, *Berichte der Dtsch. Chem. Ges.*, **1869**, 2, 140-142. <https://doi.org/10.1002/cber.18690020171>.
  22. Dewar, J., 5. On the oxidation of phenyl alcohol, and a mechanical arrangement adapted to illustrate structure in the nonsaturated hydrocarbons, *Proc. R. Soc. Edinburgh*, **1869**, 6, 82-86. <https://doi.org/DOI:10.1017/S0370164600045387>.
  23. Frenking, G.; Krapp, A., Unicorns in the world of chemical bonding models, *J. Comput. Chem.*, **2007**, 28, 15-24. <https://doi.org/10.1002/jcc.20543>.
  24. Stanger, A., What is... aromaticity: a critique of the concept of aromaticity—can it really be defined?, *Chem. Commun.*, **2009**, 15, 1939-1947.  
<https://doi.org/10.1039/B816811C>.
  25. Krygowski, T. M.; Cyrański, M. K., Structural aspects of aromaticity, *Chem. Rev.*, **2001**, 101, 1385-1420. <https://doi.org/10.1021/cr990326u>.
  26. Cyrański, M. K., Energetic aspects of cyclic pi-electron delocalization: evaluation of the methods of estimating aromatic stabilization energies, *Chem. Rev.*, **2005**, 105, 3773-3811. <https://doi.org/10.1021/cr0300845>.
  27. Poater, J.; Duran, M.; Solà, M.; Silvi, B., Theoretical evaluation of electron delocalization in aromatic molecules by means of atoms in molecules (AIM) and electron localization function (ELF) topological approaches, *Chem. Rev.* **2005**, 105, 3911-3947. <https://doi.org/10.1021/cr030085x>.
  28. Merino, G.; Vela, A.; Heine, T., Description of electron delocalization via the analysis of molecular fields, *Chem. Rev.*, **2005**, 105, 3812-3841.  
<https://doi.org/10.1021/cr030086p>.
  29. Gomes, J. A. N. F.; Mallion, R. B., Aromaticity and ring currents, *Chem. Rev.*, **2001**,

- 101, 1349-1384. <https://doi.org/10.1021/cr990323h>.
30. Heine, T.; Corminboeuf, C.; Seifert, G., The magnetic shielding function of molecules and pi-electron delocalization, *Chem. Rev.*, **2005**, *105*, 3889-3910. <https://doi.org/10.1021/cr030082k>.
  31. Lazzeretti, P., Assessment of aromaticity *via* molecular response properties, *Phys. Chem. Chem. Phys.*, **2004**, *6*, 217-223. <https://doi.org/10.1039/b311178d>.
  32. Feilchenfeld, H., A relation between the lengths of single, double and triple bonds, *J. Phys. Chem.*, **1959**, *63*, 1346-1346. <https://doi.org/10.1021/j150578a603>.
  33. Coulson, C. A.; Golebiewski, A., On perturbation calculations for the  $\pi$ -electrons and their application to bond length reconsiderations in aromatic hydrocarbons, *Proc. Phys. Soc.*, **1961**, *78*, 1310-1320. <https://doi.org/10.1088/0370-1328/78/6/335>.
  34. Freeman, P. K., Neutral homoaromaticity in some heterocyclic systems, *J. Org. Chem.*, **2005**, *70*, 1998-2001. <https://doi.org/10.1021/jo040250o>.
  35. Hückel, E., Quantentheoretische beiträge zum benzolproblem - I. Die elektronenkonfiguration des benzols und verwandter verbindungen, *Z. Phys.*, **1931**, *70*, 204-286. <https://doi.org/10.1007/BF01339530>.
  36. Hückel, E., Quantentheoretische beiträge zum problem der aromatischen und ungesättigten verbindungen. III., *Z. Phys.*, **1932**, *76*, 628-648. <https://doi.org/10.1007/BF01341936>.
  37. Clar, E.; Zander, M., 378. 1 : 12-2 : 3-10 : 11-tribenzoperylene, *J. Chem. Soc.*, **1958**, *0*, 1861-1865. <https://doi.org/10.1039/JR9580001861>.
  38. Armit, J. W.; Robinson, R., CCXI. - polynuclear heterocyclic aromatic types. Part II. Some anhydronium bases, *J. Chem. Soc. Trans.*, **1925**, *127*, 1604-1618. <https://doi.org/10.1039/CT9252701604>.
  39. Hauptmann, S., The aromatic sextet: Von E. Clar; *Z. Chem.*, **1973**, *13*, 200-200. <https://doi.org/10.1002/zfch.19730130531>.
  40. Clar, E., *Polycyclic hydrocarbons*, Springer, Berlin, Heidelberg, Germany, 1964.
  41. Solà, M., Forty years of Clar's aromatic  $\pi$ -sextet rule, *Front. Chem.* **2013**, *1*, 1-8. <https://doi.org/10.3389/fchem.2013.00022>.
  42. Breslow, R., Aromatic character, *Chem. Eng. News Arch.* **1965**, *43*, 90-100. <https://doi.org/10.1021/cen-v043n026.p090>.
  43. Breslow, R.; Brown, J.; Gajewski, J. J., Antiaromaticity of cyclopropenyl anions, *J. Am. Chem. Soc.*, **1967**, *89*, 4383-4390. <https://doi.org/10.1021/ja00993a023>.
  44. Balaban, A. T., To be or not to be ... aromatic?, *Rev. Roum. Chim.*, **2015**, *60*, 121-140.
  45. Labarre, J.-F.; Crasnier, F., *Critique of the notion of aromaticity. In electronic structure of organic compounds*, Fortschritte der Chemischen Forschung, vol. 24, Springer, Berlin, Heidelberg, Germany, 1971, pp. 33-54. <https://doi.org/10.1007/bfb0051963>.
  46. Wiberg, K. B., Properties of some condensed aromatic systems, *J. Org. Chem.*, **1997**, *62*, 5720-5727. <https://doi.org/10.1021/jo961831j>.
  47. Bühl, M.; Hirsch, A., Spherical aromaticity of fullerenes, *Chem. Rev.*, **2001**, *101*, 1153-1184. <https://doi.org/10.1021/cr990332q>.

48. Pauling, L., G. N. Lewis and the chemical bond, *J. Chem. Educ.*, **1984**, *61*, 201-201. <https://doi.org/10.1021/ed061p201>.
49. Singh, J.; Singh, S.; Meer, S.; Agrawal, V. K.; Khadikar, P. V.; Balaban, A. T., QSPR Correlations of half-wave reduction potentials of cata-condensed benzenoid hydrocarbons, *ARKIVOC*, **2006**, *15*, 104-119.
50. Chen, T. A.; Liu, R. S., Synthesis of polyaromatic hydrocarbons from bis(biaryl)diynes: large PAHs with low Clar sextets, *Chem. -Eur. J.*, **2011**, *17*, 8023-8027. <https://doi.org/10.1002/chem.201101057>.
51. Pauling, L.; Sherman, J., The nature of the chemical bond. VI. The calculation from thermochemical data of the energy of resonance of molecules among several electronic structures, *J. Chem. Phys.*, **1933**, *1*, 606-617. <https://doi.org/10.1063/1.1749335>.
52. Mo, Y., The resonance energy of benzene: a revisit, *J. Phys. Chem.*, **2009**, *113*, 5163-5169. <https://doi.org/10.1021/jp808941h>.
53. Stevenson, G. R., The determination of the resonance energy of benzene. A physical chemistry laboratory experiment, *J. Chem. Educ.*, **1972**, *49*, 781-782. <https://doi.org/10.1021/ed049p781>.
54. Pople, J. A., Molecular orbital theory of aromatic ring currents, *Mol. Phys.*, **1958**, *1*, 175-180. <https://doi.org/10.1080/00268975800100211>.
55. von Schleyer, P. R.; Jiao, H., What is aromaticity?, *Pure Appl. Chem.*, **1996**, *68*, 209-218. <https://doi.org/10.1351/pac199668020209>.
56. Hunadi, R. J., Methano-bridged compounds. 1. Correlation of the <sup>13</sup>C nuclear magnetic resonance shift average and shift of the bridge carbon with the average  $\pi$ -electron density of methano-bridged and homoaromatic compounds, *J. Am. Chem. Soc.*, **1983**, *105*, 6889-6895. <https://doi.org/10.1021/ja00361a025>.
57. Gershoni-Poranne, R.; Stanger, A., Magnetic criteria of aromaticity, *Chem. Soc. Rev.*, **2015**, *44*, 6597-6615. <https://doi.org/10.1039/C5CS00114E>.
58. Wolinski, K.; Hinton, J. F.; Pulay, P., Efficient implementation of the gauge-independent atomic orbital method for NMR chemical shift calculations, *J. Am. Chem. Soc.*, **1990**, *112*, 8251-8260. <https://doi.org/10.1021/ja00179a005>.
59. Von Ragué Schleyer, P.; Manoharan, M.; Wang, Z. X.; Kiran, B.; Jiao, H.; Puchta, R.; Van Eikema Hommes, N. J. R., Dissected nucleus-independent chemical shift analysis of  $\pi$ -aromaticity and antiaromaticity, *Org. Lett.*, **2001**, *3*, 2465-2468. <https://doi.org/10.1021/ol016217v>.
60. Schleyer, P. V. R.; Maerker, C.; Dransfeld, A.; Jiao, H.; van Eikema Hommes, N. J. R., Nucleus-independent chemical shifts: A simple and efficient aromaticity probe, *J. Am. Chem. Soc.*, **1996**, *118*, 6317-6318. <https://doi.org/10.1021/ja960582d>.
61. Barth, W. E.; Lawton, R. G., Dibenzo[Ghi,Mno]fluoranthene, *J. Am. Chem. Soc.*, **1966**, *88*, 380-381. <https://doi.org/10.1021/ja00954a049>.
62. Gholami, M. M.; Tykwinski, R. R., Oligomeric and polymeric systems with a cross-conjugated  $\pi$ -framework, *Chem. Rev.*, **2006**, *106*, 4997-5027. <https://doi.org/10.1021/cr0505573>.
63. Scholl, R.; Meyer, K., Synthese des anti-diperi-dibenz-Coronens und dessen abbau zum coronen (Hexabenzobenzol). (Mitbearbeitet von horst v. Hoeßle und solon brissimdji), *Dtsch. Chem. Ges.*, **1932**, *65*, 902-915.

- <https://doi.org/10.1002/cber.19320650546>.
64. Bharat, R. B.; Bally, T.; Valente, A.; Cyrański, M. K.; Dobrzycki, Ł.; Spain, S. M.; Rempała, P.; Chin, M. R.; King, B. T., Quadrannulene: a nonclassical fullerene fragment, *Angew. Chem. Int. Ed. Engl.*, **2010**, *49*, 399-402. <https://doi.org/10.1002/anie.200905633>.
  65. Kumar, B.; King, B. T., Synthesis of 1,8,9,16-tetrakis(trimethylsilyl)tetra-cata-tetrabenzoquadrannulene, *J. Org. Chem.*, **2012**, *77*, 10617-10622. <https://doi.org/10.1021/jo3015648>.
  66. Yamamoto, K.; Harada, T.; Nakazaki, M.; Naka, T.; Kai, Y.; Harada, S.; Kasai, N., Synthesis and characterization of [7]circulene, *J. Am. Chem. Soc.*, **1983**, *105*, 7171-7172. <https://doi.org/10.1021/ja00362a025>.
  67. Pun, S. H.; Wang, Y.; Chu, M.; Chan, C. K.; Li, Y.; Liu, Z.; Miao, Q., Synthesis, structures, and properties of heptabenzo[7]circulene and octabenzo[8]circulene, *J. Am. Chem. Soc.*, **2019**, *141*, 9680-9686. <https://doi.org/10.1021/jacs.9b03910>.
  68. Kroto, H. W.; Heath, J. R.; O'Brien, S. C.; Curl, R. F.; Smalley, R. E., C60: buckminsterfullerene, *Nature*, **1985**, *318*, 162-163. <https://doi.org/10.1038/318162a0>.
  69. Chen, F.; Hong, Y. S.; Shimizu, S.; Kim, D.; Tanaka, T.; Osuka, A., Synthesis of a tetrabenzotetraaza[8]circulene by a "Fold-in" oxidative fusion reaction, *Angew. Chem. Int. Ed. Engl.*, **2015**, *54*, 10639-10642. <https://doi.org/10.1002/anie.201505124>.
  70. Serizawa, Y.; Akahori, S.; Kato, S.; Sakai, H.; Hasobe, T.; Miyake, Y.; Shinokubo, H., Synthesis of tetrasilatetrathia[8]circulenes by a fourfold intramolecular dehydrogenative silylation of C-H bonds, *Chem. -Eur. J.*, **2017**, *23*, 6948-6952. <https://doi.org/10.1002/chem.201700729>.
  71. Xiong, X.; Deng, C. L.; Minaev, B. F.; Baryshnikov, G. V.; Peng, X. S.; Wong, H. N. C., Tetrathio and tetraseleno[8]circulenes: synthesis, structures, and properties, *Chem. -Asian J.*, **2015**, *10*, 969-975. <https://doi.org/10.1002/asia.201403028>.
  72. Liljefors, T.; Wennerström, O., Molecular mechanics calculations on the structures and conformational properties of [8]circulene and some related phane compounds, *Tetrahedron*, **1977**, *33*, 2999-3003. [https://doi.org/10.1016/0040-4020\(77\)88037-X](https://doi.org/10.1016/0040-4020(77)88037-X).
  73. Salcedo, R.; Sansores, L. E.; Picazo, A.; Sansón, L., [8]circulene. Theoretical approach, *J. Mol. Struct.: THEOCHEM*, **2004**, *678*, 211-215. <https://doi.org/10.1016/j.theochem.2004.03.020>.
  74. Hellwinkel, D.; Reiff, G., Cyclooctatetraene systems flattened by steric constraints, *Angew. Chem. Int. Ed. Engl.*, **1970**, *9*, 527-528 <https://doi.org/10.1002/anie.197005271>.
  75. Hellwinkel, D.; Reiff, G., Durch sterische zwänge eingeebnete cyclooctatetraen-systeme, *Angew. Chem. Int. Ed. Engl.*, **1970**, *82*, 516-517. <https://doi.org/10.1002/ange.19700821309>.
  76. Erdtman, H. G. H., Studies on the formation of complex oxidation and condensation products of phenols. A contribution to the investigation of the origin and nature of humic acid. Part I. Studies of the reactivity of simple monocyclic quinones, *Proc. R. Soc. A Math. Phys. Eng. Sci.*, **1933**, *143*, 177-191. <https://doi.org/10.1098/rspa.1933.0212>.
  77. Nielsen, C. B.; Brock-Nannestad, T.; Hammershøj, P.; Reenberg, T. K.; Schau-Magnussen, M.; Trpceviski, D.; Hensel, T.; Salcedo, R.; Baryshnikov, G. V.; Minaev,

- B. F.; Pittelkow, M., Azatrioxa[8]circulenes: planar anti-aromatic cyclooctatetraenes, *Chem. -Eur. J.*, **2013**, *19*, 3898-3904. <https://doi.org/10.1002/chem.201203113>.
78. Dadvand, A.; Cicoira, F.; Chernichenko, K. Y.; Balenkova, E. S.; Osuna, R. M.; Rosei, F.; Nenajdenko, V. G.; Perepichka, D. F., Heterocirculenes as a new class of organic semiconductors, *Chem. Commun.*, **2008**, 5354-5356. <https://doi.org/10.1039/b809259a>.
79. Nakamura, Y.; Aratani, N.; Shinokubo, H.; Takagi, A.; Kawai, T.; Matsumoto, T.; Yoon, Z. S.; Kim, D. Y.; Ahn, T. K.; Kim, D.; Muranaka, A.; Kobayashi, N.; Osuka, A., A directly fused tetrameric porphyrin sheet and its anomalous electronic properties that arise from the planar cyclooctatetraene core, *J. Am. Chem. Soc.*, **2006**, *128*, 4119-4122. <https://doi.org/10.1021/ja057812l>.
80. Baryshnikov, G. V.; Karaush, N. N.; Minaev, B. F., The electronic structure of heteroannelated cyclooctatetraenes and their UV-VIS absorption spectra, *Chem. Heterocycl. Compd.*, **2014**, *50*, 349-363. <https://doi.org/10.1007/s10593-014-1482-7>.
81. Shen, M.; Ignatyev, I. S.; Xie, Y.; Schaefer, H. F., [7]circulene: a remarkably floppy polycyclic aromatic C<sub>28</sub>H<sub>14</sub> Isomer, *J. Phys. Chem.*, **1993**, *97*, 3212-3216. <https://doi.org/10.1021/j100115a024>.
82. Dopfer, J. H.; Wynberg, H., Synthesis and properties of some heterocirculenes, *J. Org. Chem.*, **1975**, *40*, 1957-1966. <https://doi.org/10.1021/jo00901a019>.
83. Högberg, H.-E.; Brandänge, S.; Lindström, B.; Enzell, C. R.; Enzell, C. R.; Swahn, C.-G., Cyclo-oligomerization of quinones. V. The acid catalyzed reactions of alpha-naphthoquinone with phenols, *Acta Chem. Scand.*, **1973**, *27*, 2559-2566. <https://doi.org/10.3891/acta.chem.scand.27-2559>.
84. Kwiatkowski, J. S.; Leszczyński, J.; Teca, I., Molecular structure and infrared spectra of furan, thiophene, selenophene and their 2,5-N and 3,4-N derivatives: density functional theory and conventional post-Hartree-Fock MP2 studies, *J. Mol. Struct.*, **1997**, *436-437*, 451-480. [https://doi.org/10.1016/S0022-2860\(97\)00125-7](https://doi.org/10.1016/S0022-2860(97)00125-7).
85. Liebermann, C., Ueber das verhalten von benzo- und  $\alpha$ -naphthochinon gegen schwefelsäure, *Dtsch. Chem. Ges.*, **1885**, *18*, 966-968. <https://doi.org/10.1002/cber.188501801200>.
86. Erdtman, H. G. H., Studies on the formation of complex oxidation and condensation products of phenols. Part III. Rearrangements of oxidation-reduction type in the diquinone Group, *Proc. R. Soc. A Math. Phys. Eng. Sci.*, **1933**, *143*, 223-227. <https://doi.org/10.1098/rspa.1933.0214>.
87. Erdtman, H. G. H.; Högberg, H.-E., Cyclooligomerisation of quinones, *Tetrahedron Lett.*, **1970**, *11*, 3389-3392. [https://doi.org/10.1016/S0040-4039\(01\)98484-9](https://doi.org/10.1016/S0040-4039(01)98484-9).
88. Högberg, H.-E.; Klitgaard, N. A.; Bernatek, E.; Galy, J.; Pearson, W. B.; Meisalo, V. Cyclo-oligomerization of quinones. III. The action of strong acids on 1,4-naphthoquinone, *Acta Chem. Scand.*, **1972**, *26*, 309-316. <https://doi.org/10.3891/acta.chem.scand.26-0309>.
89. Högberg, H.-E.; Leander, K.; Lünig, B.; Rosenblom, J.; Pilotti, Å., Cyclo-oligomerization of quinones. IV. The action of strong acids on 2,3-dialkyl-p-benzoquinones, *Acta Chem. Scand.*, **1972**, *26*, 2752-2758. <https://doi.org/10.3891/acta.chem.scand.26-2752>.
90. Erdtman, H. G. H.; Högberg, H.-E., The structure of a termolecular condensation product obtained by the action of strong acids on toluquinone, *Heterocycles*, **1977**, *8*,

- 171-174. [https://doi.org/10.3987/s\(s\)-1977-01-0171](https://doi.org/10.3987/s(s)-1977-01-0171).
91. Erdtman, H. G. H.; Högberg, H.-E., The acid-catalysed oligomerisation of p-benzoquinone, *Tetrahedron*, **1979**, *35*, 535-540. [https://doi.org/10.1016/0040-4020\(79\)80152-0](https://doi.org/10.1016/0040-4020(79)80152-0).
  92. Nakamura, Y.; Aratani, N.; Osuka, A., Experimental and theoretical investigations into the paratropic ring current of a porphyrin sheet., *Chem. -Asian J.*, **2007**, *2*, 860-866. <https://doi.org/10.1002/asia.200700112>.
  93. Nakamura, Y.; Aratani, N.; Furukawa, K.; Osuka, A., Synthesis and characterizations of free base and Cu(II) complex of a porphyrin sheet, *Tetrahedron*, **2008**, *64*, 11433-11439. <https://doi.org/10.1016/j.tet.2008.08.072>.
  94. Pawlicki, M.; Garbicz, M.; Szterenber, L.; Latos-Grazyński, L., Oxatriphyrins(2.1.1) incorporating an *ortho*-phenylene motif, *Angew. Chem. Int. Ed. Engl.*, **2015**, *54*, 1906-1909. <https://doi.org/10.1002/anie.201410595>.
  95. Chandra, B.; Mahanta, S. P.; Pati, N. N.; Baskaran, S.; Kanaparthi, R. K.; Sivasankar, C.; Panda, P. K., Calix[2]bispyrrolylarenes: new expanded calix[4]pyrroles for fluorometric sensing of anions via extended  $\pi$ -conjugation, *Org. Lett.*, **2013**, *15*, 306-309. <https://doi.org/10.1021/ol3032158>.
  96. Shimizu, M.; Nagao, I.; Tomioka, Y.; Hiyama, T., Palladium-catalyzed annulation of vic-bis(pinacolatoboryl)alkenes and -phenanthrenes with 2,2'-dibromobiaryls: facile synthesis of functionalized phenanthrenes and dibenzo[*g,p*]chrysenes, *Angew. Chem. Int. Ed. Engl.*, **2008**, *47*, 8096-8099. <https://doi.org/10.1002/anie.200803213>.
  97. Seven, Ö.; Qu, Z. W.; Zhu, H.; Bolte, M.; Lerner, H. W.; Holthausen, M. C.; Wagner, M., Synthesis, coupling, and condensation reactions of 1,2-diborylated benzenes: an experimental and quantum-chemical study, *Chem. -Eur. J.*, **2012**, *18*, 11284-11295. <https://doi.org/10.1002/chem.201201547>.
  98. Davis, F.; Higson, S., *Macrocycles: construction, chemistry and nanotechnology applications*, John Wiley & Sons, 2011, pp. 16-33. <https://doi.org/10.1002/9780470980200.ch2>.
  99. Pellegrin, M., Contribution à l'étude de la réaction de Fittig, *Recl. Trav. Chim. Pays-Bas Belg.*, **2010**, *18*, 457-465. <https://doi.org/10.1002/recl.18990181203>.
  100. Parekh, V. C.; Guha, P. C., Synthesis of p, p-Diphenylene Disulfide, *J. Indian Chem. Soc.*, **1934**, *11*, 95-100.
  101. Brown, C. J.; Farthing, A. C., Preparation and structure of di-*p*-Xylylene, *Nature*, **1949**, *164*, 915-916. <https://doi.org/10.1038/164915b0>.
  102. Cram, D. J.; Steinberg, H., Macro rings. I. Preparation and spectra of the paracyclophanes, *J. Am. Chem. Soc.*, **1951**, *73*, 5691-5704. <https://doi.org/10.1021/ja01156a059>.
  103. Vögtle, F.; Neumann, P., Zur nomenklatur der phane-II, *Tetrahedron*, **1970**, *26*, 5847-5873. [https://doi.org/10.1016/0040-4020\(70\)80023-0](https://doi.org/10.1016/0040-4020(70)80023-0).
  104. Mitchell, R. H.; Boekelheide, V., Transformation of sulfide linkages to carbon-carbon double bond. Syntheses of cis- and trans-15,16-dimethyldihydropyrene and trans-15,16-dihydropyrene, *J. Am. Chem. Soc.*, **1974**, *96*, 1547-1557. <https://doi.org/10.1021/ja00812a045>.
  105. Pascal, R. A.; Grossman, R. B.; Engen, D. Van., Synthesis of in-

- [34,10][7]metacyclophane: projection of an aliphatic hydrogen toward the center of an aromatic ring, *J. Am. Chem. Soc.*, **1987**, *109*, 6878-6880. <https://doi.org/10.1021/ja00256a067>.
106. Lemmerz, R.; Nieger, M.; Vögtle, F., New highly strained adamantanophanes, *J. Chem. Soc. Chem. Commun.*, **1993**, *14*, 1168-1170. <https://doi.org/10.1039/C39930001168>.
107. Vögtle, F.; Dohm, J.; Rissanen, K., The first clamped and strongly deformed adamantane, *Angew. Chem. Int. Ed. Engl.*, **1990**, *29*, 902-904. <https://doi.org/10.1002/anie.199009021>.
108. Pascal, R. A. J.; McMillan, W. D.; Van Engen, D., 9,18-diphenyltetrabenz(a,c,h,j)anthracene: a remarkably twisted polycyclic aromatic hydrocarbon, *Chem. Inf.*, **1987**, *18*, 62-62. <https://doi.org/10.1002/chin.198702152>.
109. Pascal, R. A.; Van Engen, D., The solid state structure of 9,11,20,22-tetraphenyltetrabenz[a,c,l,n]pentacene-10,21-dione: a longitudinally twisted molecular ribbon, *Tetrahedron Lett.*, **1987**, *28*, 293-294. [https://doi.org/10.1016/S0040-4039\(00\)95710-1](https://doi.org/10.1016/S0040-4039(00)95710-1).
110. Pascal, R. A.; Grossman, R. B., A comment on the structure and proton NMR spectrum of 2,8,17-trithia[45,L2][9]metacyclophane, *J. Org. Chem.*, **1987**, *52*, 4616-4617. <https://doi.org/10.1021/jo00229a036>.
111. Aita, K.; Ohmae, T.; Takase, M.; Nomura, K.; Kimura, H.; Nishinaga, T., Dithieno[3,4-b:3',4'-d]thiophene-annelated antiaromatic planar cyclooctatetraene with olefinic protons, *Org. Lett.*, **2013**, *15*, 3522-3525. <https://doi.org/10.1021/ol401125f>.
112. Nishinaga, T.; Ohmae, T.; Aita, K.; Takase, M.; Iyoda, M.; Arai, T.; Kunugi, Y., Antiaromatic planar cyclooctatetraene: a strategy for developing ambipolar semiconductors for field effect transistors, *Chem. Commun.*, **2013**, *49*, 5354-5356. <https://doi.org/10.1039/c3cc41764f>.
113. Harrison, I. T., The effect of ring size on threading reactions of macrocycles, *J. Chem. Soc. Chem. Commun.*, **1972**, 231-232. <https://doi.org/10.1039/C39720000231>.
114. Eisch, J. J., Karl Ziegler: master advocate for the unity of pure and applied research, *J. Chem. Educ.*, **1983**, *60*, 1009-1014. <https://doi.org/10.1021/ed060p1009>.
115. Wiberg, K. B., The concept of strain in organic chemistry, *Angew. Chem. Int. Ed. Engl.*, **1986**, *25*, 312-322. <https://doi.org/10.1002/anie.198603121>.
116. Petrucci, R.H.; Harwood, W.S. and Herring, F., Various generalizations of metric spaces and fixed point theorems, *RACSAM*, **2015**, *109*, 175-198. <https://doi.org/10.1007/s13398-014-0173-7.2>.
117. Bumpus, J. A., A theoretical investigation of the ring strain energy, destabilization energy, and heat of formation of CL-20, *Adv. Phys. Chem.*, **2012**, 1-7. <https://doi.org/10.1155/2012/175146>.
118. Prelog, V.; Schenker, K., Zur kenntnis des kohlenstoffringes. 61. Mitteilung über die oxydation von cyclodecenen zu cyclodecandiolen-(1,6), eine transannulare reaktion, *Helv. Chim. Acta*, **1952**, *35*, 2044-2053. <https://doi.org/10.1002/hlca.19520350634>.
119. Eisch, J. J., Karl Ziegler: master advocate for the unity of pure and applied research, *J. Chem. Educ.*, **1983**, *60*, 1009-1014. <https://doi.org/10.1021/ed060p1009>.
120. Martí-Centelles, V.; Burguete, M. I.; Luis, S. V., Macrocycle synthesis by chloride-

- templated amide bond formation, *J. Org. Chem.*, **2016**, *81*, 2143-2147.  
<https://doi.org/10.1021/acs.joc.5b02676>.
121. Prakash, G. K. S.; Yan, P.; Török, B.; Bucsi, I.; Tanaka, M.; Olah, G. A., Gallium(III) trifluoromethanesulfonate: a water-tolerant, reusable Lewis acid catalyst for Friedel-Crafts reactions, *Catal. Lett.*, **2003**, *85*, 1-6. <https://doi.org/10.1023/A:1022133227407>.
  122. Haupt, M., *Synthesis and investigation of diazadioxo[8]circulene-based cyclophane systems*, M. Sc. thesis, University of Copenhagen, Department of Chemistry, Copenhagen, 2016.
  123. Joensson, M. H., *Synthesis and properties of a cyclophane incorporating a diazadioxo[8]circulene*, M. Sc. thesis, University of Copenhagen, Department of Chemistry, Copenhagen, 2017.
  124. Xu, J.; Wei, Z.; Du, Y.; Pu, S., Facile electrosyntheses of high-strength and highly-conductive poly(1,12-bis(carbazolyl) dodecane) films, *Mater. Lett.*, **2007**, *61*, 2486-2490. <https://doi.org/10.1016/j.matlet.2006.09.042>.
  125. Koizumi, T. A.; Tsutsui, K.; Tanaka, K., Selective formation of inter- and intramolecular A-D-A  $\pi$ - $\pi$  stacking: solid-state structures of bis(pyridiniopropyl)benzenes, *Eur. J. Org. Chem.*, **2003**, 4528-4532. <https://doi.org/10.1002/ejoc.200300310>.
  126. Kumar, K.; Shin Wang, S.; N. Sukenik, C., Synthesis, characterization, and chemistry of bridgehead-functionalized bicyclo[2.2.2]octanes: reactions at neopentyl sites, *J. Org. Chem.*, **2002**, *49*, 665-670. <https://doi.org/10.1021/jo00178a018>.
  127. Goldsmith, R. H.; Vura-Weis, J.; Scott, A. M.; Borkar, S.; Sen, A.; Ratner, M. A.; Wasielewski, M. R., Unexpectedly similar charge transfer rates through benzo-annulated bicyclo[2.2.2]octanes, *J. Am. Chem. Soc.*, **2008**, *130*, 7659-7669. <https://doi.org/10.1021/ja8004623>.
  128. Martins, A.; Marquardt, U.; Kasravi, N.; Alberico, D.; Lautens, M., Synthesis of substituted benzoxacycles via a domino ortho-alkylation/Heck coupling sequence, *J. Org. Chem.*, **2006**, *71*, 4937-4942. <https://doi.org/10.1021/jo060552l>.
  129. He, Z.; Ye, G.; Jiang, W., Imine macrocycle with a deep cavity: guest-selected formation of syn/anti configuration and guest-controlled reconfiguration, *Chem. -Eur. J.*, **2014**, *21*, 3005-3012. <https://doi.org/10.1002/chem.201405912>.
  130. Beletskaya, I. P.; Cheprakov, A. V., Copper in cross-coupling reactions: the post-Ullmann chemistry, *Coord. Chem. Rev.*, **2004**, *248*, 2337-2364. <https://doi.org/10.1016/j.ccr.2004.09.014>.
  131. Bisceglia, J. A.; Orelli, L. R., Recent progress in the Horner-Wadsworth-Emmons reaction, *Curr. Org. Chem.*, **2015**, *19*, 744-775. <https://doi.org/10.2174/1385272819666150311231006>.
  132. Oullette, R. J., Rawn, J. D., *Principles of Organic Chemistry*, Elsevier, 2015, pp. 239-258. <https://doi.org/10.1016/c2014-0-02430-6>.